APPLICATION OF COMPREHENSIVE 2–DIMENSIONAL LIQUID CHROMATOGRAPHY FOR THE ANALYSIS OF COMPLEX PHENOLIC FRACTIONS

by

Kathithileni Martha Kalili

Thesis presented in partial fulfilment of the requirements for the degree of ***Master of Science (Chemistry)***

at

Stellenbosch University

Department of Chemistry and Polymer Science
Faculty of Science

Supervisor: Dr. A.J. de Villiers

December 2009

Declaration

By submitting this thesis electronically, I declare that the entirety of the work contained therein is my own, original work, that I am the owner of the copyright thereof (unless to the extent explicitly otherwise stated) and that I have not previously in its entirety or in part submitted it for obtaining any qualification.

Date: 27 October 2009

Summary

The separation of apple, cocoa and green tea phenolic compounds by comprehensive 2-dimensional liquid chromatography (2-D-LC) has been studied. In the first dimension, phenolic compounds were separated according to polarity by hydrophilic interaction chromatography (HILIC) on a diol stationary phase with a mobile phase containing acetonitrile, methanol, acetic acid and water. Gradient reversed-phase (RP) LC using a C18 column with fluorescence detection was employed in the second dimension to separate compounds according to hydrophobicity. Compounds were identified using negative electrospray ionisation mass spectrometry (ESI-MS) coupled to both HILIC and RP separations.

The coupling of HILIC and RP separations proved to be especially beneficial since this provided simultaneous information on both the polarity and hydrophobicity of phenolics. The low degree of correlation ($r^2 < 0.21$) between the two LC modes afforded peak capacities in excess of 3000 for the off-line method. An on-line method was also developed utilizing a short, small particle-packed column to provide fast separation in the second dimension. A 1 mm i.d. column was used in the first dimension for the on-line system to reduce injection volumes onto the second dimension column. A significantly lower practical peak capacity was measured for the on-line system, due largely to the reduction in second dimension peak capacity. On the other hand, analysis could be performed in an automated fashion using the on-line system reducing the risk of sample alteration and guaranteeing better operation reliability and reproducibility. Especially the off-line comprehensive HILIC × RP-LC method developed demonstrated its utility in the analysis of various groups of phenolic compounds including proanthocyanidins, phenolic acids, flavonols and flavonol conjugates in a variety of natural products.

Opsomming

Die skeiding van fenoliese komponente in appel, kakao en groen tee is deur middel van 'comprehensive' 2-dimensionele vloeistof chromatografie (2-D-LC) bestudeer. Hidrofiliese interaksie chromatografie (HILIC) is gebruik om die fenoliese komponente in die eerste dimensie te skei op grond van polariteit, deur gebruik te maak van 'n diol stationêre fase en mobiele fase bestaande uit asetonitriel, metanol, asynsuur en water. 'n Gradiënt omgekeerde fase (RP) LC analisie op 'n C18 kolom met fluorosensie deteksie is in die tweede dimensie gebruik om fenole volgens hidrofobisiteit te skei. Negatiewe elektrosproei-ionisasie massa spektometrie (ESI-MS) gekoppel aan HILIC en RP skeidings is gebruik vir identifikasie van fenole.

Die koppeling van HILIC en RP skeidings veral voordelig deurdat dit gelyktydige informasie verskaf het oor die polariteit sowel as die hidrofobisiteit van die fenoliese komponente. Die lae graad van korrelasie ($r^2 < 0.21$) tussen die twee LC metodes was verantwoordelik vir piek kapasiteite bo 3000 vir die af-lyn metode. 'n Aanlyn metode was ontwikkel deur gebruik te maak van 'n kort, klein partikel gepakte kolom om vinnige skeiding in die tweede dimensie te verseker. 1 mm i.d. kolom was gebruik in die eerste dimensie vir die aanlyn sisteem om die inspuit volume op die tweede dimensie kolom te verminder. Aansienlike laer praktiese piek kapasiteit was gemeet vir die aanlyn sisteem, grootliks toegeskryf aan die reduksie in die tweede dimensie piek kapasitiet. Aan die ander kant, analise kan geoutomatiseerd uitgevoer word deur gebruik te maak van die aanlyn sisteem, wat monster alterasie, beter betroubaarheid en reproduseerbaarhied verseker. Veral die ontwikkelde af-lyn 'comprehensive' HILIC × RP-LC metode toon demonstreerbare voordele vir die analiese van verskeie groepe fenoliese komponente, insluitende proantosianiede, fenoliese sure, flavonole en gekonjugeerde flavonole in 'n verskeidenheid natuurlike produkte.

Acknowledgements

I would like to thank the following people and institutions for their various contributions, otherwise this study would not have been realised:

My most sincere gratitude goes to my supervisor, Dr André de Villiers for his guidance and immense help offered throughout this study and the preparation of this thesis as well as for financial support, I can never thank him enough.

I am indebted to the National Research Foundation (NRF, South Africa), Stellenbosch University and the National Endowment Fund (Namibia) for financial support.

Dr Marietjie Stander is thanked for assisting with the LC-MS analysis.

Thanks to Prof Harald Pasch and Dr Frank David for serving as internal and external examiners, respectively.

Thanks to Berhane Weldergergis and the Chemistry and Polymer Science department staff members for all the assistance rendered.

Friends and family, thanks for all forms of support and encouragement.

And above all, thanks to the Almighty for his protection, guidance and for making everything possible.

Table of Contents

Chapter 3

Chapter 4

Chapter 5

Chapter 1

General Introduction

Phenolics are compounds possessing an aromatic ring with one or more hydroxyl functional groups, which are widely distributed in nature. These compounds have been studied quite substantially over the years. The interest in the study of phenolic compounds stems from the wide range of sensory properties and biological activities that these compounds are known to possess. Although these bioactive roles have been known for decades, complete characterisation of these compounds is not yet fully established. In order to understand the roles that these compounds play in the human health and food quality, it is necessary to investigate their mechanisms of action and bioavailability [1]. This is only possible using reliable analytical methods that would allow their accurate detection and quantification in natural products as well as various biological systems [1]. However, due to difficulty of analysis presented by the diverse and complex structures of phenolic compounds, the analysis of these compounds remains challenging.

The separation of phenolic compounds has been studied for years in pursuit of improved analytical techniques. High performance liquid chromatography (HPLC) is the method of choice for phenolic analysis. Although HPLC methods provide valuable analytical results, they do not provide sufficient resolving power for complete resolution of complex samples [2]. This is in part due to the limited separation space available for conventional 1-dimensional LC. Coupling multiple separation techniques is an established approach to increase the separation space and consequently peak capacity of a chromatographic system. This study was thus aimed at investigating alternative separation strategies that would enable improved separation of phenolic compounds. Comprehensive 2-dimensional liquid chromatography (2-D LC) techniques were explored in this regard.

References

[1] D.S. Barbosa, J. Consum. Protect. Food Safety 2 (2007) 407.
[2] P.Q. Tranchida, P. Dugo, G. Dugo, L. Mondello, J. Chromatogr. A 1054 (2004) 3.

Chapter 2

High Performance Liquid Chromatography

2.1. Chromatographic separation

Chromatography is a separation method by which analyte molecules are separated based on their differential partitioning between two phases, the stationary and mobile phases [1-4]. The stationary phase is immobilised, typically in a column, while the mobile phase flows over the stationary phase. The stationary phase commonly consists of either solid particles or a viscous liquid coated on the surface of solid particles or on the wall of a capillary tube. The mobile phase can either be a gas (gas chromatography), a liquid (liquid chromatography) or a supercritical fluid (supercritical fluid chromatography).

2.2. High Performance Liquid Chromatography (HPLC)

HPLC is a chromatographic technique which uses high pressure to force solvents through a packed bed of very small particles to achieve separation [5]. This modern form of liquid chromatography evolved from conventional gravity-fed liquid chromatography, which is still widely used for preparative chemistry and biochemistry [5]. HPLC is the single most widely used separation technique, and finds application in various fields of science such as agriculture, forensics, medicine, environment, pharmaceutical, etc. The technique has demonstrated its suitability for the analysis of diverse non-volatile, thermally labile and high molecular weight compounds such as carbohydrates, proteins, nucleic acids, polymers, etc.

2.2.1. Separation modes in HPLC

The power of modern HPLC lies in numerous options that exist to tune selectivity. Using diverse modes of separation, each based on different separation principles, separation can be effected using various approaches depending on the physico-chemical properties of the analytes of interest. The different separation mechanisms include adsorption chromatography, partition chromatography, ion exchange chromatography (IEX), affinity chromatography (AC) and size exclusion chromatography (SEC). Separation is governed by intermolecular interactions such as dipole-dipole, dipole-induced, hydrogen bonding, dispersion and electrostatic

interactions between the analytes and the mobile- and stationary phases. Only the HPLC modes used in this study are briefly described here.

2.2.1.1. Normal phase liquid chromatography (NP-LC)

Normal phase LC is a form of both adsorption and partition chromatography which employs a polar stationary phase and non-polar or weakly polar mobile phases. In NP-LC, polar stationary phases such as bare silica or support-bonded amino (NH_2), diol or cyano (CN) phases are used together with non-polar or weakly polar organic solvents such as hexane, dichloromethane, ethyl acetate and isopropanol. Polar and/or aqueous solvents are also used in several instances depending on the analyte/ stationary phase properties. This mode of separation came to be so known due to historic reasons: because chromatography was first performed using a polar stationary phase and a non-polar mobile phase, this mode was termed "normal" phase LC [6]. NP-LC offers separation based on the polarity of the analytes. A more polar solvent has higher elution strength and analytes are eluted in order of increasing polarity. NP-LC is useful for compounds which are insoluble in water, for synthesis monitoring and analysis of polymers. However, due to the highly polar nature of the stationary phases used in adsorption NP-LC, the presence of polar solvents in the mobile phase can lead to strong binding of these polar components by the stationary phase, resulting in relatively long column equilibration times and poor reproducibility [7].

2.2.1.2. Hydrophilic interaction chromatography (HILIC)

Hydrophilic interaction chromatography is a variant of NP-LC, which uses polar stationary phases and polar aqueous mobile phases. Although the practice of HILIC dates back to the 1950s, this separation mode has been referred to as NP-LC until recently when Alpert [8] proposed the term HILIC to distinguish it from the classical NP-LC which uses non-aqueous mobile phases. In HILIC, retention increases with the hydrophilicity of analytes and decreases with the polarity of the mobile phase [7,8]. The separation mechanism of HILIC is not yet fully understood and various mechanisms have been postulated. Separation in HILIC is thought to occur as a result of partitioning of analytes between a water layer immobilised on a hydrophilic stationary phase and the weakly hydrophobic mobile phase [7-10]. This method was

designed for the separation of polar or ionised analytes with limited retention in RP-LC [9,11]. Classically, HILIC has only been used in the analysis of sugars and oligosaccharides [7,10] until 1990 when Alpert [8] demonstrated its potential for other compounds such as amino acids, proteins, peptides, organic acids and bases as well as oligonucleotides. Since then, the application of HILIC has been extended to other compounds including cosmetics [12], pharmaceuticals [13,14] and flavonoids [15,16]. A range of hydrophilic stationary phases suitable or specially designed for HILIC analyses are commercially available, with the choice depending on the application [8].

2.2.1.3. Reversed phase liquid chromatography (RP-LC)

Reversed phase LC is a form of partition chromatography which employs a non-polar or weakly polar stationary phase and relatively polar, normally aqueous mobile phases. Support-based stationary phases such as octyldecyl (C_{18}), octyl (C_8), hexyl phenyl (C_6-Ph) and cyano (CN) phases are commonly used in combination with mobile phases consisting of water, methanol, acetonitrile, tetrahydrofuran or mixtures thereof. RP-LC offers separation on the basis of hydrophobicity. Analyte molecules partition between the polar mobile phase and the non-polar stationary phase, and more polar compounds are less retained than non-polar ones. However, the elution order is not always predictable due to other factors such as solvent properties, pH and temperature that also affect selectivity. RP is by far the most popular LC mode. Reasons for this include: ability to separate a wide range of compounds (e.g. acids, bases and neutrals), high reproducibility, relatively straightforward method development since separation principles are well-known, RP-LC provides faster column equilibration than non-aqueous adsorption separations and the fact that water, commonly used as mobile phase, is cheap and freely available.

2.3. HPLC instrumentation

A typical HPLC instrument consists of a solvent delivery unit, sample injector, pressure transducer, pulse dampener, column, detector and a computer to control the instrument and collect data (**Figure 2.1**). Modern HPLC instruments include an autosampler and a column heating compartment for accurate temperature control.

Each of these components governs the chromatographic performance of an HPLC instrument.

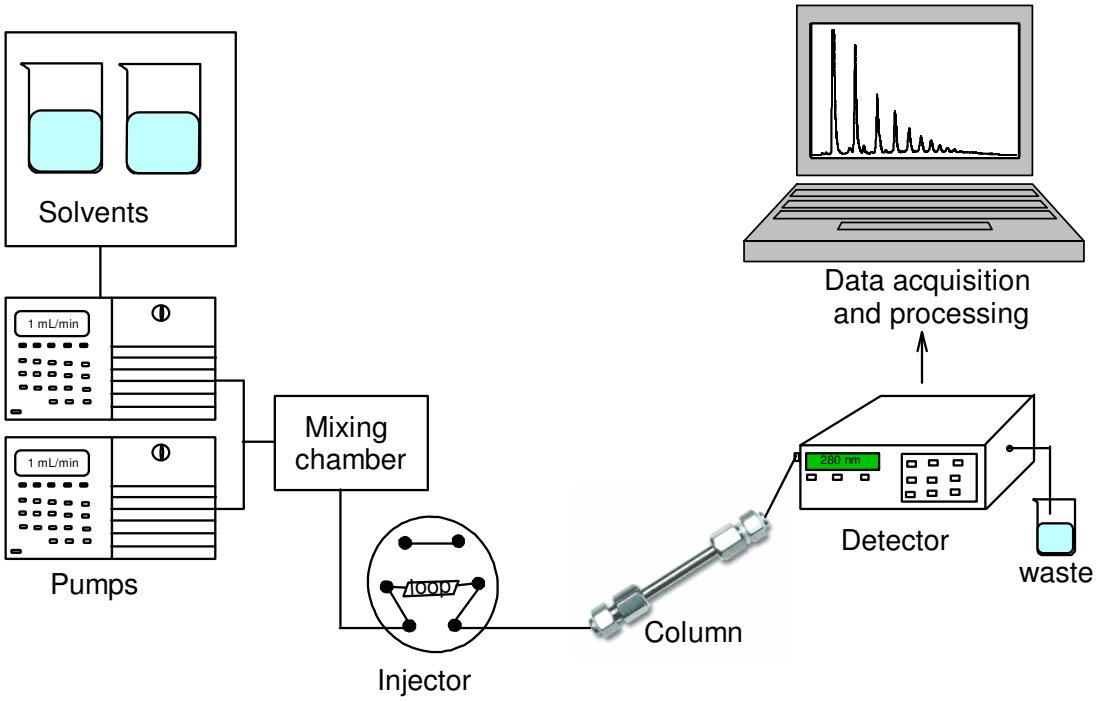

Figure 2.1: A schematic diagram of an HPLC instrument.

2.3.1. Solvent delivery system

The solvent delivery unit is composed of the solvent reservoirs and the pumps. Solvents play an essential role in an LC separation and high purity solvents are a necessity for reliable analytical results. It is of utmost importance that the solvents be filtered prior to use in the HPLC system to remove any particulate matter which might be present to avoid damage or clogging of the pumps, injector or column. In addition, the solvents need to be degassed before use so as to remove any dissolved gases which could lead to the formation of bubbles in the system. Bubble formation may lead to unsteady and irreproducible flow rates, erratic gradient profiles or result in increased baseline noise. Degassing is done via ultrasonication, sparging of the mobile phase with an inert gas of low solubility to force any dissolved gases out of solution, or by use of an on-line degasser consisting of a vacuum pumping system and membrane.

The main driving force behind an HPLC instrument is the pump. An HPLC pump is required to generate a highly reproducible and pulse-free flow in the range of 0.1 to 10 mL/min at pressures up to 6000 pounds per square inch (psi) (6000 psi = 400 bar).

Three types of pumps, namely: reciprocating pumps, syringe or displacement pumps and pneumatic or constant pressure pumps are used in HPLC instrumentation. Each pumping system has advantages and disadvantages. The reciprocating pump is the most commonly used, and about 90% of commercially available HPLC systems are equipped with this kind of pump. The reciprocating pump consists of a small cylindrical chamber which is alternately filled and emptied with the mobile phase by the back and forth motion of a piston. This produces a pulsed flow, which requires dampening to avoid excessive baseline noise. The pump head is equipped with inlet and outlet check valves, which maintain the flow in one direction. The inlet check valve prevents backward flow of the mobile phase into the solvent reservoir while the outlet check valve prevents backward flow from the column into the pump. This pump is advantageous in that it has a small internal volume, high output pressure, constant flow rates and is compatible with gradient elution. The displacement pump consists of a large, syringe-like chamber with a plunger which is driven by a stepper motor, while in the pneumatic pump the mobile phase is delivered through the movement of a piston or diaphragm by pressurised gas. The displacement pump has limited solvent compatibility, while the pneumatic pump can only provide output pressures up to 2000 psi and it is not suitable for gradient elution [6].

Elution in HPLC is performed either in the isocratic or gradient mode. In isocratic elution, the mobile phase composition remains constant throughout the analysis, while gradient elution involves stepwise or continuous changing of the mobile phase composition as a function of time. Gradient elution is generally useful for samples containing analytes comprising a wide retention range, where isocratic elution does not separate the compounds in a reasonable time [17-19]. In effect, gradient elution provides an increase in solvent strength, resulting in reduced retention factor (k) values of the later eluting compounds, which would otherwise be poorly detected or quantified. Gradient elution, relative to isocratic elution, offers advantages of improved resolution, better detection and quantitation of strongly retained compounds and shorter analysis times [17,18]. For these reasons, most HPLC analyses are carried out in the gradient mode. In order to enable gradient execution, earlier HPLC instruments are equipped with a gradient programmer, which is used for programming the solvent composition as a function of time. With modern HPLC instruments, a

computer is used to control all system components as well as to acquire and process data.

Another notable component of the pumping unit is the mixing chamber. In the mixing chamber, solvents are mixed in order to get a uniform composition. This mixing can either be done before the solvent reaches the pump (low-pressure mixing) or after passing through the pump (high-pressure mixing). Solvent degassing is most critical for high-pressure mixing because mixing happens in a small chamber under high pressure and the presence of gases in the mobile phase at this stage could lead to bubble formation upon decompression.

2.3.2. Injection system

A two-position 6-port injection valve is commonly used to introduce the sample onto the column. The valve has high pressure capability up to at least 400 bar. Sample loops of different volumes can be used depending on the injection volume. The valve can be switched between two positions, namely the load and inject positions. In the load position, the mobile phase flows from the pump to the column, bypassing the sample loop, while in the inject position, the flow is directed from the pump through the sample loop to the column (**Figure 2.2**). The fact that the valve can be switched between two positions allows one to load the sample at atmospheric pressure without stopping the flow. Modern autosamplers allow automated injection of samples without user intervention by combining a 6-port valve with a syringe and needle to place the sample in the loop.

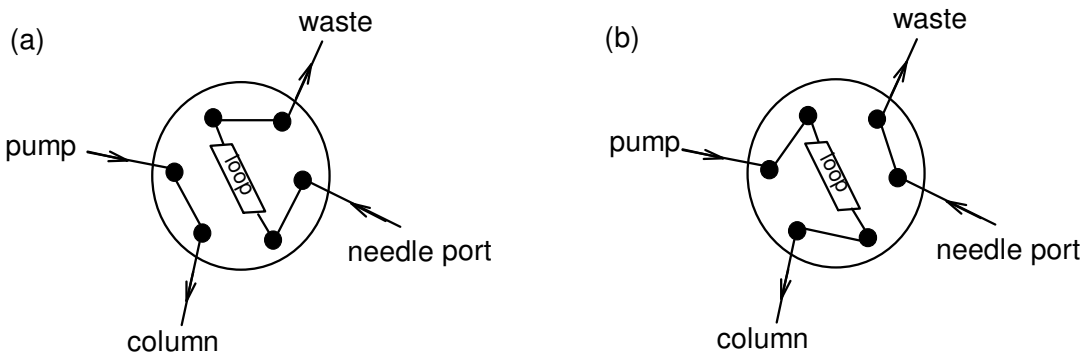

Figure 2.2: A diagram of a 2-position 6-port valve used for injection in HPLC. The diagram shows the port connections when the valve is in the (a) load and (b) inject positions.

2.3.3. The HPLC column

A column is regarded as the heart of an HPLC system since this is where separation takes place. HPLC columns are usually made out of stainless steel to withstand high pressures generated by the flow of mobile phase through a packed bed of small particles. In addition, the material used for the column should be chemically inert.

Typical HPLC columns range between 1.5-30 cm in length and the particle sizes range between 3-10 µm. Columns with internal diameters (i.d.) between 1-4.6 mm are primarily used for analytical chromatography, with 2-4.6 mm i.d. considered to provide the best compromise between efficiency and convenience [17]. Columns with i.d. between 4-10 mm and 10-25.4 mm are used for semi-preparative and preparative applications, respectively. The internal diameter of HPLC columns (at least 1 mm to ~ 10 mm) is not known to play any significant effect on the column performance [7]. However, because the flow rate is proportional to the column diameter, increase in column diameter is accompanied by increase in flow rate and consequently, high solvent consumption [7]. In addition, the sample dilution factor is higher in larger-bore columns than in smaller-bore columns, therefore increase in column diameter should be accompanied by proportional increase in injection volume if sensitivity is to be maintained [2,7]. Besides low solvent consumption, smaller-bore columns can be particularly useful if a small amount of sample is available and the analytes are present in low concentrations [2,7].

The efficiency of a chromatographic separation is determined by the amount of band broadening i.e., how broad the peaks are [5]. The separation efficiency of a chromatographic column is measured by the number of theoretical plates (N), defined as:

$$N = 16\left(\frac{t_R}{w_b}\right)^2 = 5.54\left(\frac{t_R}{w_h}\right)^2 = \frac{L}{H} \qquad (\mathbf{2.1})$$

where t_R is the analyte retention time (min), w_b is the base peak width (min), w_h is the peak width at half height (min), L is the column length (mm) and H is the theoretical plate height (mm or µm).

The contribution of various physical processes that take place inside the column to band broadening is described by the van Deemter equation:

$$H = A + \frac{B}{u_0} + Cu_0 \qquad (\mathbf{2.2})$$

where:

H = theoretical plate height, which relates the variance of a band to the distance travelled through the column (mm)

u_0 = mobile phase flow velocity (mm/sec)

A = the multiple path term, which is independent of flow rate

B = the longitudinal diffusion term, which is inversely proportional to flow rate

C = the finite equilibration time between the mobile and stationary phases, also called the mass transfer term, which is directly proportional to flow rate.

All three terms contribute to band broadening in packed columns. This is in addition to extra-column band broadening resulting from diffusion in system volume i.e. outside the column from the point of injection to detection.

When operating at optimal conditions, a general deduction obtained from the van Deemter curve (H-u_0 plot) is that $H \approx 2d_p$. In this instance, **equation 2.1** becomes:

$$N = \frac{L}{2d_p} \qquad (\mathbf{2.3})$$

where d_p is the particle diameter (µm). This implies that the efficiency of an HPLC column increases with decrease in particle size and increase in column length. However, small particles have higher resistance to solvent flow [5], which implies higher operating pressures. Due to this constraint, columns longer than 30 cm cannot be used if pressures are to be kept within the instrument pressure range. Ultra high pressure LC (UHPLC) systems which can withstand pressures up to 15 000 psi (1000 bar), and short columns packed with small particles sizes (< 2 µm) are now commercially available from some manufacturers and these offer highly efficient, fast separations.

In order to prolong the lifetime of analytical columns, it is recommended that guard columns packed with the stationary phase similar to that of the analytical columns be placed before the analytical column.

2.3.4. Detection

Detection forms an essential part of an HPLC system. This allows monitoring of the eluate exiting the column for the presence of analytes [2,4,17,20]. An ideal detector should be sensitive to low concentrations of analytes, provide a linear response, be non-destructive, insensitive to fluctuations in temperature and mobile phase composition and should not broaden analytes peaks [2,5,6,17,20]. Various types of detectors have been developed for use in HPLC; detectors used in this study will be discussed briefly.

2.3.4.1. Ultraviolet (UV) detection

UV detection is one of the most commonly used modes of detection in HPLC. These detectors have gained popularity because of their sensitivity to a wide range of compounds, insensitivity to temperature changes, ease of use, compatibility with gradient elution and affordability [2,17]. A UV detector works on the principle of Beer-Lambert law:

$$Absorbance = \log \frac{I_0}{I} = \varepsilon bc \qquad (\mathbf{2.4})$$

where:

I_0 = intensity of the incident light

I = intensity of the transmitted light

b = path length of the cell (cm)

ε = molar absorptivity or molar extinction coefficient ($M^{-1}cm^{-1}$)

c = concentration of the light absorbing species in the sample (M).

The Beer-Lambert law states that absorbance is directly proportional to the concentration of the light absorbing species in the sample and the molar absorptivity (ε) of the analyte at the specified wavelength. The UV detector measures the difference between the incident light and the transmitted light. Light from the lamp passes through the flow cell and is transmitted onto a diode that measures the light intensity. However, for an analyte molecule to be detected by UV, it must possess a chromophore containing an atom or group of atoms containing valence electrons with low excitation energies, which allows UV absorption [6,17]. It is also of the essence that a mobile phase with acceptable UV transmittance at the selected wavelength be

used, in order to maximise detection sensitivity with respect to analyte molecules [2,17,18].

There are various types of UV detectors which are used in HPLC namely, fixed wavelength (FW), variable wavelength (VW) and photodiode array (PDA) detectors. FW detectors utilize mercury lamps which emit intense radiation at 254 nm, or zinc lamps which emit at 214 nm. The FW detector comprises of a series of focusing lenses and slits to focus the source light on the flow cell and then the transmitted light onto the diode. VW detectors use deuterium lamps which emit over the range 180-400 nm, or tungsten lamps for the visible wavelength range (400-700 nm). The VW detector is equipped with a diffraction grating (located between the lamp and the flow cell) which selects a single wavelength. Light from the lamp enters the grating assembly via the entrance slit and is focused on the grating by a mirror. Monochromatic light of the selected wavelength is focused onto a second mirror and then exits via the exit slit. The VW detector, as opposed to the FW detector, offers the possibility of scanning the entire wavelength range in order to determine the absorption maximum for the compound of interest [20].

PDA detectors use deuterium or tungsten lamps which provide radiation in the full spectral range between 190-800 nm. In the PDA detector, the grating assembly is placed after the flow cell: therefore the entire range of wavelengths from the source enters the flow cell. The transmitted light then passes through a dispersive element (e.g. a prism) which disperses the light into different wavelengths, each of which is detected by a diode. The PDA detector allows monitoring of the entire spectrum of all analytes as they elute [2,18,20]. This feature led to the popularity of the PDA detector as it makes it a powerful qualitative tool, particularly for mixtures of compounds with different spectra [21].

2.3.4.2. Fluorescence detector (FLD)

Some compounds exhibit luminescence property, i.e. when they are irradiated with light in the UV region they undergo electronic excitation and emit light of a higher wavelength [5,18,20]. Emission can occur either instantaneously (fluorescence) or after a certain time delay (phosphorescence) [5]. In the fluorescence detector, light

from the lamp passes through the excitation filter, which provides monochromatic light of the desired wavelength for the excitation of sample molecules [17,18,20]. The exciting light passes through the effluent in the flow cell, causing target sample molecules to emit light of a higher wavelength [17,18,20]. The emission filter is placed at the right angle (90°) to the excitation filter, allowing only a small fraction of the scattered light from the excitation source to reach the photomultiplier tube (PMT), thereby minimising background noise [18]. In this case, only the light emitted by the sample molecules is quantified as the emission signal [18,22]. A fluorescence detector is at least three orders of magnitude more sensitive than an UV detector [18]. In addition to sensitivity, fluorescence detection offers an added advantage of selectivity, since few compounds possess fluorescent properties [18,21]. At the same time, the fact that only few compounds fluoresce, makes fluorescence detection amenable to a very narrow range of analytes. Although several fluorescent derivatisation reagents have been developed in order to increase the utility of fluorescence, derivatisation adds an extra step of sample treatment to the analysis and the stability of the derivatisation products is critical [18]. Because fluorescence is unaffected by matrix effects, it is ideally suited for complex sample matrices and trace-level analysis [17]. In contrast, fluorescence emission is to a certain extent influenced by a number of environmental factors such as solvents, pH, temperature and concentration [2,18,20,22]. Therefore, each of the parameters requires careful consideration for maximum sensitivity and to avoid self-absorption, which can occur if the analyte concentration is too high [20,22].

2.3.4.3. Mass spectrometric (MS) detection

MS detection has found considerable use in HPLC over the years. The combination of liquid chromatography and mass spectrometry, abbreviated LC-MS, represents a very significant step which allows structural elucidation of separated compounds. MS is currently the most powerful detection mode available in HPLC and has become the method of choice for the analysis of complex samples. MS involves production, separation and detection of ions [4,21]. Since only charged species are detectable, the first step in MS detection involves ionisation of the analyte molecules [18]. After ionisation, ions are sorted based on their mass-to-charge (*m/z*) ratios and focused in

the mass analyser [18]. MS techniques are distinguished based on the ionisation source. Common ionisation techniques used in MS include electron impact (EI), atmospheric pressure chemical ionisation (AP-CI), atmospheric pressure electrospray ionisation (AP-ESI), thermospray (TSP), fast atom bombardment (FAB) and matrix-assisted laser desorption ionisation (MALDI). As for the ion source, the choice depends mainly on the compatibility of the ion source with the introduction method (e.g. HPLC, GC) and the resolution of the instrument with the targeted mass range of the analytes [18]. These ionisation techniques are far too broad to be covered within the context of this thesis, only aspects of AP-ESI will be discussed briefly.

The breakthrough in ESI was first described in the 1980s by John Fenn, who received the Nobel Prize in Chemistry in 2002 together with Koichi Tanaka and Kurt Wuthrich, for the development of methods for structural elucidation of biological macromolecules using ESI, MALDI and NMR, respectively [23]. In ESI, the LC eluate is transferred into the API source through a metal capillary, which is set to a high voltage (3-6 kV) [23-27]. The action of the high electric field at the metal capillary together with the surrounding high-speed N_2 flow, results in the creation of charged droplets (**Figure 2.3**) [4,5,23,24].

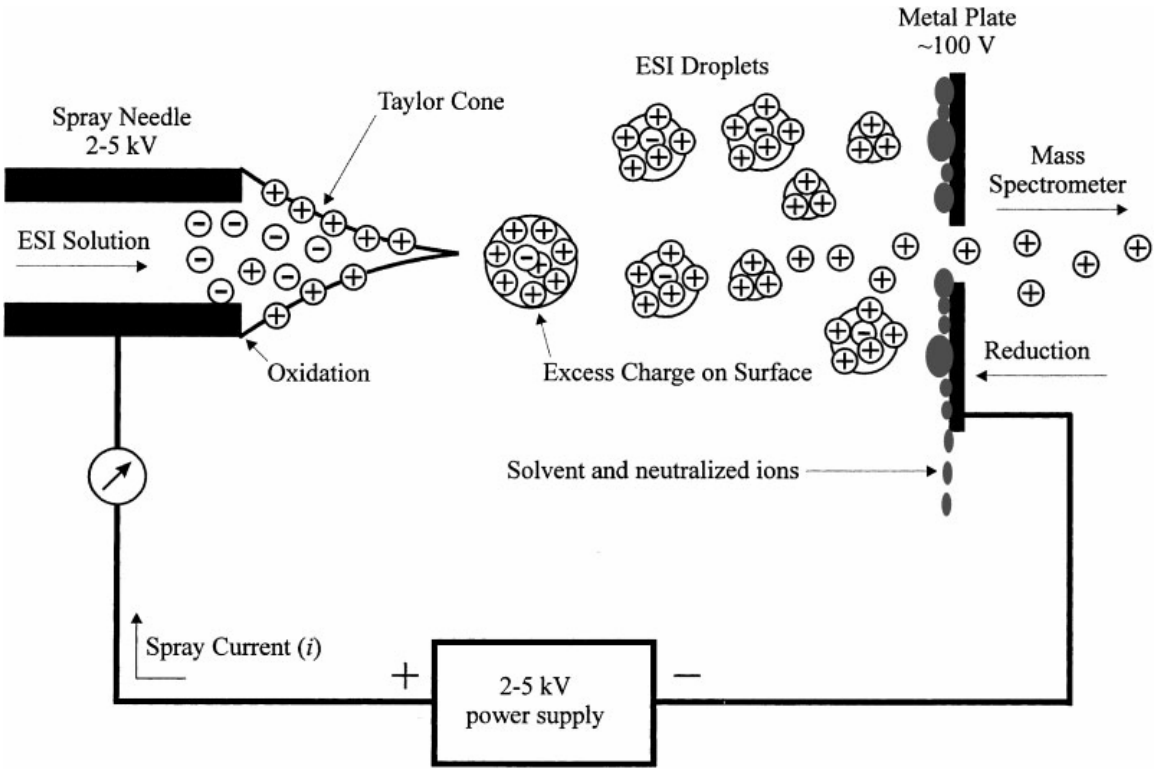

Figure 2.3: A schematic diagram of electrospray ionisation [28].

The droplets are evaporated by a heating device located in the source, which concentrates the droplets and increases their charge density [29]. The increase in charge-to-surface area due to evaporation results in Coulombic explosion, releasing smaller droplets [4,23,25-27]. This process is repeated until very small, highly charged droplets capable of producing gas-phase ions are formed [4,25,26]. These gas-phase ions can then be analysed in the mass spectrometer on the basis of their *m/z* ratios [4,28]. The charge on the droplet surface can be positive or negative depending on the polarity of the capillary voltage [5,23]. The ions may be either singly- or multiply charged. Multiple charging allows detection of high molecular weight compounds when using mass analysers with limited scan ranges [4,18,23].

Various mass analysers such as ion trap (ITP), quadrupole, triple-quadrupole, time-of-flight (TOF), magnetic and electrostatic sectors and Fourier transform ion cyclotron resonance (FT-ICR) have been developed. The triple quadrupole and the time-of-flight are the most commonly used mass analysers in combination with HPLC.

The quadrupole mass analyser consists of four parallel rods arranged in a symmetrical manner [18]. The diagonally opposed rods are connected together electrically with a fixed radio-frequency (RF) and direct current (DC) voltage applied to them [5,18,30]. The ions from the source are focused and travel along the quadrupole between the rods [5]. For a certain range of voltages, only ions with certain *m/z* ratios have stable trajectories and will reach the detector, while ions with unstable trajectories collide with the rods to form neutral molecules [5,6]. The RF potential is varied so that ions of different *m/z* ratios can be focused onto the detector for their mass spectrum to be constructed [5]. The triple-quadrupole mass analyser consists of three sets of quadrupole rods arranged in series [30]. The first and the third quadrupoles are used as mass filters while the middle quadrupole is a collisionally induced dissociation (CID) source [18,30]. MS/MS spectra of analyte parent ions can be generated in this manner by first selecting the parent ion in the first quadrupole, followed by CID in the second quadrupole and subsequent sorting of fragment ions in the third quadrupole [18,30].

In the time-of-flight mass spectrometer, ions of different *m/z* ratios are accelerated through the flight tube under the influence of applied voltage [18]. Since the ions are

given the same kinetic energy, their velocities differ inversely with their masses, therefore ions reach the detector at different times (times of flight) in order of increasing mass [6,18,30]. The resolution of the TOF-MS is measured based on its ability to accurately determine times of flight for different ions [18,30]. This is affected by different factors such as the length of the flight tube, the accelerating voltages and devices as well as the differences in the ions present in a sample [18,30]. Mass resolution can be improved by increasing the length of the flight tube so as to increase the flight distance, which is usually achieved by using reflectrons and similar devices [18,30]. Such technologies have led to the high resolution currently achievable with TOF-MS instruments. For this reason, these instruments are now the most popular in LC-MS due to simplicity, larger mass range and suitability for routine operation [18,30]. Despite the high purchase and running costs and requirement of specialised personnel to operate sophisticated instruments such as the LC-MS, the technique offers a powerful analytical tool and it is therefore indispensable for identification of complex non-volatile samples.

2.4. Limitations of 1-D HPLC separations

Since the advent of chromatography, the field has continuously been developed in pursuit of improved chromatographic performance. This is due to the ever-increasing need for improved separating power required for the analysis of complex samples. The resolving power of a chromatographic separation system is measured in terms of peak capacity (n_p) [31]. Peak capacity is defined as the maximum number of peaks that can be separated at a given resolution within a given separation window [3,32-34]. For any single separation mechanism, resolution is limited either by the selectivity of the stationary phase or by the attainable efficiency [33]. Selectivity can be tuned by changing the stationary phase, mobile phase composition, pH or temperature. The peak capacity, on the other hand, is limited by the number of theoretical plates (N) and the separation space [33]. The peak capacities for isocratic and gradient analyses [34] are given by **equations 2.5 and 2.6**, respectively:

$$n_p = 1 + \frac{\sqrt{N}}{4}\ln(k+1) \qquad (\mathbf{2.5})$$

where N is the column plate count and k is the retention factor for the last eluting compound.

$$n_p = 1 + \frac{t_g}{\overline{w}} \qquad (\mathbf{2.6})$$

where t_g is the gradient run time (min) and $\overline{w}$ is the average peak width (min).

From the theory of chromatography, it is well known that N of a chromatographic separation can be increased by increasing the column length or by decreasing the particle size. However, both approaches are technically limited because they are accompanied by significant increase in pressure, and HPLC instrumentation and columns are limited in terms of maximum operating pressure (the limit for current commercial instruments is ~ 1 200 bar). Therefore, increasing the separation space is another approach to enhance peak capacity. This can be achieved by coupling multiple, non-correlated (orthogonal) separation mechanisms and subjecting the sample to both separation mechanisms [33].

The following discussion will focus on the most important means currently available to increase the resolving power of particularly HPLC separations. However, these topics are far too broad to be covered comprehensively within the context of this thesis and thus only brief summaries of particularly their benefits are discussed and the reader is referred to various articles [35-45] covering these topics in full for more detailed information.

2.5. Ultrahigh pressure LC (UHPLC)

The benefit of reducing the particle size of the stationary phase has long been known in HPLC: it is well established that reducing the particle size leads to increased separation efficiency in packed columns. This is because small particles provide more uniform flow through the column, thus reducing the A term of the van Deemter equation (equation 2, section 2.3.3) [5], and because smaller particles offer a short distance through which the analyte must diffuse in the mobile phase, which reduces the C term of the van Deemter equation [5,39]. This is evident from the van Deemter curves obtained for columns packed with different particle sizes (**Figure 2.4**), which

is the plot of the plate height (H) as a function of linear velocity (u_0). Another deduction that can be obtained from the van Deemter curves is the fact that reduction in particle size leads to increase in optimal linear velocity (u_{opt}), while the efficiency-loss above this value is reduced.

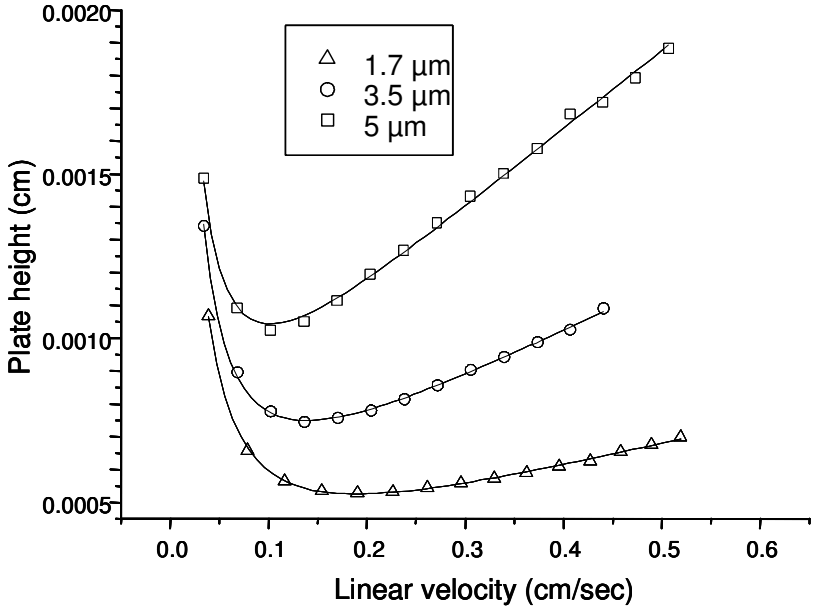

Figure 2.4: Experimental van Deemter curves for 1.7, 3.5 and 5 µm HPLC columns [41].

However, the reduction in particle size is accompanied by increase in pressure because small particles have high resistance to solvent flow [5]. This is clearly evident from Darcy's law [39,46], which relates the pressure drop across the column (ΔP, psi) to the eluent viscosity (η, cP), column length (L), linear velocity (u_0), column particle diameter (d_p) and column permeability (K_0) :

$$\Delta P = \frac{K_0 \eta L}{d_p^{\,2}} u_0 = \frac{K_0 \eta N H}{d_p^{\,2}} u_0 \qquad (\mathbf{2.7})$$

Darcy's law shows that the pressure drop is inversely proportional to the square of the particle diameter. The optimum linear velocity is inversely proportional to the particle diameter and is given by:

$$u_{opt} = \frac{3D_m}{d_p} \qquad (\mathbf{2.8})$$

where D_m is the analyte's diffusion coefficient in the mobile phase [39]. **Equations 2.7 and 2.8** imply that the pressure drop at optimal linear velocity is inversely proportional to $d_p^{\,3}$ [39]. This necessitates that, for the same pressure drop, a decrease

in particle size will have to be coupled with reduction in column length, linear velocity or an increase in temperature (to reduce the mobile phase viscosity). This means that the same efficiency is achieved much faster with the combination of higher linear velocities and shorter columns packed with small particles. For the same column length, higher efficiencies are achievable on small particle-packed columns, but only if the operating pressure is increased. For instance, columns packed with 1.5 µm could not be made longer than 3.3 cm due to pressure constraints and could therefore not provide efficiency of more than 10 000 plates [39]. Due to pressure limitation, this potential benefit could not be realised with conventional HPLC instrument having maximum operating pressures of 400 bar. This remained the case until late 1990s when MacNair *et al* [39,40] developed an LC system with pressure capability as high as 4 100 – 5 000 bar (60 000 – 72000 psi). This technology came to be known as "ultrahigh pressure liquid chromatography (UHPLC)" and led to the commercialisation of columns packed with < 2 µm particles, and instrumentation with maximum operating pressures of ~1 200 bar (17 400 psi).

2.6. High temperature LC (HTLC)

Temperature is an important parameter in liquid chromatography which affects selectivity, retention and mobile phase viscosity [35-37,43,47,48]. Yet, in the past, temperature has been under-utilised as a parameter for tuning LC separations, partly due to the unavailability of thermally stable stationary phases and suitable instrumentation [47,48]. Until recently, most LC separations were carried out at ambient temperature [37,48]. The realisation of the potential of temperature as a tuneable parameter for selectivity control or improved chromatographic efficiency [37], prompted the development of presently available thermally stable stationary phases and instrumentation. Increase in temperature is coupled with a reduction in mobile phase viscosity and an increase in analyte diffusion, which implies faster mass transfer of analytes between the mobile and stationary phase, improved efficiency at higher flow rates and reduction in analysis time [2,5,36,37,43,45,47-52].

The effect of temperature on column performance is clearly depicted in **Figure 2.5**, where theoretical van Deemter curves obtained at different temperatures are shown.

From the figure, it is apparent that the minimum plate height (H_{min}) is not affected by temperature, but higher optimal linear velocities are attained at higher temperatures.

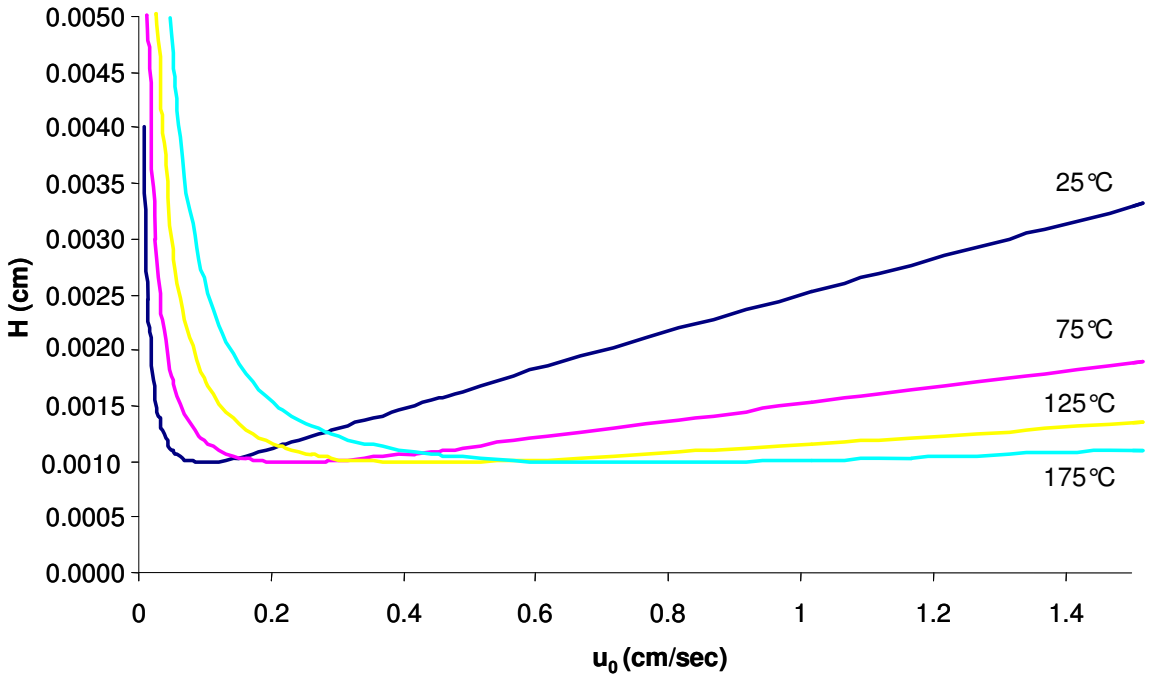

Figure 2.5: Theoretical van Deemter curves on a 5 µm column, showing the effect of temperature on the plate height (H) and linear velocity (u_0) [52].

In addition, temperature elevation is associated with an increase in eluting strength of the mobile phase, alteration in selectivity and changes in dissociation equilibria for ionisable compounds [43,45]. The effect of temperature on selectivity change is illustrated by the Van't Hoff equation:

$$\ln k = -\frac{\Delta H}{RT} + \frac{\Delta S}{R} + \ln \Phi \qquad (\mathbf{2.9})$$

where k is the retention factor, ΔH (Jmol^{-1}) and ΔS (JK^{-1}mol^{-1}) are the enthalpy and entropy of solute transfer from the mobile phase to the stationary phase, respectively, R is the universal gas constant (JK^{-1}mol^{-1}), T is the temperature (K) and Φ is the phase ratio of the column. Since variations in temperature results in changes in enthalpy (ΔH) or entropy (ΔS), this could result in changes in the retention of analytes depending on the extent to which the analyte is affected by such changes [36].

Temperature tuning has the same effect as changing the mobile phase composition, although the effect is much smaller [36]. For instance, Chen and Horvath [53] showed that while maintaining the same eluent strength, a 5°C increase in temperature has the

same effect on retention of neutral compounds as a 1% increase in acetonitrile content for temperatures between 30-80°C. The effect of temperature on retention is ascribed to the fact that the polarity of water decreases with increase in temperature and hence the eluotropic strength of water increases at high temperatures [54,55]. The possibility of using pure water as the eluent has also been explored at temperatures over 100°C [55,56]. This signifies that HTLC is a promising approach towards "green" LC, which could do away with high consumption of costly and toxic solvents currently used in LC, to enable safer, cheaper and environmentally friendly LC practices [54].

This approach, however, is presented with a series of limitations, including:

(i) the eluent strength cannot be changed during an analysis unless temperature programming is performed (this is nowadays possible),

(ii) highly retained non-polar solutes may not elute even at high temperatures,

(iii) there is a limited number of thermally stable stationary phases suitable for superheated water chromatography, and

(iv) peak distortion or band broadening may be a problem if strong organic solvents are to be injected for analytes with limited solubility in water [43,45].

Since the use of higher linear velocities is possible without loss of efficiency when working at high temperatures, this means that the analysis time can effectively be reduced [2,52]. For this reason, temperature elevation is particularly useful for 2-D LC analyses, more especially in the second dimension which needs to be carried out relatively fast. In fact, the combination of elevated temperature and ultra high pressure offers an attractive approach to faster and highly efficient separations. However, the success of this application is largely dependent on the thermal stability of the analytes [47,57]. Temperature elevation may also lead to degradation of the stationary phase and shorten the column lifetime [5,47]. Therefore, thorough studies on the thermal stability of analytes and stationary phases are required if the benefits of this technique are to be realised [47,51].

2.7. Multidimensional LC (MD-LC)

Generally, 1-dimensional chromatographic techniques are incapable of providing resolution of complex samples consisting of many components (e.g. > 100) [32]. This remains the case even if the separation space is theoretically large enough to accommodate all compounds in a sample if they were evenly spaced. This occurs as a result of random distribution of peaks across the separation space [58], making it impossible to utilise the entire available space. Davis *et al* [58-61] used the statistical method of overlap (SMO) theory to explain component overlap phenomena in both one- and two- dimensional systems. They showed that any random chromatogram can never contain more than 37% of its theoretical maximum peaks and no more than 18% of components will be detected as single peaks. They further showed that in order for a single component of a mixture to provide a 90% probability of appearing as an isolated peak, the chromatogram must be at least 95% empty [58]. Since peak overlap is unavoidable, 1-dimensional separations will certainly fail to resolve complex samples such as those encountered in, for example, natural products. As the number of components to be resolved increases, the degree of overlap also increases, necessitating more powerful separation methods. The degree of overlap suggests coupling of two or more mutually independent (orthogonal) separations so that components overlapping in one dimension will be separated in the other.

Multidimensional (MD) LC techniques were therefore developed as a means of overcoming the limited resolving power of conventional 1-dimensional LC techniques. A MD chromatographic separation refers to a technique in which more than one separation mechanism is applied to the analysis of a sample [32,33]. In MD separation systems, different separation mechanisms are combined, and improved resolution is provided because the separation space is effectively increased [33]. If orthogonal retention mechanisms are combined, the theoretical peak capacity of a MD separation is the product of the peak capacities in each dimension [32,33,49,62-64].

For a chromatographic system to be defined as truly multidimensional, certain criteria must be met, namely:

(i) The sample must be subjected to two or more uncorrelated (i.e. orthogonal) separation mechanisms,

(ii) Any two components separated in the first dimension must remain separated in consecutive dimensions,

iii) The elution profiles from both dimensions must be maintained [32,64-66].

The design of multidimensional systems therefore requires careful selection and optimisation of certain parameters in order to achieve practical peak capacities as close to the theoretical maximum as possible.

2.7.1. General aspects of multidimensional separations

Dimensionality: Sample dimensionality is a concept that was introduced by Giddings [67] to describe the amenability of a sample to multidimensional separations. He explained that the retention of analytes in a sample is dependent on the structural properties (referred to as "dimensions") of the analytes. Each independent characteristic structural property of the analytes in the sample represents separate dimension for that particular sample. Therefore, if the analytes in a sample can only be separated on the basis of one structural property, the sample is mono-dimensional [33,49,67]. It would be pointless to subject this sample to multiple separation mechanisms as only one dimension would provide selectivity and no additional information would be gained from a secondary separation [33,49,67]. Giddings further stated that increasing the system dimensionality can only be beneficial if the sample dimensionality is greater or equal to the system dimensionality. However, if the sample dimensionality exceeds that of the system, it results in a chaotic separation pattern as not all the sample components will be resolved [67]. Although it becomes practically very hard to increase separation dimensionality above two, the concept provides a useful starting point for designing multidimensional systems [33].

Sampling rate: The sampling rate of the first dimension peaks is another crucial aspect that needs to be considered in the design of a 2-D separation. It has been demonstrated that the peak capacity of the first dimension separation (and consequently of the 2-D system) can be greatly reduced due to under-sampling of the first dimension peaks [68-70]. Therefore, in order to maintain the first dimension resolution, it is required that each first dimension peak be sampled at least three times to avoid peak capacity loss due to under-sampling [69,70]. However, sampling rates

of at least 2 fractions per first dimension peak provide a better compromise between the sampling rate and the second dimension analysis time [68]. In order to achieve satisfactory first dimension sampling, an extremely slow first dimension separation, or a very fast second dimension analysis is implied. Due to this demand, column dimensions used in each dimension need to be well-matched. Using linear velocities below the optimal value will result in loss of efficiency in the first dimension and loss of peak capacity. Usually, a microbore column operated at a low flow rate is employed in the first dimension in order to provide sample volumes which are compatible for injecting onto the second dimension without splitting the flow. This minimises the dilution factor of the sample and improves sensitivity in the second dimension and at the same time allows for focussing of analytes at the head of the secondary column [63,65]. A short column with a conventional internal diameter (i.d.) is typically used in the second dimension for faster separations and higher loadability. The use of high linear velocities as required for fast analysis in the second dimension is limited by increase in pressure. In order to circumvent this problem, fast second dimension analysis can be achieved through the use of high temperature together with thermally stable columns or monolithic columns.

Peak capacity: The total peak capacity (n_T) of a 2-D separation should ideally be equal to the product of the peak capacities in the first (n_1) and second (n_2) dimensions [32,33,49,62-64], and is given by:

$$n_T = n_1 \times n_2 \qquad (\mathbf{2.10})$$

However, this is hardly ever achieved in practice because it is rare (if at all possible) to obtain a completely orthogonal system due to retention correlations which always exist between separation modes [33,63]. In addition, extra peak broadening effects, including the sampling rate of the first dimension peaks, also lead to loss of peak capacity in 2-D separations. Several statistical and mathematical approaches have been developed to account for these effects and provide more accurate practical peak capacities [71-75]. Only the methods of Liu *et al* [71], which accounts for orthogonality in the estimation of the 2-D peak capacity calculation, and that of Li *et al* [75], which accounts for under-sampling, will be discussed briefly.

Liu *et al* [71] used a geometrical approach to factor analysis to estimate the orthogonality of a 2-D separation, and derived equations accounting for this parameter in the calculation of the practical peak capacity. Since two sets of independent retention data are obtained in 2-D separations, the method of Liu *et al* [71] assumes that each set of retention data can be taken as an independent vector. Therefore, there are two independent vectors associated with any 2-D separation and the correlation between these two vectors can be calculated using the scaled retention factors of analytes separated in each dimension. The correlation matrix (C) is then given by:

$$C' = \left(\frac{1}{N'-1}\right) k'^{T}\, k' \qquad (\mathbf{2.11})$$

where k' is the matrix of the scaled retention factors, k'^{T} is the transpose of the matrix of the scaled retention factors and N' is the number of retention data for each vector, which is also equal to the number of components in a 2-D plot. This correlation matrix can be shown as:

$$C' = \begin{bmatrix} 1 & \cdots & C1j \\ \vdots & \vdots & \vdots \\ Ci1 & \cdots & 1 \end{bmatrix} \qquad (\mathbf{2.12})$$

where $C_{ij} = C_{ji}$ and is the quantitative measure of the correlation between two sets of vectors (retention data), which is the orthogonality of the 2-D system. When $C_{ij} = 1$, a totally correlated system is obtained and when $C_{ij} = 0$, a totally orthogonal system is obtained [71].

Most 2-D separation systems lie between perfect correlation (i.e. when identical separation mechanisms are used) and perfect orthogonality (i.e. when non-correlated separation mechanisms are selected) [71]. Therefore, the available separation space is reduced to a fraction of the orthogonal case if correlation exists between the selected separation modes [76]. A graphical representation of the 2-D retention space with a peak spreading angle (β) is shown in **Figure 2.6**.

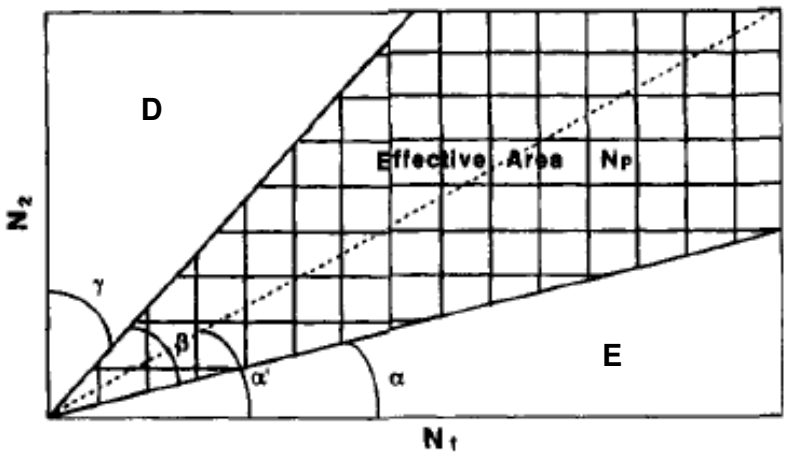

Figure 2.6: An effective non-orthogonal 2-D retention space when the spreading angle is β [71].

The gridded area in **Figure 2.6** is the effective area occupied by peaks in a 2-D separation space, while areas D and E becomes unavailable due to correlation [71]. In this instance, angles α, α', β and γ as well as unavailable areas D and E are calculated using **equations 2.13-2.18**:

$\alpha' = \tan^{-1} (n_2/n_1)$ (**2.13**)

$\beta = \cos^{-1} (r)$, r is the square root of the correlation coefficient (**2.14**)

$\alpha = \alpha'(1-2\beta/\pi)$ (**2.15**)

$\gamma = \pi/2 - \alpha - \beta$ (**2.16**)

$D = \frac{1}{2} n_2^2 \tan \gamma$ (**2.17**)

$E = \frac{1}{2} n_1^2 \tan \alpha$ (**2.18**)

The practical peak capacity (n_p) is then calculated using:

$n_p = n_T - (D + E)$ (**2.19**)

$= n_T - \frac{1}{2} [n_2^2 \tan \gamma + n_1^2 \tan \alpha]$ (**2.20**)

In a 2-D separation, it is generally required that the peaks eluting from the first dimension column be sampled at least 3 times in order to avoid loss of resolution achieved in the first dimension due to under-sampling [68-70]. However, this requirement is not obeyed in most instances, which often results in loss of peak capacity [68]. In view of this, several authors developed both mathematical and statistical models to account for this effect in the calculation of the 2-D peak capacity when sufficient sampling of the first dimension peaks is not done. The method of Davis *et al* [77] is a modification of previous work by other authors [68-70] on the investigation of the sampling problem in 2-D chromatographic separations. The approach of Davis *et al* [77] differed from that of previous authors in the sense that

they assessed the effect of under-sampling on randomly simulated peaks across the entire chromatogram, as opposed to a single pair of peaks used by previous authors [68-70]. These authors included an average sampling correction factor (<β>) in the calculation of the first dimension peak capacity to correct for under-sampling and the product rule is then used to calculate the effective peak capacity. The average sampling correction factor is given by:

$$< \beta >= \sqrt{1 + 0.214\left(\frac{t_s}{{}^1\sigma}\right)^2} \qquad (\mathbf{2.21})$$

where t_s is the first dimension sampling time and ${}^1\sigma$ is the first dimension peak standard deviation before sampling [77]. The effective 2-D peak capacity is then calculated using:

$$n'_{p,2D} = \frac{n_1 n_2}{< \beta >} = \frac{n_1 n_2}{\sqrt{1 + 0.21\left(\frac{t_s}{{}^1\sigma}\right)^2}} \text{ valid for } 0.2 \le \frac{t_s}{{}^1\sigma} \le 16 \qquad (\mathbf{2.22})$$

The method of Li *et al* [75] is an extension of the method of Davis *et al* [77], which includes the sampling correction factor (also referred to as the peak broadening factor) for under-sampling of the first dimension peaks. The effective 2-D peak capacity according to Li *et al* [75] is then given by:

$$n'_{p,2D} = \frac{n_1 n_2}{\sqrt{1 + 3.35\left(\frac{{}^2t_c n_1}{{}^1t_g}\right)^2}} \qquad (\mathbf{2.23})$$

where ${}^2t_c$ is the second dimension cycle time, which is equal to the sampling time and ${}^1t_g$ is the first dimension gradient time.

Although these methods [71,75] seek to address the issue of accurate determination of 2-D peak capacities, they deal with different parameters which all need to be assessed in the computation of the peak capacity. Due to lack of consensus on the appropriate method, chromatographers often opt for whatever method they find suitable to calculate the peak capacity of their 2-D separations, which makes it impossible to compare results in literature. Therefore, this issue need to be addressed in order to ensure consistency and comparison of results for different separation systems.

2.7.2. Instrumental aspects of 2-D LC systems

Two approaches, heart-cutting and comprehensive analyses, may be employed in 2-D LC separations. In the heart-cutting approach, only certain fractions (regions of interest) of the first dimension separation are analysed in the second dimension. In contrast, the entire sample is subjected to both separation mechanisms in comprehensive 2D-LC. Two-dimensional analyses can also be performed in either on-line or off-line fashion. In the on-line setup, fractions from the first dimension are directly transferred to the second dimension for subsequent analysis. This is usually done by means of switching valve(s) equipped with sampling loops or trapping columns which alternately trap the fractions from the first dimension at defined time intervals. **Figure 2.7** shows two on-line configurations utilising different switching valve configurations. In all instances, the first dimension eluate is alternately trapped in one of the loops while secondary separation of the second loop fraction is carried out using a second pump. Once the cycle is completed, the valve(s) is/are switched so that the content of the other loop can be analysed. This is repeated throughout the entire first dimension separation.

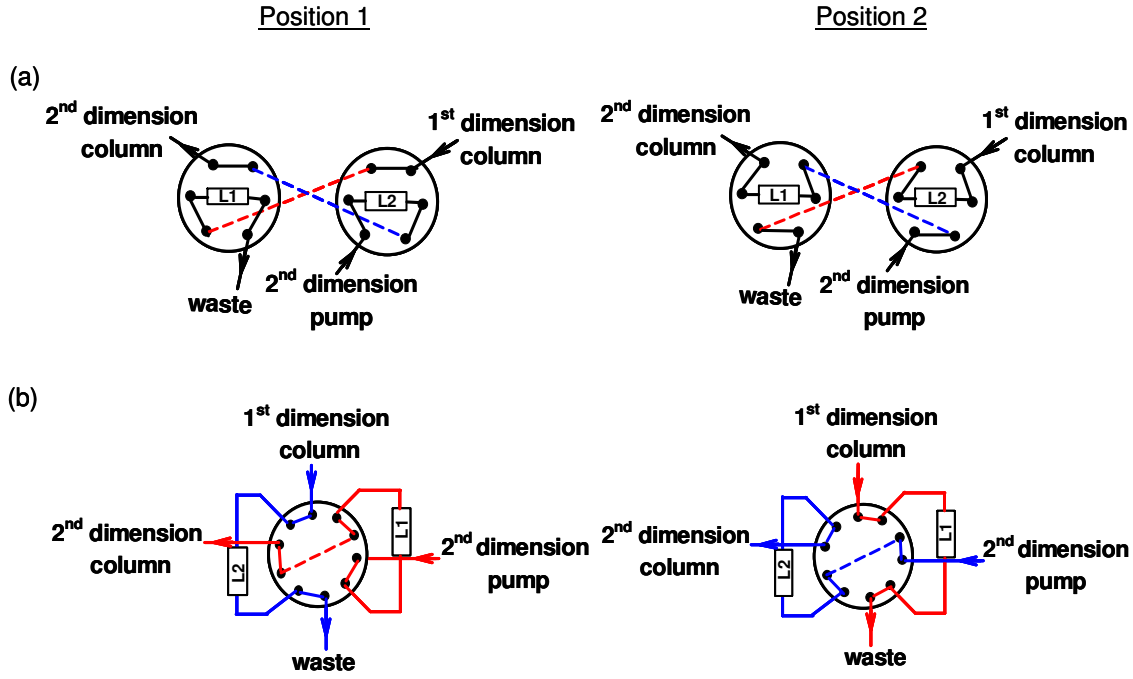

Figure 2.7: Experimental configurations for on-line comprehensive 2-D LC systems using (a) two 6-port switching valves and (b) a 2-position 10-port switching valve.

It is of the essence that the fraction transferred to the second dimension column should be fully analysed prior to the subsequent transfer in order to avoid the "wrap-

around" effect (where analytes from the previous analysis elute in the separation space of the next transfer), which results in chaotic band displacement [78]. This requires that the second dimension analysis time be equal or less than the first dimension sampling time [63,78]. Fast separations in the second dimension can be achieved by using monolithic columns, which permit higher flow rates with low backpressures [62] because of their high permeability and good mass-transfer properties [79]. Alternatively, high temperature can be employed to reduce the mobile phase viscosity and allow faster flow rates without exceeding system pressure limits. Thermally stable phases such as carbon-coated zirconia columns are generally used for this purpose.

Alternatively, two parallel secondary columns can be used in the second dimension. This offers an advantage of increased second dimension analysis time, thereby leading to higher second dimension peak capacity [79]. The overall peak capacity of the 2-D system is therefore greatly enhanced, at the cost of instrument complexity [79]. In addition, a stop-flow approach can also be used whereby the two columns are connected via a two position 6-port valve with no sampling loops. Each fraction of the first dimension eluate is transferred directly to the second dimension column. When a specific fraction has been transferred, the valve is switched and the first dimension flow is stopped, while the second dimension analysis of the transferred fraction is carried out. When the second dimension analysis is complete, the primary flow is started again for the next transfer and the process is repeated until the whole analysis is completed. Although this approach allows for automation, less risk of sample alteration and longer analysis time in the second dimension and hence improved peak capacities, this could lead to excessive band broadening of the first dimension peaks [78].

In the off-line setup, fractions from the first dimension are collected and subsequently analysed on another column. This can be done on the same or another instrument, often with evaporation performed prior to re-injection to reconcentrate the sample. Because the off-line approach places less demand on the second dimension analysis time, very high practical peak capacities are attainable.

Because LC offers a wide range of separation mechanisms with different selectivities, this implies a good number of theoretically possible combinations for 2-D LC systems

[65]. However, some combinations are impractical due to solvent immiscibility and/or mobile/stationary phases incompatibilities [65], therefore these parameters need to be carefully considered when designing 2-D LC methods. In addition, injection of large volumes of solvents that may be immiscible, differ greatly in viscosity or may be strong solvents, perturbs the retention process and jeopardises the focusing of analytes at the head of the second dimension column, resulting in peak distortion [80,81]. Solvent and mobile/stationary phase incompatibilities are of less concern for the off-line approach, since evaporation and reconstitution is possible between the two dimensions. However, successful coupling of two LC systems in an on-line manner is complicated by the considerations outlined above. The principal advantages and disadvantages associated with on-line and off-line analyses are summarised in **Table 2.1**.

Table 2.1: Advantages and disadvantages of on-line and off-line comprehensive 2-D LC techniques.

	On-line	**Off-line**
Advantages	- Automation - Faster - Better reproducibility	- Higher peak capacities - Ease of operation - Allows combination of non-compatible LC modes with evaporation of solvents and redissolution prior to second dimension analysis - The sample can be concentrated before second dimension analysis for better sensitivity
Disadvantages	- Complicated instrumental configuration and expensive - Require specific interfaces	- Time consuming - Difficult to automate - Poor reproducibility - Risk of sample loss, contamination and /or degradation

The choice of the approach largely depends on the problem at hand. High peak capacities are attained when using the off-line approach but there is a risk of analyte loss and/or degradation. On-line analyses on the other hand, are faster and highly reproducible, but specific, costly interfaces are required. The stop-flow approach can however, provide a better compromise between peak capacity and automation, but the possibility of excessive peak broadening cannot be ruled out.

2.7.3. 2-D LC applications

Multidimensional LC techniques have been successfully applied in the separation of real-world samples. Applications of MD techniques are covered extensively throughout this thesis, and therefore, only selected applications will be highlighted. Erni & Frei [82] reported the groundbreaking work in 2-D LC, by combining gel permeation chromatography (GPC) and RP-LC to separate complex plant extracts. This was followed by the work of Bushey & Jorgenson [83] who employed IEX and SEC in the analysis of proteins. The combination of NP-LC and RP-LC has also been employed in the separation of a variety of samples including lemon and citrus oil extracts [84] red orange essential oil [85], carotenoids [86] and polymers [87]. Tian *et al* [88] developed a NP-LC × RP-LC method to separate traditional Chinese medicine with the use of a vacuum-evaporation interface, to avoid injection of NP solvents onto the RP column. SEC × liquid chromatography/liquid chromatography at critical conditions (LC/LC-CC) have also been employed in the analysis of polymers [89-91]. RP-LC × RP-LC has also been widely evaluated in the analysis of various samples such as steroid mixtures and sulphonamide drugs [79], phenolic compounds [92-98] and polymers [99]. Quite recently, the combination of SFC and RP-LC has been used in the separation of a lemon oil extract [100] and fatty acids of fish oil [101].

In summary, 2-dimensional chromatography allows the combination of (ideally) uncorrelated separations, which provides significantly improved separation in a 2-dimensional space. Although data analysis can be a daunting task, presentation of data in a 2-D space greatly aids data interpretation, since it is easier to compare different samples by means of visual inspection in a 2-dimensional space than in a 1-dimensional space. Developing 2-dimensional methods can be quite challenging and rather lengthy in comparison to one-dimensional separations [78]. However, the vast

amount of information obtainable from a 2-D separation makes the effort worthwhile [78]. For this reason, comprehensive 2-D chromatographic techniques are indispensable tools for the analysis of complex samples.

List of symbols

$\overline{w}$	average peak width, min
k'^{T}	transpose of the matrix of the scaled retention factors, dimensionless
η	mobile phase viscosity, cP
β	peak spreading angle, dimensionless
π	pi, dimensionless
Φ	stationary-to-mobile phase ratio of the column, dimensionless
α, α′ and γ	angles, dimensionless
ΔH	change in enthalpy of solute transfer from the mobile phase to the stationary phase, $Jmol^{-1}$
ΔP	pressure drop across the column, psi
ΔS	change in entropy of solute transfer from the mobile phase to the stationary phase, $JK^{-1}mol^{-1}$
$<\beta>$	sampling correction factor (peak broadening factor), dimensionless
${}^{1}\sigma$	first dimension peak standard deviation before sampling, min
${}^{1}t_g$	first dimension gradient time, min
${}^{2}t_c$	second dimension cycle time, min
A	multiple path term, dimensionless
B	longitudinal diffusion term, dimensionless
C	finite equilibration time between the mobile- and stationary phase, dimensionlesss
C'	correlation matrix, dimensionless
$C_{ij} = C_{ji}$	quantitative measure of the correlation between two sets of retention data, dimensionless
D and E	unavailable areas in a 2-D separation space, dimensionless
D_m	analyte diffusion coefficient in the mobile phase, dimensionless
d_p	particle diameter, µm
H	plate height, mm
k	retention factor, dimensionless

k'	matrix of the scaled retention factors, dimesnionless
K_0	column permeability, dimensionless
L	column length, mm
N	number of theoretical plates, dimensionless
N'	number of retention data in each dimension, dimensionless
$n'_{p,2D}$	effective 2-D peak capacity, dimensionless
n_1	peak capacity in the first dimension, dimensionless
n_2	peak capacity in the second dimension, dimensionless
n_p	peak capacity, dimensionless
n_T	total peak capacity, dimensionless
r	square root of the correlation coefficient (r^2), dimensionless
R	universal gas constant, $JK^{-1}mol^{-1}$
T	temperature, Kelvins (K)
t_g	gradient time, min
t_R	retention time, min
t_s	first dimension sampling time, min
u_0	mobile phase linear velocity, mm/sec
u_{opt}	optimal linear velocity, mm/sec
w_b	base peak width, min
w_h	peak width at half height, min

2.8. References

[1] C.F. Simpson, in C.F. Simpson (Editor), Techniques in liquid chromatography, Wiley Heyden Ltd., West Sussex, 1982, p. 1.

[2] V.R. Meyer, Practical high-performance liquid chromatography, 4th ed., John Wiley & Sons, Chichester, 2004.

[3] J. Cazes, R.P.W. Scott, Chromatography theory, Marcel Dekker, Inc., New York, 2002.

[4] W.M.A. Niessen, Liquid chromatography-mass spectrometry, 3rd ed., CRC Press, New York, 2006.

[5] D.C. Harris, Quantitative Chemical Analysis, W.H. Freeman and Co., New York, 1999.

[6] D.A. Skoog, F.J. Holler, T.A. Nieman, Principles of Instrumental Analysis, 5th ed., Saunders College Publishing Philadelphia, 1998.

[7] U.D. Neue, HPLC Columns: Theory, technology and practice, Wiley-VCH, Inc., New York, 1997.

[8] A.J. Alpert, J. Chromatogr. A 499 (1990) 177.

[9] D.V. McCalley, U.D. Neue, J. Chromatogr. A 1192 (2008) 225.

[10] P. Hemström, K. Irgum, J. Sep. Sci. 29 (2006) 1784.

[11] J. Pesek, M.T. Matyska, LC-GC N. Am. 25 (2007) 480.

[12] P. Dallet, L. Labat, E. Kummer, J.P. Dubost, J. Chromatogr. B 742 (2000) 447.

[13] C. McClintic, D. Remick, J. Peterson, D. Risley, J. Liq. Chromatogr. Relat. Technol. 26 (2003) 3093.

[14] X. Wang, W. Li, H.T. Rasmussen, J. Chromatogr. A 1083 (2005) 58.

[15] A. Yanagida, H. Murao, M. Ohnishi-Kameyama, Y. Yamakawa, A. Shoji, M. Tagashira, T. Kanda, H. Shindo, Y. Shibusawa, J. Chromatogr. A 1143 (2007) 153.

[16] H. Zhang, Z. Guo, F. Zhang, Q. Xu, X. Liang, J. Sep. Sci. 31 (2008) 1623.

[17] L.R. Snyder, J.J. Kirkland, Introduction to modern liquid chromatography, John Wiley & Sons, Inc., New York, 1974.

[18] L.R. Snyder, J.J. Kirkland, J.L. Glajch, Practical HPLC method development, 2nd ed., John Wiley & Sons, Inc., New York, 1997.

[19] B.A. Bidlingmeyer, Practical HPLC methodology and applications, John Wiley & Sons, Inc., New York, 1992.

[20] B.B. Wheals, in C.F. Simpson (Editor), Techniques in liquid chromatography, Wiley Heyden Ltd., West Sussex, 1982, p. 121.

[21] G.D. Christian, Analytical Chemistry, 6th ed., John Wiley & Sons, Inc., MA, 2004.

[22] P.C. Sadek, Troubleshooting HPLC systems, a bench manual, John Wiley & Sons, Inc., New York, 2000.

[23] S.L. Gelhaus, I.A. Blair, in P.G. Pearson, L.C. Wienkers (Editors), LC-MS Analysis in drug metabolism studies, Informa Health Care, 2008.

[24] R. Kostiainen, T.J. Kauppila, J. Chromatogr. A 1216 (2009) 685.

[25] P. Kebarle, L. Tang, Anal. Chem. 65 (1993) 972A.

[26] P. Kebarle, J. Mass Spectrom. 35 (2000) 804.

[27] R.B. Cole, J. Mass Spectrom. 35 (2000) 763.

[28] N.B. Cech, C.G. Enke, Mass Spectrom. Rev. 20 (2001) 362.

[29] M.G. Ikonomou, A.T. Blades, P. Kebarle, Anal. Chem. 62 (1990) 957.

[30] R.E. Ardrey, Liquid chromatography-Mass spectrometry: An introduction, John Wiley & Sons, Ltd., Chichester, 2003.
[31] R.A. Shellie, P.R. Haddad, Anal. Bioanal. Chem. 386 (2006) 405.
[32] J.C. Giddings, in H.J. Cortes (Editor), Multidimensional Chromatography: techniques and applications, Marcel Dekker, Inc., New York, 1990, p. 1.
[33] S.P. Dixon, I.D. Pitfield, D. Perrett, Biomed. Chromatogr. 20 (2006) 508.
[34] U.D. Neue, J. Chromatogr. A 1184 (2008) 107.
[35] C.V. McNeff, B. Yan, D.R. Stoll , R.A. Henry, J. Sep. Sci 30 (2007) 1672.
[36] T. Greibrokk, T. Andersen, J. Chromatogr. A 1000 (2003) 743.
[37] E. Lundanes, T. Greibrokk, in E. Grushka, N. Grinberg (Editors), Advances in Chromatography, CRC Press, MA, 2006, p. 45.
[38] J.M. Cunliffe, S.B. Adams-Hall, T.D. Maloney, J. Sep. Sci. 30 (2007) 1214.
[39] J.E. MacNair, K.C. Lewis, J.W. Jorgenson, Anal. Chem. 69 (1997) 983.
[40] J.E. MacNair, K.D. Patel, J.W. Jorgenson, Anal. Chem. 71 (1999) 700.
[41] A. de Villiers, F. Lestremau, R. Szucs, S. Gelebart, F. David, P. Sandra, J. Chromatogr. A 1127 (2006) 60.
[42] J.W. Dolan, J. Chromatogr. A 965 (2002) 195.
[43] S. Heinisch, J.-L. Rocca, J. Chromatogr. A 1216 (2009) 642.
[44] N. Wu, J.A. Lippert, M.L. Lee, J. Chromatogr. A 911 (2001) 1.
[45] T. Greibrokk, T. Andersen, J. Sep. Sci. 24 (2001) 899.
[46] G. Guiochon, J. Chromatogr. A 1126 (2006) 6.
[47] F.D. Antia, C. Horvath, J. Chromatogr. 435 (1988) 1.
[48] H. Chen, C. Horvath, J. Chromatogr. A 705 (1995) 3.
[49] D.R. Stoll, X. Li, X. Wang, P.W. Carr, S.E.G. Porter, S.C. Rutan, J. Chromatogr. A 1168 (2007) 3.
[50] D.R. Stoll, J.D. Cohen, P.W. Carr, J. Chromatogr. A 1122 (2006) 123.
[51] J.D. Thompson, P.W. Carr, Anal. Chem. 74 (2002) 1017.
[52] F. Lestremau, A. de Villiers, F. Lynen, A. Cooper, R. Szucs, P. Sandra, J. Chromatogr. A 1138 (2007) 120.
[53] M.H. Chen, C. Horváth, J. Chromatogr. A 788 (1997) 51.
[54] F. Lynen, P. Sandra, in 39th SACI National Convention, Stellenbosch, South Africa, 2008, p. 47.
[55] Y. Yang, M. Belghazi, A. Lagadec, D.J. Miller, S.B. Hawthorne, J. Chromatogr. A 810 (1998) 149.
[56] F. Lynen, J.M.D. Heijl, F.E. Du Prez, R. Brown, R. Szucs, P. Sandra, Chromatographia 66 (2007) 143.
[57] U.D. Neue, J.R. Mazzeo, J. Sep. Sci. 24 (2001) 921.
[58] J.M. Davis, J.C. Giddings, Anal. Chem. 55 (1983) 418.
[59] J.M. Davis, J.C. Giddings, Anal. Chem. 57 (1985) 2168.
[60] K. Rowe, J.M. Davis, Anal. Chem. 67 (1995) 2981.
[61] J.M. Davis, J.C. Giddings, Anal. Chem. 57 (1985) 2178.
[62] P.J. Schoenmakers, G. Vivo-Truyols, W.M.C. Decrop, J. Chromatogr. A 1120 (2006) 282.
[63] P. Dugo, F. Cacciola, T. Kumm, G. Dugo, L. Mondello, J. Chromatogr. A 1184 (2008) 353.
[64] Z. Liu, M.L. Lee, J. Microcol. Sep. 12 (2000) 241.
[65] P.Q. Tranchida, P. Dugo, G. Dugo, L. Mondello, J. Chromatogr. A 1054 (2004) 3.
[66] J.C. Giddings, Anal. Chem. 56 (1984) 1258A.
[67] J.C. Giddings, J. Chromatogr. A 703 (1995) 3.

[68] K. Horie, H. Kimura, T. Ikegami, A. Iwatsuka, N. Saad, O. Fiehn, N. Tanaka, Anal. Chem. 79 (2007) 3764.
[69] R.E. Murphy, M.R. Schure, J.P. Foley, Anal. Chem. 70 (1998) 1585.
[70] J.V. Seeley, J. Chromatogr. A 962 (2002) 21.
[71] Z. Liu, D.G. Patterson, M.L. Lee, Anal. Chem. 67 (1995) 3840.
[72] J.M. Davis, P.W. Carr, Anal. Chem. 81 (2009) 1198.
[73] N.E. Watson, J.M. Davis, R.E. Synovec, Anal. Chem. 79 (2007) 7924.
[74] M. Gilar, P. Olivova, A.E. Daly, J.C. Gebler, Anal. Chem. 77 (2005) 6426.
[75] X. Li, D.R. Stoll, P.W. Carr, Anal. Chem. 81 (2009) 845.
[76] M. Gray, G.R. Dennis, P. Wormell, R. Andrew Shalliker, P. Slonecker, J. Chromatogr. A 975 (2002) 285.
[77] J.M. Davis, D.R. Stoll, P.W. Carr, Anal. Chem. 80 (2008) 461.
[78] A.R. Shalliker, M.J. Gray, in E. Grushka, N. Grinberg (Editors), Advances in Chromatography, CRC Press, New York, 2006, p. 177.
[79] I. François, A. de Villiers, B. Tienpont, F. David, P. Sandra, J. Chromatogr. A 1178 (2008) 33.
[80] S. Udrescu, A. Medvedovici, V. David, J. Sep. Sci. 31 (2008) 2939.
[81] S. Keunchkarian, M. Reta, L. Romero, C. Castells, J. Chromatogr. A 1119 (2006) 20.
[82] F. Erni, R.W. Frei, J. Chromatogr. A 149 (1978) 561.
[83] M.M. Bushey, J.W. Jorgenson, Anal. Chem. 62 (1990) 161.
[84] I. François, A. de Villiers, P. Sandra, J. Sep. Sci. 29 (2006) 492.
[85] P. Dugo, M. Herrero, D. Giuffrida, T. Kumm, G. Dugo, L. Mondello, J. Agric. Food Chem. 56 (2008) 3478.
[86] P. Dugo, V. Skerikova, T. Kumm, A. Trozzi, P. Jandera, L. Mondello, Anal. Chem. 78 (2006) 7743.
[87] P. Jandera, J. Fischer, H. Lahovská, K. Novotná, P. Cesla, L. Kolárová, J. Chromatogr. A 1119 (2006) 3.
[88] H. Tian, J. Xu, G. Yafeng, J. Sep. Sci. 31 (2008) 1677.
[89] H. Pasch, M. Adler, F. Rittig, S. Becker, Macromol. Rapid Commun. 26 (2005) 438.
[90] D. Knecht, F. Rittig, R.F.M. Lange, H. Pasch, J. Chromatogr. A 1130 (2006) 43.
[91] A. van der Horst, P.J. Schoenmakers, J. Chromatogr. A 1000 (2003) 693.
[92] M. Kivilompolo, T. Hyotylainen, J. Chromatogr. A 1145 (2007) 155.
[93] E. Blahová, P. Jandera, F. Cacciola, L. Mondello, J. Sep. Sci. 29 (2006) 555.
[94] F. Cacciola, P. Jandera, E. Blahová, L. Mondello, J. Sep. Sci. 29 (2006) 2500.
[95] F. Cacciola, P. Jandera, Z. Hajdu, P. Cesla, L. Mondello, J. Chromatogr. A 1149 (2007) 73.
[96] T. Hájek, V. Skeríková, P. Cesla, K. Vynuchalová, P. Jandera, J. Sep. Sci. 31 (2008) 3309.
[97] F. Cacciola, P. Jandera, L. Mondello, J. Sep. Sci. 30 (2007) 462.
[98] P. Dugo, F. Cacciola, M. Herrero, P. Donato, L. Mondello, J. Sep. Sci. 31 (2008) 3297.
[99] M.J. Gray, G.R. Dennis, P.J. Slonecker, R.A. Shalliker, J. Chromatogr. A 1041 (2004) 101.
[100] I. Francois, A.S. Pereira, F. Lynen, P. Sandra, J. Sep. Sci. 31 (2008) 3473.
[101] I. François, P. Sandra, J. Chromatogr. A 1216 (2009) 4005.

Chapter 3

Proanthocyanidins

3.1. Occurrence, basic chemistry and importance

Phenolic compounds are ubiquitous in nature and constitute by far the largest and most widely distributed group of compounds throughout the plant kingdom [1,2]. Polyphenols are secondary metabolites synthesised in plants during the normal development processes and are present in considerable amounts in different parts of plants [1,3].

Phenolic compounds comprise simple phenols, phenolic acids, coumarins, flavonoids, stilbenes, lignins and lignans. The phenolic acids are subdivided into benzoic acid derivatives, which are based on a C_6-C_1 skeleton, and cinnamic acid derivatives, which are based on a C_6-C_3 skeleton [4]. The coumarins are phenolic acids derivatives composed of a benzene ring fused with an oxygen heterocycle [4]. Lignins are polymers of C_6-C_3 units [5], while lignans are composed of two phenylpropane units [6]. Flavonoids are subdivided into different classes, whose structures are all based on a C_6-C_3-C_6 skeleton and only differ at the central heterocyclic ring (**Figure 3.1**) [4]. These include flavonols, flavones, flavanones, anthocyanidins, and flavanols (catechins and tannins). Tannins are grouped into hydrolysable and non-hydrolysable or condensed tannins (proanthocyanidins). Hydrolysable tannins are esters of phenolic acids and sugars or their derivatives, which yield a sugar and a phenolic acid moiety upon hydrolysis [4]. The sugar is usually glucose or a polysaccharide while the phenolic acid is either gallic acid in the case of gallotannins or ellagic acid in the case of ellagitannins [4,7,8]. Proanthocyanidins are polymers of flavan-3-ol monomeric units which form coloured anthocyanidins upon heating in an acidic medium [2,4,7,9-11]. Because of their wide distribution in nature, proanthocyanidins constitute the second largest class of natural phenolic compounds after lignin, and form an integral part of the human diet [7,12-14].

Various classes of proanthocyanidins are found in nature, with monomeric units differing by the hydroxylation pattern and stereochemistry of the asymmetric carbons of the heterocyle (**Figure 3.2a**) [10,15]. Procyanidins and prodelphinidins are the most common classes, while propelargonidins are less common [10,15]. Procyanidins form the largest class of proanthocyanidins and are made up of catechin and epicatechin monomeric units. Prodelphinidins consist of gallocatechin and

epigallocatechin monomeric units, while propelargonidins consist of afzelechin and epiafzelechin units. In addition, (epi)catechin and (epi)gallocatechin could be esterified by gallic acid to form (epi)catechin/(epi)gallocatechin gallate monomeric units. The monomeric units are usually linked through C4 → C6 or C4 → C8 bonds (B type), or, less commonly, an additional ether linkage could result from oxidative coupling of C2 → O7 or C2 → O5 to give A type oligomers (**Figure 3.2**) [2,10,13,14,16-21]. Oligomers consisting of mixed procyanidin, prodelphinidin and/or propelargonidin constituent units are also found in nature [14]. The size of proanthocyanidins is expressed as the degree of polymerisation (DP) [13,14,22].

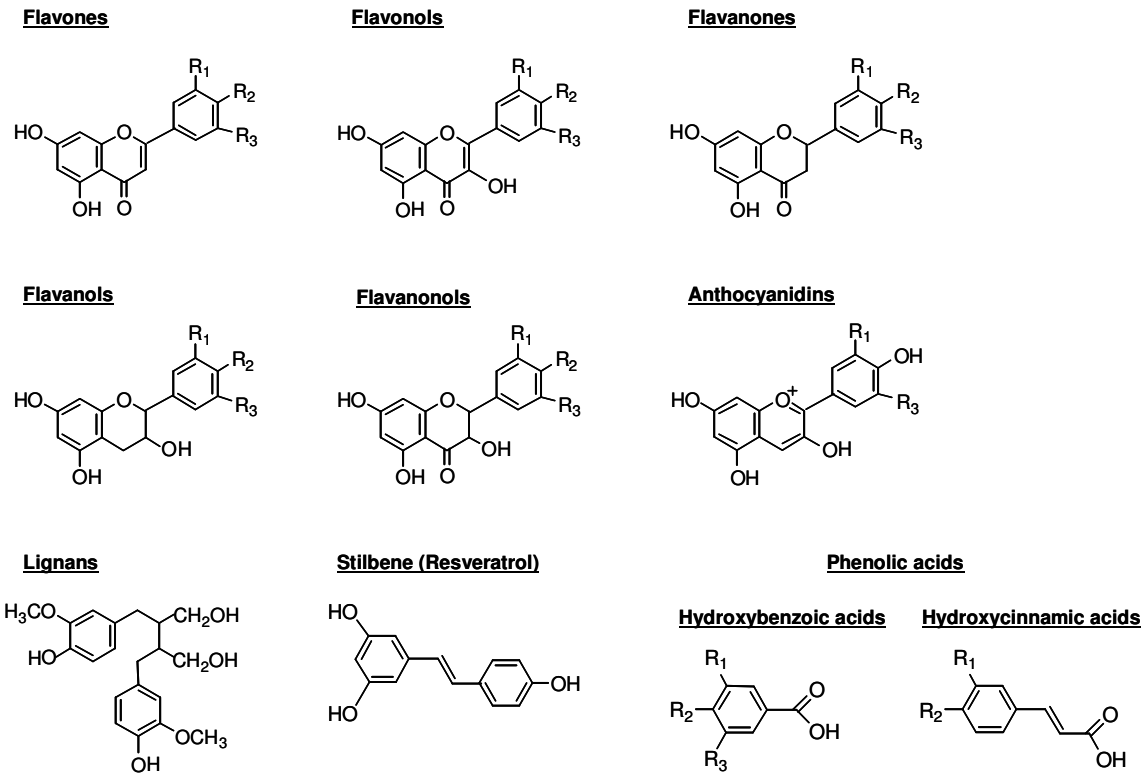

Figure 3.1: Structures of various classes of phenolic compounds.

(a)

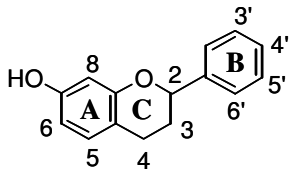

Proanthocyanidin type	3	5	8	3'	4'	5'
Procassinidin	H	H	H	H	OH	H
Probutinidin	H	H	H	OH	OH	H
Proapigeninidin	H	OH	H	H	OH	H
Proluteolinidin	H	OH	H	OH	OH	H
Protricetinidin	H	OH	H	OH	OH	OH
Prodistenidin	OH	OH	H	H	H	H
Propelargonidin	OH	OH	H	H	OH	H
Procyanidin	OH	OH	H	OH	OH	H
Prodelphinidin	OH	OH	H	OH	OH	OH
Proguibourtinidin	OH	H	H	H	OH	H
Profisetinidin	OH	H	H	OH	OH	H
Prorobinetinidin	OH	H	H	OH	OH	OH
Proteracacinidin	OH	H	OH	H	OH	H
Promelacacinidin	OH	H	OH	OH	OH	H

(b)

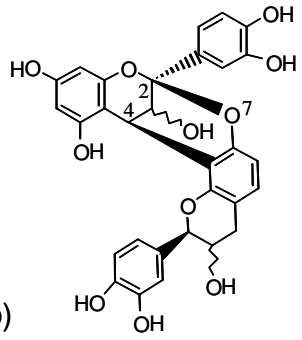

(c)

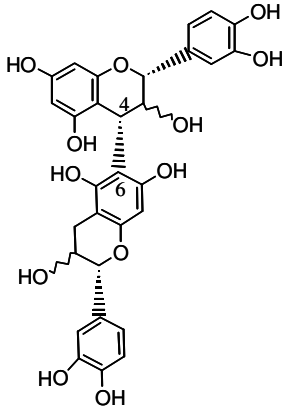

(d)

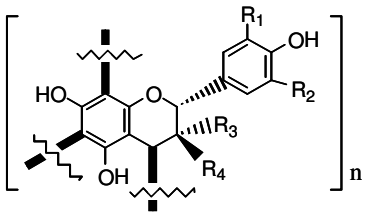

Figure 3.2: Structures of (a) proanthocyanidin monomeric units, (b) an A-type procyanidin dimer, (c) a C4 → C6 B-type procyanidin dimer and (d) a general polymerisation pattern for proanthocyanidins.

Flavan-3-ols are the most numerous phenolic compounds and represent about 25-50% of red wine [23], 50-70% of grape seed [24] and about 95% of cacao bean [1,25] total phenolic constituents. Tea catechins constitute about 30-35% of fresh tea leaves, 10-15% of unprocessed (green) tea and 8-21% of fermented (black) tea [26,27].

Extensive research in the fields of health, nutrition and medicine indicate that polyphenols exhibit a wide range of physiological effects including anti-oxidant, anti-microbial, anti-allergy, anti-inflammatory, anti-carcinogenic and anti-hypertensive activities [12,14,16-20,28-34]. For example, red wine procyanidins were found to inhibit atherosclerosis through suppression of endothelin-1, a peptide with a vasoconstricting effect [23]. A cacao pentameric procyanidin was found to selectively inhibit growth of human breast cancer cells [35]. Green tea catechins were found to show, amongst others, antioxidant, anti-hypertensive, anti-depressant and anti-inflammatory activities [9,26], while grape seed procyanidins were found to exhibit

antioxidant activity *in vivo* [24]. Proanthocyanidins are also thought to be involved in defence against ultraviolet radiation or aggression by pathogens [6,7]. Moreover, proanthocyanidins play various roles in determining quality of plant foods such as colour and chemical stability, astringency, bitterness, etc [13,36]. They are known to precipitate proteins in saliva, which is responsible for the astringent taste sensation upon consumption of tannin-rich food [1,7]. Astringency is most pronounced in unripe food and improves with ripeness [6]. Flavan-3-ols also play a part in the browning reactions in grapes and wine [34]. More importantly, these compounds react with anthocyanins to form complex pigments resulting in colour stability of red wines [34,36,37] and loss of astringency [34].

3.2. Extraction and purification of proanthocyanidins

Numerous extraction and purification methods for polyphenols have been developed. However, only methods pertaining to proanthocyanidins will be covered in depth, those of flavonols and phenolic acids will only be mentioned briefly in some instances, since these are the only classes of phenolic compounds that were dealt with in this study. Despite extensive research done on the analysis of phenolic compounds, complete characterisation of these compounds in food has not yet been fully established due to the difficulty of analysis presented by their diverse and complex structures. Improved analytical methods for purification of standards are required to allow detailed investigation of their physiological properties and accurate quantification of polyphenols in foods.

Most solvent systems used in the extraction of phenolic compounds are not specific for certain classes of compounds and in most cases, extraction is followed by sample clean-up to separate the various classes of compounds. For example, 60-70% methanol in water can be used to extract both phenolic acids and flavonoids [38-41]. Proanthocyanidins are mostly extracted from their sample matrices using aqueous acetone and/or methanol solutions or mixtures thereof. For example, 70% aqueous acetone has been employed in the extraction of cocoa [28,42,43], mangosteen pericarps [44] and pine bark [16] proanthocyanidins. 80% aqueous acetone was found better for cocoa liquor [43], while 60% acetone afforded apple [45] proanthocyanidins. On the other hand, 70% aqueous methanol has been successfully

used in the extraction of hawthorn [46] and cacao bean [47] proanthocyanidins. For grape seed proanthocyanidins, various solvent systems including 60% aqueous acetone [47], 50% aqueous methanol [48], 75% aqueous methanol [49] and 80% aqueous methanol followed by 75% aqueous acetone [50,51] have been used while 60% aqueous acetone [52] and 67% aqueous acetone [53] have been used for the extraction of grape skin proanthocyanidins. However, these solvent systems are only effective in the extraction of low oligomers, since high molecular weight (MW) compounds are insoluble in these extraction solvents [1,54].

Some modifiers such as acetic acid are added to the extracting solvents to suppress ionisation and improve the extractability of the compounds. For instance, Lazarus *et al* [18] and Gu *et al* [17,22] used acetone-water-acetic acid (70:29.5:0.5, %v/v/v) mixtures in the extraction of proanthocyanidins from various foods and beverages. Wollgast *et al* [31] used acetone-water-acetic acid (70:29.8:0.2, %v/v/v) in the extraction of chocolate procyanidins while Passos *et al* [55] used 5% acetic acid in methanol to extract grape seeds proanthocyanidins. However, care needs to be taken when acidified extraction solvents are used to avoid hydrolysis of the acid labile interflavanoid bonds present in proanthocyandins [2]. In addition, antioxidants such as sodium metabisulphite and ascorbic acid can also be added to the extraction solvents to enhance the stability of the compounds [56]. Escribano-Bailon *et al* [57] used 0.5 g/L ascorbic acid in methanol in the extraction of grape seed procyanidins while Peng & Jay-Allemand [56] used both ascorbic acid and sodium metabisulphite in their extraction solvents to prevent oxidation of compounds. This is also highly recommended when long term storage of the extract is desired in order to minimise oxidation [2]. On the contrary, quantification methods based on redox reactions, such as the Folin-Ciocalteu method, become unusable when antioxidative agents are added to the extract, therefore care should be taken in the selection of extraction solvents [2]. After extraction, the sample is usually concentrated by evaporating excess solvents under reduced pressure at ~ 40 °C to avoid sample degradation.

Standard purifications procedures such as solid-phase extraction (SPE), liquid-liquid extraction (LLE) and column chromatography (CC) are used to clean up extracts prior to analysis [34]. SPE is not only used in the purification of extracts but in

fractionation and enrichment of samples as well. Fractionation on an SPE cartridge is generally achieved through utilisation of different solvent systems of varying elution strengths in combination with pH adjustments such that certain classes of compounds are retained while others are eluted. For example, Sun *et al* [58] successfully fractionated red wine phenolics into various classes using C18 cartridges. The procedure involved dealcoholisation and neutralisation of the wine before loading it onto a pre-conditioned cartridge. Elution started with washing with distilled water (pH 7) to elute the phenolic acids, followed by a washing step with ethyl acetate to elute monomeric flavanols and oligomeric procyanidins, before washing with acidified methanol and acidified 75% aqueous acetone for elution of polymeric and higher polymeric proanthocyanidins, respectively. The various classes of compounds were then subjected to HPLC analysis for further separation. Lazarus *et al* [18] used a two-step SPE method to elute proanthocyanidins from various samples including grape seed extracts, green tea, peanut skins and nutmeat, apple, almond seedcoat, red wine and grape juice using acetone, water and acetic acid (70:29.5:0.5, %v/v/v) solvent systems.

Sephadex LH-20 chromatography has also been successfully employed in the fractionation of proanthocyanidins in various samples [47,57]. Prior *et al* [59] employed Sephadex-LH-20 to clean up and enrich procyanidin extracts from blueberries and cranberries using sequential elution starting with 20% aqueous methanol for removal of sugars and phenolic acids, followed by 60% aqueous methanol to remove flavonols and anthocyanins and then 100% methanol for elution of procyanidins prior to HPLC analysis. Sephadex LH-20 column chromatography used to be one of the preferred purification techniques for proanthocyanidins, because this technique provides residue-free solutions which are ideally suited for structural elucidation by degradation or analytical techniques such as nuclear magnetic resonance (NMR) or mass spectrometry (MS) [1]. However, this is more and more being replaced by SPE because of the simplicity, versatility and speed of this technique. Although these procedures are effective, they are very laborious and care should be taken to avoid loss and/or degradation of compounds.

3.3. Analysis of proanthocyanidins

Various separation techniques such as high performance liquid chromatography (HPLC), thin layer chromatography (TLC) and capillary electrophoresis (CE) have been employed in the qualitative and quantitative studies of proanthocyanidins [1]. Lea [60] developed a TLC method on silica plates to separate cider procyanidins according to molecular weight (MW), and oligomers up to heptamers were separated. This was later improved by Rigaud *et al* [47] using a normal phase liquid chromatography (NP-LC) column and mobile phases composed of dichloromethane, methanol, water and formic acid to achieve good separation of cacao beans and grape seeds procyanidins up to pentamers. Another NP-LC method developed by Yanagida *et al* [33] utilised hexane-acetone mobile phases and a silica column to achieve separation of apple procyanidins up to DP 5. However, poor separations were achieved with this method due to limited solubility of high MW compounds in the mobile phase. Therefore, Shoji *et al* [19] later improved this method by increasing the polarity of the mobile phase. They used hexane-methanol-ethyl acetate mobile phases instead and were able to achieve good separation up to octamers. Quiet recently, promising separation of procyanidins according to DP (up to tetradecamers) was achieved by hydrophilic interaction chromatography (HILIC) (though referred to as normal phase LC) on a diol stationary phase using acetonitrile-methanol-water-acetic acid mobile phases [13]. Furthermore, Yanagida *et al* [30] also developed a different HILIC method for the separation of apple oligomeric proanthocyanidins utilising a TSKgel amide-80 column and aqueous acetonitrile mobile phases to achieve separation according to MW up to decamers. Although improved separations according to DP have been achieved by these two modes of separation, complete separation is still not possible and these methods do not provide resolution of isomers.

Reversed phase (RP) LC is currently the most common method for the isomeric analysis of proanthocyanidins. Typically, C18 columns are used with aqueous acetonitrile or methanol and acid/buffer modifiers as mobile phases. Gradients are generally applied from a high water content to a low water content [2]. Compounds are eluted based on the substitution pattern, stereochemistry and polarity [61] and the order is not related to DP [2,31]. The popularity of this method is attributed to its ability to separate isomers, although only resolution of up to tetramers has been

achieved to date [2,19,62]. The resolution of higher oligomeric isomers has not been achieved due to the fact that the number of isomers increases with increasing DP, causing peak overlap and resulting in unresolved "bumps" in RP separations [2,18,28,31,63]. RP-LC has been employed in the separation and identification of isomeric proanthocyanidins from various samples. For instance, Escribano-Bailon *et al* [57] utilised a C18 column with aqueous acetonitrile-formic acid mobile phase in the separation of grape seed proanthocyanidins to achieve isomeric resolution up to tetramers. In similar studies, RP-LC has been used for isomeric separation and/or quantitation of proanthocyanidins in samples such as chocolate [31,43], pine bark [16], green tea [64-66], nectarines, peaches and plums [67], grape seeds [68], etc.

Capillary electrophoresis (CE) offers an effective alternative approach to HPLC. Various electromigration techniques have been successfully applied to the analysis of catechins in different foods. Horie *et al* [69] first employed capillary zone electrophoresis (CZE) to the analysis of catechins, caffeine and ascorbic acid in green tea infusions. Due to limited and imprecise detection of caffeine and ascorbic acid with this method, they later improved it by adding sodium dodecyl sulphate (SDS) to the buffer to facilitate separation by micellar electrokinetic chromatography (MEKC) under basic conditions [70]. However, catechins were found to be unstable in basic buffers, therefore MEKC with acidic buffers was applied to the analysis and quantification of catechins and caffeine in black and green tea extracts [71], cacao and chocolate [72,73] and resulted in better stability. Pomponio *et al* [74] also evaluated the effect of various alcohols on the selectivity of microemulsion electrokinetic chromatography (MEEKC) for the separation of green tea catechins using SDS and *n*-heptane under acidic conditions. Although both acidic, neutral and basic buffers were used in different CE methods, high efficiencies, stability and reproducibility for these compounds were only obtained under acidic conditions [71,74].

In addition to the analytical techniques mentioned above, colourimetric methods such as the Folin-Ciocalteau, dimethylaminocinnamaldehyde (DMACA), vanillin- acid and butanol-HCl assays are used for the quantification of polyphenols. The Folin-Ciocalteu assay is used for the determination of the total polyphenol content, therefore it is not specific for any class of polyphenols [75]. Aldehydes are known to become highly electrophilic and thus very reactive towards unsaturated compounds (such as

flavanols) when in solution containing strong mineral acids [76]. In the DMACA assay, proanthocyanidins are reacted with DMACA in the presence of a mineral acid to yield coloured DMACA-flavanol adducts with maximum absorbance between 632-640 nm depending on the solvent used [76]. However, this has only been observed with DMACA, other aldehydes resulted in adducts that absorbs maximally at lower wavelengths [76].

In the vanillin-acid assay, vanillin reacts with the meta-substituted ring of the proanthocyanidins in the presence of an acid catalyst to produce red adducts which absorb maximally around 500 nm [77]. The vanillin reaction is highly sensitive to water, the colour yield is readily quenched in the presence of very small amounts of water [77]. Other factors such as the solvent type, temperature, vanillin concentration, nature and concentration of the acid as well as the type of standards are also known to influence the reaction [78]. In this reaction, sulphuric acid has been found to be a better catalyst than hydrochloric acid at similar concentrations [78].

The butanol-HCl assay involves acid-catalysed oxidative cleavage of proanthocyanidins to give coloured anthocyanidins which exhibit maximum absorbance around 550 nm [77,79]. This assay is greatly affected by the presence of trace impurities of transition metal ions in the reaction mixture and consistent yields have only been obtained when iron salts were added [79]. In addition, this assay is highly dependent on other factors including the amount of water present in the reaction mixture and the acid-butanol ratio [77,79]. The DMACA assay is preferred over the vanillin assay because this method is simple, sensitive and suffers less from interferences with anthocyanins [2]. The vanillin-acid assay is used exclusively for flavanols while the butanol-HCl and DMACA assays are specific for proanthocyanidins [1,28,62]. However, these assays only give an estimation of the total flavanol content and not of individual oligomers [28]. Although these methods are still widely used in the determination of phenolic contents of various samples, they are highly dependent on many factors and therefore need to be used with extreme care [78].

Other techniques such as partial acid hydrolysis, thiolysis and enzymatic hydrolysis are used to determine the constituent units of proanthocyanidin oligomers

[17,47,57,80,81]. The butanol-acid assay is the most commonly used acid hydrolysis technique for the determination of proanthocyanidins constituent units [78]. In thiolysis, proanthocyanidins are heated in the presence of an acid and benzyl mercaptan to yield a free terminal unit and a benzylthioether derivative of the extension unit [82]. Enzymatic degradation is performed by incubating proanthocyanidins with the tannase enzyme in a buffer solution [47]. Rigaud *et al* [47,82] confirmed the composition of unknown grape seed proanthocyanidin dimers, trimers and tetramers using microthiolysis and/or enzymatic degradation followed by HPLC analysis of the formed products.

Another method similar to thiolysis is phloroglucinol degradation, which involves acid hydrolysis of proanthocyanidins in the presence of a nucleophilic reagent (phloroglucinol) to produce a free terminal unit and a phloroglucinol adduct of the extension unit [2,61]. Koupai-Abyazani *et al* [61] developed this method and employed it in the structural elucidation of sainfoin proanthocyanidins using RP-HPLC with UV detection. Although A type proanthocyanidins were found to be resistant to thiolytic degradation [80,83], Le Roux *et al* [84] successfully characterised A type procyanidins in litchi pericaps using thioacidolysis, NMR and ESI-MS following NP-LC fractionation. A comparison of the two thiolytic reagents by Mathews *et al* [80] indicated that higher yields are obtained with benzyl mercaptan than with phloroglucinol and for this reason, they recommended benzyl mercaptan for depolymerisation reactions, despite its toxicity and unpleasant smell.

For positive identification of compounds, spectroscopic techniques such as NMR, MS and fourier transform infrared (FT-IR) are employed. More information is gained when these techniques are hyphenated with chromatographic separation. MS facilitates identification of compounds when coupled to HPLC by providing the mass spectral information. However, MS cannot distinguish between isomers with the same mass-to-charge (*m/z*) ratio. IR and particularly NMR are useful for isomeric structural elucidation.

The robustness of NMR in structural elucidation lies in its ability to provide chemical environment information of each proton and carbon nucleus in a molecule as well as the linkages between nearby nuclei [1,85]. This provides useful information from

which compounds skeletons and substitution patterns can be deduced [85]. This requires that samples be highly purified and be prepared in good yields for good sensitivity and neatly resolved spectra. Fractionation of extracts using polyamide and/or Sephadex LH-20 column chromatography are some of the techniques used in the preparative isolation of proanthocyanidins prior to NMR. Hatano *et al* [42] subjected a cacao liquor extract to Sephadex LH-20, MCI-gel CHP 20P, Diaion HP-20 and/or Toyopearl HW-40 chromatography for preparative purification of monomeric, dimeric and trimeric procyanidin glycosides.

However, structural determination of proanthocyanidins by NMR is complicated by conformational isomerism which may occur in solution [86]. This results from steric interactions in the vicinity of the interflavanoid bonds, allowing free rotation of the flavanoid units that often leads to broadening or duplication of resonances in the ^{1}H or ^{13}C NMR spectra of these compounds [2,86]. Conformational isomerism has only been found to prevail at low temperatures, spectra acquired at elevated temperatures resulted in first order spectra [87]. Another way of overcoming or limiting the free rotation barriers is through derivatisation of the hydroxyl groups into permethyl ether 3-O-acetates groups, which are more stable at high temperatures [88]. On the contrary, Shoji *et al* [89] obtained first order ^{1}H NMR spectra at low temperatures (-20 °C or -40 °C) for apple procyanidins without acetylation.

NMR has been employed in various studies for structural determination of proanthocyanidins. For example, Davis *et al* [90] used 2-D proton-carbon correlation and 1-D nuclear overhauser effect (NOE) difference experiments in the assignment of tea proanthocyanidins using acetone-d_6. Although various solvents have been employed in different NMR studies, deuterated methanol has been found to serve as the best solvent for both ^{1}H and ^{13}C NMR experiments [86]. Other solvents such as acetone-d_6, acetone-d_6/H_2O, acetone-d_6/D_2O and DMSO-d_6 are presented with a series of drawbacks such as proton exchange, limited solubility or difficulty of recovery of sample [86].

Due to commercial unavailability of oligomeric proanthocyanidin standards, some quantitative studies for proanthocyanidins employ catechin monomers as standards to estimate higher oligomers as catechin equivalents [10,18]. Since monomers and

oligomers have different extinction coefficients, this method cannot be used for accurate determination of oligomers [10,18]. For this reason, researchers have developed methods for purification of oligomers for much more accurate quantification. These procedures are very time consuming, stressing the need for a reliable analytical method which can be applied on a commercial scale.

3.4. Detection

Because of the high efficiency and robustness of the technique, HPLC is one of the commonly used techniques for proanthocyanidin analysis. Fluorescence and UV detection are the most widely used modes of detection for proanthocyanidins. The photodiode array (PDA) detector is preferred over variable-wavelength or UV-Vis detectors due to its ability to detect different compounds at multiple wavelengths. UV absorbance spectra can be very useful in the identification of compounds. For example, flavan-3-ols show an absorption band in the UV region between 270-280 nm, flavones and flavonols show two bands between 310-370 nm and 250-295 nm [10], while phenolic acids show two bands between 225-235 nm and 290-330 nm [4]. Since most phenolic compounds absorb UV at around 280 nm, UV detection cannot be used for selective detection of proanthocyanidins [10,18,75]. In order to overcome this limitation, Treutter [76] developed a method that allowed selective detection of catechins and proanthocyanidins around 640 nm following their post-column derivatisation with DMACA. Cho *et al* [91] also measured the fluorescence quantum yield of epicatechin polymers with 4β→8 interflavan bonds and found the optimum excitation and emission wavelengths to be around 280 nm and 320 nm, respectively. Since proanthocyanidins are the only phenolic compounds which exhibit fluorescence properties [37,62], fluorescence detection is preferred because of selectivity and higher sensitivity compared to UV detection [1,2,13,18,28,37]. Coupling fluorescence with UV detection facilitates identification of phenolic compounds since fluorescence reduces interference from other compounds.

Reversed phase LC coupled with fluorescence and/or MS detection is currently the most powerful method for the isomeric analysis of proanthocyanidins. Ionisation techniques such as atmospheric pressure chemical ionisation (AP-CI) and electrospray ionisation (ESI) are used for hydrophilic, ionic and polar organic compounds [92,93].

Because of its high ionisation efficiency, ESI is the most common ionisation technique used for the study of proanthocyanidins. ESI is effective in both positive and negative modes depending on the analysis conditions. Addition of salts has also been found to enhance ionisation in some cases, especially when non-aqueous solvents are used. Hammerstone *et al* [29] first developed an on-line NP-LC-ESI-MS method which allowed simultaneous separation and identification of singly linked oligomeric procyanidins up to decamers in cocoa and chocolate extracts. This method was later applied by Lazarus *et al* [18] in the detection of proanthocyanidins from various foods and beverages. They were able to identify singly and/or doubly linked proanthocyanidin oligomers up to dodecamers in apple, heptamers in grape seeds and almonds, nonamers in cinnamon and octamers in peanuts. Gu *et al* [94] employed both NP-LC-MS/MS and thiolytic degradation in the screening of various foods and beverages for the presence of proanthocyanidins. A combination of RP-LC with ESI-MS has also been effectively employed in the characterisation of chocolate [31], pine bark [16] and wine [49,95] procyanidins.

Other MS techniques such as matrix-assisted laser desorption ionisation time-of-flight MS (MALDI TOF/MS) [19,32,33,48,96] and fast-atom bombardment MS (FAB-MS) [96] have also been utilised in the characterisation of proanthocyanidins. Ohnishi-Kameyama *et al* [96] confirmed presence of up to pentadecameric procyanidin oligomers in an apple extract by MALDI-TOF/MS using *trans*-3-indoleacrylic acid as the matrix with addition of a silver salt to aid ionisation. They were also able to detect up to undecameric procyanidin oligomers using FAB-MS in both positive and negative modes. Shoji *et al* [19] and Yang *et al* [48] applied both NP-LC-ESI-MS and MALDI-TOF/MS in the characterisation of apple and grape seed procyanidins, respectively. Recently, Es-Safi *et al* [97] characterised proanthocyanidin oligomers from pear juice with DP up to 25 using ESI/MS, MALDI/TOF/MS and NMR.

Electrochemical detection (ECD) is another detection system used for compounds which exhibit oxidation-reduction potentials such as flavonoids. Hayes *et al* [98,99] and Subagio *et al* [100] applied ECD in the quantitative determination of catechin and epicatechin in beer and cacao. In both instances, ECD offered enhanced sensitivity and selectivity over UV detection. In addition, ECD has the ability to reduce matrix

effects and it is unaffected by changes in mobile phase gradients, which facilitates quantification and identification of analytes [1,98-100].

3.5. 2-Dimensional LC (2-D-LC) analysis of proanthocyanidins

NP-LC and RP-LC are the methods of choice for the analysis of proanthocyanidins. However, 1-dimensional LC methods do not provide sufficient resolving power for complete separation of complex samples. Comprehensive 2-D LC techniques theoretically offer an enhanced resolving power necessary for improved separation of complex samples, but only by combining orthogonal separation mechanisms [101-109].

Blahova *et al* [110] assessed the combinations of octadecyl (C18), pentafluorophenylpropyl (F5) and polyethyleneglycol (PEG) silica-based columns in the separation of natural phenolic antioxidant standards. The selectivity of a C18 column was found to be strongly correlated to that of the F5 column ($r^2 = 0.999$) as compared to that of the C18 with the PEG ($r^2 = 0.657$). Serial coupling of the C18 and PEG columns provided better separation of compounds that were not well separated on single columns. Cacciola *et al* [111-113] and Hajek *et al* [114] applied 2-D LC methods to the analysis of natural phenolic acids and/or flavone antioxidants in beer and wine samples, or to selected polyphenolic standards. These authors used combinations of serially coupled and/or single PEG-silica, phenyl silica and C18 columns in the first dimension and a single or two parallel monolithic Chromolith C18 or zirconia carbon columns in the second dimension. Although single PEG and C18 columns exhibited low correlation with the zirconia column ($r^2 < 0.1$), relative to the serially coupled PEG and C18 with the zirconia column ($r^2 > 0.3$), better resolution of compounds was achieved when serially coupled PEG and C18 columns were used in the first dimension with the zirconia column in the second dimension. Also, the use of two parallel zirconia columns in the second dimension allowed sufficient separation times in the second dimension resulting in enhanced peak capacities.

Kivilompolo *et al* [115,116] employed on-line RP-LC × RP-LC using ion pair chromatography in the second dimension for comprehensive 2-D LC analysis of phenolic acids and monomeric procyanidins in wines and juices. These authors

obtained very low correlation between these retention mechanisms and peak capacities in excess of 300 were reported. Although high peak capacity values were obtained, these values were calculated as a product of the peak capacities in each dimension. This method overestimates the 2-D peak capacity, as it does not account for parameters such as under-sampling of the first dimension peaks and orthogonality, factors upon which the peak capacity of a 2-D separation is highly dependent.

Dugo *et al* [117] also employed a microbore phenyl column and a Chromolith/ Ascentis Express C18 column for comprehensive 2-D LC analysis of polyphenolic standards and red wine. Although good baseline separation of compounds was obtained in this work, only a small portion of the separation space was used due to high correlation ($r^2 > 0.8$) between the retention mechanisms exhibited by the two columns. As a consequence, low practical peak capacities (relative to those theoretically achievable) were obtained for this 2-D system. Nevertheless, such peak capacities are not achievable with conventional 1-D methods.

None of these methods was designed exclusively for the analysis of proanthocyanidins and most of the reported compounds are phenolics that can be separated by 1-D LC. However, this suggests that 2-D LC separations are promising tools for improved separations of complex samples such as proanthocyanidin fractions, especially if highly orthogonal systems are selected. Moreover, this could provide a breakthrough into the sought after reliable analytical methods necessary for the analysis of such compounds to enable their complete characterisation.

3.6. References

[1] J. Wollgast, E. Anklam, Food Res. Int. 33 (2000) 423.
[2] W. Hümmer, P. Schreier, Mol. Nutr. Food Res. 52 (2008) 1381.
[3] M. Naczk, F. Shahidi, J. Chromatogr. A 1054 (2004) 95.
[4] P. Ribereau-Gayon, Plant Phenolics, Hafner Publishing Company, Inc., New York, 1972.
[5] H.A. Stafford, Phytochemistry 27 (1988) 1.
[6] C. Manach, A. Scalbert, C. Morand, C. Remesy, L. Jimenez, Am. J. Clin. Nutr. 79 (2004) 727.
[7] C. Santos-Buelga, A. Scalbert, J. Sci. Food Agric. 80 (2000) 1094.
[8] M.N. Clifford, A. Scalbert, J. Sci. Food Agric. 80 (2000) 1118.
[9] W.-S. Jeong, A.-N. Kong, Pharm. Biol. 42 (2004) 84.
[10] C. Santos-Buelga, C. Garcia-viguera, F.A. Tomas-Barberan, in C. Santos-Buelga, G. Williamson (Editors), Methods in polyphenol analysis, The Royal Society of Chemistry, Cambridge, 2003, p. 102.
[11] V. Cheynier, H. Fulcrand, in C. Santos-Buelga, G. Williamson (Editors), Methods in polyphenol analysis, The Royal Society of Chemistry, Cambridge, 2003, p. 284.
[12] H.J. Li, M.L. Deinzer, Anal. Chem. 79 (2007) 1739.
[13] M.A. Kelm, J.C. Johnson, R.J. Robbins, J.F. Hammerstone, H.H. Schmitz, J. Agric. Food Chem. 54 (2006) 1571.
[14] L. Gu, M.A. Kelm, J.F. Hammerstone, Z. Zhang, G. Beecher, J. Holden, D. Haytowitz, R.L. Prior, J. Mass Spectrom. 38 (2003) 1272.
[15] P.M. Aron, J.A. Kennedy, Mol. Nutr. Food Res. 52 (2008) 79.
[16] M. Karonen, J. Loponen, V. Ossipov, K. Pihlaja, Anal. Chim. Acta 522 (2004) 105.
[17] L. Gu, M. Kelm, J.F. Hammerstone, G. Beecher, D. Cunningham, S. Vannozzi, R.L. Prior, J. Agric. Food Chem. 50 (2002) 4852.
[18] S.A. Lazarus, G.E. Adamson, J.F. Hammerstone, H.H. Schmitz, J. Agric. Food Chem. 47 (1999) 3693.
[19] T. Shoji, S. Masumoto, N. Moriichi, T. Kanda, Y. Ohtake, J. Chromatogr. A 1102 (2006) 206.
[20] Y.J. Hong, F.A. Tomas-Barberan, A.A. Kader, A.E. Mitchell, J. Agric. Food Chem. 54 (2006) 2405.
[21] L.J. Porter, Z. Ma, B.G. Chan, Phytochemistry 30 (1991) 1657.
[22] L. Gu, S.E. House, X. Wu, B. Ou, R.L. Prior, J. Agric. Food Chem. 54 (2006) 4057.
[23] R. Corder, W. Mullen, N.Q. Khan, S.C. Marks, E.G. Wood, M.J. Carrier, A. Crozier, Nature 444 (2006) 566.
[24] M. García-Marino, J.C. Rivas-Gonzalo, E. Ibáñez, C. García-Moreno, Anal. Chim. Acta 563 (2006) 44.
[25] K.A. Cooper, E. Campos-Gimenez, D. Jimenez-Alvarez, K. Nagy, J.L. Donovan, G. Williamson, J. Agric. Food Chem. 55 (2007) 2841.
[26] T.L. Lunder, in Mou-Tang Huang, Chi-Tang Ho, C.Y. Lee (Editors), Phenolic compounds in Food and their effects on health II, American Chemical Society, New York, 1992, p. 114.

[27] D.A. Balentine, in Chi-Tang Ho, Chang. Y. Lee, M.-T. Huang (Editors), Phenolic compounds in food and their effects on health I, American Chemical Society, Washington, DC, 1992, p. 102.
[28] G.E. Adamson, S.A. Lazarus, A.E. Mitchell, R.L. Prior, G. Cao, P.H. Jacobs, B.G. Kremers, J.F. Hammerstone, R.B. Rucker, K.A. Ritter, H.H. Schmitz, J. Agric. Food Chem. 47 (1999) 4184.
[29] J.F. Hammerstone, S.A. Lazarus, A.E. Mitchell, R. Rucker, H.H. Schmitz, J. Agric. Food Chem. 47 (1999) 490.
[30] A. Yanagida, H. Murao, M. Ohnishi-Kameyama, Y. Yamakawa, A. Shoji, M. Tagashira, T. Kanda, H. Shindo, Y. Shibusawa, J. Chromatogr. A 1143 (2007) 153.
[31] J. Wollgast, L. Pallaroni, M.-E. Agazzi, E. Anklam, J. Chromatogr. A 926 (2001) 211.
[32] A. Yanagida, T. Kanda, T. Shoji, M. Ohnishi-Kameyama, T. Nagata, J. Chromatogr. A 855 (1999) 181.
[33] A. Yanagida, T. Kanda, T. Takahashi, A. Kamimura, T. Hamazono, S. Honda, J. Chromatogr. A 890 (2000) 251.
[34] S. Pati, I. Losito, G. Gambacorta, E. La Notte, F. Palmisano, P.G. Zambonin, J. Mass Spectrom. 41 (2006) 861.
[35] D. Ramljak, L.J. Romanczyk, L.J. Metheny-Barlow, N. Thompson, V. Knezevic, M. Galperin, A. Ramesh, R.B. Dickson, Mol. Cancer Ther. 4 (2005) 537.
[36] M. Dell'Agli, A. Busciala, E. Bosisio, Cardiovasc. Res. 63 (2004) 593.
[37] S. Gómez-Alonso, E. García-Romero, I. Hermosín-Gutiérrez, J. Food Comp. Anal. 20 (2007) 618.
[38] M. Ganzera, C. Egger, C. Zidorn, H. Stuppner, Anal. Chim. Acta 614 (2008) 196.
[39] R. Tsao, R. Yang, J.C. Young, H. Zhu, J. Agric. Food Chem. 51 (2003) 6347.
[40] R. Tsao, R. Yang, J. Chromatogr. A 1018 (2003) 29.
[41] L.-Z. Lin, J.M. Harnly, J. Agric. Food Chem. (2008).
[42] T. Hatano, H. Miyatake, M. Natsume, N. Osakabe, T. Takizawa, H. Ito, T. Yoshida, Phytochemistry 59 (2002) 749.
[43] M. Natsume, N. Osakabe, M. Yamagishi, T. Takizawa, T. Nakamura, H. Miyatake, T. Hatano, T. Yoshida, Biosci. Biotechnol. Biochem. 64 (2000) 2581.
[44] C. Fu, A.E.K. Loo, F.P.P. Chia, D. Huang, J. Agric. Food Chem. 55 (2007) 7689.
[45] L. Michodjehoun-Mestres, J.-M. Souquet, H. Fulcrand, E. Meudec, M. Reynes, J.-M. Brillouet, Food Chem. 114 (2009) 989.
[46] U. Svedstrom, H. Vuorela, R. Kostiainen, K. Huovinen, I. Laakso, R. Hiltunen, J. Chromatogr. A 968 (2002) 53.
[47] J. Rigaud, M.T. Escribano-Bailon, C. Prieur, J.M. Souquet, V. Cheynier, J. Chromatogr. A 654 (1993) 255.
[48] Y. Yang, M. Chien, J. Agric. Food Chem. 48 (2000) 3990.
[49] S. Gonzalez-Manzano, C. Santos-Buelga, J.J. Perez-Alonso, J.C. Rivas-Gonzalo, M.T. Escribano-Bailon, J. Agric. Food Chem. 54 (2006) 4326.
[50] I. Spranger, B. Sun, A.M. Mateus, V.t. de Freitas, J.M. Ricardo-da-Silva, Food Chem. 108 (2008) 519.
[51] B. Sun, G.P. Belchior, J.M. Ricardo-da-Silva, M.I. Spranger, J. Chromatogr. A 841 (1999) 115.

[52] J.-M. Souquet, V. Cheynier, F. Brossaud, M. Moutounet, Phytochemistry 43 (1996) 509.
[53] J.A. Kennedy, Y. Hayasaka, S. Vidal, E.J. Waters, G.P. Jones, J. Agric. Food Chem. 49 (2001) 5348.
[54] E.C. Bate-Smith, Phytochemistry 14 (1975) 1107.
[55] C.P. Passos, S.M. Cardoso, M.R.M. Domingues, P. Domingues, C.M. Silva, M.A. Coimbra, Food Chem. 105 (2007) 1457.
[56] S. Peng, C. Jay-Allemand, J. Chem. Ecol. 17 (1991) 887.
[57] T. Escribano-Bailon, Y. Gutierrez-Fernandez, J.C. Rivas-Gonzalo, C. Santos-Buelga, J. Agric. Food Chem. 40 (1992) 1794.
[58] B. Sun, M.C. Leandro, V. de Freitas, M.I. Spranger, J. Chromatogr. A 1128 (2006) 27.
[59] R.L. Prior, S.A. Lazarus, G. Cao, H. Muccitelli, J.F. Hammerstone, J. Agric. Food Chem. 49 (2001) 1270.
[60] A.G.H. Lea, J. Sci. Food Agric. 29 (1978) 471.
[61] M.R. Koupai-Abyazani, J. McCallum, B.A. Bohm, J. Chromatogr. A 594 (1992) 117.
[62] R.L. Prior, L. Gu, Phytochemistry 66 (2005) 2264.
[63] A.W. Taylor, E. Barofsky, J.A. Kennedy, M.L. Deinzer, J. Agric. Food Chem. 51 (2003) 4101.
[64] A. Kiehne, C. Lakenbrink, U.H. Engelhardt, Z Lebensm Unters Forsch A 205 (1997) 153.
[65] D. Del Rio, A.J. Stewart, W. Mullen, J. Burns, M.E.J. Lean, F. Brighenti, A. Crozier, J. Agric. Food Chem. 52 (2004) 2807.
[66] M. Friedman, C.E. Levin, S.-H. Choi, E. Kozukue, N. Kozukue, J. Food Sci. 71 (2006) C328.
[67] F.A. Tomas-Barberan, M.I. Gil, P. Cremin, A.L. Waterhouse, B. Hess-Pierce, A.A. Kader, J. Agric. Food Chem. 49 (2001) 4748.
[68] Z. Peng, Y. Hayasaka, P.G. Iland, M. Sefton, P. Hoj, E.J. Waters, J. Agric. Food Chem. 49 (2001) 26.
[69] H. Horie, T. Mukai, K. Kohata, J. Chromatogr. A 758 (1997) 332.
[70] H. Horie, K. Kohata, J. Chromatogr. A 802 (1998) 219.
[71] C.C.T. Wörth, M. Wießler, O.J. Schmitz, Electrophoresis 21 (2000) 3634.
[72] R. Gotti, S. Furlanetto, S. Pinzauti, V. Cavrini, J. Chromatogr. A 1112 (2006) 345.
[73] R. Gotti, J. Fiori, F. Mancini, V. Cavrini, Electrophoresis 25 (2004) 3282.
[74] R. Pomponio, R. Gotti, B. Luppi, V. Cavrini, Electrophoresis 24 (2003) 1658.
[75] V.L. Singleton, R. Orthofer, R.M. Lamuela-Raventós, P. Lester, in Methods in Enzymology, Academic Press, 1999, p. 152.
[76] D. Treutter, J. Chromatogr. A 467 (1989) 185.
[77] A.E. Hagerman, L.G. Butler, P. Lester, in Methods in Enzymology, Academic Press, 1994, p. 429.
[78] P. Schofield, D.M. Mbugua, A.N. Pell, Anim. Feed Sci. Technol. 91 (2001) 21.
[79] L.J. Porter, L.N. Hrstich, B.G. Chan, Phytochemistry 25 (1985) 223.
[80] S. Matthews, I. Mila, A. Scalbert, B. Pollet, C. Lapierre, C.L.M. HerveduPenhoat, C. Rolando, D.M.X. Donnelly, J. Agric. Food Chem. 45 (1997) 1195.
[81] S. Guyot, N. Marnet, J.F. Drilleau, J. Agric. Food Chem. 49 (2001) 14.

[82] J. Rigaud, J. Perez-Ilzarbe, J.M.R. Da Silva, V. Cheynier, J. Chromatogr. A 540 (1991) 401.
[83] J.J. Karchesy, R.W. Hemingway, J. Agric. Food Chem. 34 (1986) 966.
[84] E. Le Roux, T. Doco, P. Sarni-Manchado, Y. Lozano, V. Cheynier, Phytochemistry 48 (1998) 1251.
[85] J.-L. Wolfender, K. Ndjoko, K. Hostettmann, in C. Santos-Buelga, G. Williamson (Editors), Methods in polyphenol research, The Royal Society of Chemistry, Cambridge, 2003, p. 128.
[86] L.J. Porter, in J.B. Harborne (Editor), The Flavanoids: advances in research since 1986., Chapman & Hall, London, 1994, p. 23.
[87] A.C. Fletcher, L.J. Porter, E. Haslam, R.K. Gupta, J. Chem. Soc., Perkin Trans. 1 (1977) 1628
[88] P.J. Steynberg, J.P. Steynberg, B.C.B. Bezuidenhoudt, D. Ferreira, J. Chem. Soc., Perkin Trans. 1 (1995) 3005
[89] T. Shoji, M. Mutsuga, T. Nakamura, T. Kanda, H. Akiyama, Y. Goda, J. Agric. Food Chem. 51 (2003) 3806.
[90] A.L. Davis, Y. Cai, A.P. Davies, J.R. Lewis, Magn. Reson. Chem. 34 (1996) 887.
[91] D. Cho, R. Tian, L.J. Porter, R.W. Hemingway, W.L. Mattice, J. Am. Chem. Soc. 112 (1990) 4273.
[92] R. Kostiainen, T.J. Kauppila, J. Chromatogr. A 1216 (2009) 685.
[93] H.P. Nguyen, K.A. Schug, J. Sep. Sci. 31 (2008) 1465.
[94] L. Gu, M.A. Kelm, J.F. Hammerstone, G. Beecher, J. Holden, D. Haytowitz, R.L. Prior, J. Agric. Food Chem. 51 (2003) 7513.
[95] H. Fulcrand, S. Remy, J.M. Souquet, V. Cheynier, M. Moutounet, J. Agric. Food Chem. 47 (1999) 1023.
[96] M. Ohnishi-Kameyama, A. Yanagida, T. Kanda, T. Nagata, Rapid Commun. Mass Spectrom. 11 (1997) 31.
[97] N.-E. Es-Safi, S. Guyot, P.-H. Ducrot, J. Agric. Food Chem. 54 (2006) 6969.
[98] P.J. Hayes, M.R. Smyth, I. McMurrough, Analyst 112 (1987) 1205.
[99] P.J. Hayes, M.R. Smyth, I. McMurrough, Analyst 112 (1987) 1197.
[100] A. Subagio, P. Sari, N. Morita, Phytochem. Anal. 12 (2001) 271.
[101] D.R. Stoll, X. Li, X. Wang, P.W. Carr, S.E.G. Porter, S.C. Rutan, J. Chromatogr. A 1168 (2007) 3.
[102] P. Dugo, F. Cacciola, T. Kumm, G. Dugo, L. Mondello, J. Chromatogr. A 1184 (2008) 353.
[103] P. Jandera, J. Fischer, H. Lahovská, K. Novotná, P. Cesla, L. Kolárová, J. Chromatogr. A 1119 (2006) 3.
[104] P.Q. Tranchida, P. Dugo, G. Dugo, L. Mondello, J. Chromatogr. A 1054 (2004) 3.
[105] P. Dugo, V. Skerikova, T. Kumm, A. Trozzi, P. Jandera, L. Mondello, Anal. Chem. 78 (2006) 7743.
[106] S.P. Dixon, I.D. Pitfield, D. Perrett, Biomed. Chromatogr. 20 (2006) 508.
[107] I. François, A. de Villiers, P. Sandra, J. Sep. Sci. 29 (2006) 492.
[108] P.E. Toups, M.J. Gray, G.R. Dennis, N. Reddy, M.A. Wilson, R.A. Shalliker, J. Sep. Sci. 29 (2006) 481.
[109] C.J. Venkatramani, A. Patel, J. Sep. Sci. 29 (2006) 510.
[110] E. Blahová, P. Jandera, F. Cacciola, L. Mondello, J. Sep. Sci. 29 (2006) 555.
[111] F. Cacciola, P. Jandera, E. Blahová, L. Mondello, J. Sep. Sci. 29 (2006) 2500.

[112] F. Cacciola, P. Jandera, Z. Hajdu, P. Cesla, L. Mondello, J. Chromatogr. A 1149 (2007) 73.
[113] F. Cacciola, P. Jandera, L. Mondello, J. Sep. Sci. 30 (2007) 462.
[114] T. Hájek, V. Skeríková, P. Cesla, K. Vynuchalová, P. Jandera, J. Sep. Sci. 31 (2008) 3309.
[115] M. Kivilompolo, T. Hyötyläinen, J. Sep. Sci. 31 (2008) 3466.
[116] M. Kivilompolo, V. Oburka, T. Hyotylainen, Anal. Bioanal. Chem. 391 (2008) 373.
[117] P. Dugo, F. Cacciola, M. Herrero, P. Donato, L. Mondello, J. Sep. Sci. 31 (2008) 3297.

Chapter 4

Off-line Comprehensive 2-Dimensional Hydrophilic Interaction × Reversed Phase Liquid Chromatography Analysis of Procyanidins*

*Published as K.M. Kalili, A. de Villiers, J. Chromatogr. A 1216 (2009) 6274.

4.1. Introduction

Proanthocyanidins are a group of polyphenolic compounds found widespread throughout the plant kingdom [1], and comprise oligomeric or polymeric phenols composed of flavan-3-ol monomeric units joined through interflavanoid linkages [2]. Monomeric units are most frequently linked through C4 → C6 or C4 → C8 bonds (B-type), or, less commonly, a second interflavanoid bond could result from oxidative coupling of C2 → O7 to form A-type oligomers (**Figure 4.1**) [3-9]. Proanthocyanidins are further subdivided into procyanidins, prodelphinidins and propelargonidins [5]. Procyanidins form the largest class of proanthocyanidins [3] and are made up exclusively of catechin and epicatechin flavan-3-ol units. Prodelphinidins contain gallocatechin and epigallocatechin units, while propelargonidins comprise afzelechin and epiafzelechin building blocks. In addition, monomeric units consisting of gallic acid esters of (epi)catechin and (epi)gallocatechin ((epi)catechin/(epi)gallocatechin gallate) are also found in nature.

Proanthocyanidins are the second most abundant natural phenolic compounds following lignin and form an essential part of the human diet [4,10], as they are present in common foods such as apples, berries, cocoa, grapes, wine, etc. These compounds have been studied extensively in recent years in the fields of health, nutrition and medicine [1,3,11]. This is due to the growing body of evidence suggesting that they exhibit a diversity of physiological effects such as anti-oxidant, anti-microbial, anti-allergy, anti-inflammatory, anti-carcinogenic and anti-hypertensive activities [1-3,5-8,10-16].

In spite of considerable advances, the separation of proanthocyanidins remains a challenge owing to the complexity of their structures, particularly their degree of polymerisation (DP), a key feature which determines their physico-chemical properties [12,14,15,17]. Improved separation methods for these compounds are required for, amongst others, *in vivo* studies of their physiological activities [12,15]. Reversed phase liquid chromatography (RP-LC) coupled with fluorescence and/or mass spectrometry (MS) detection is currently the most powerful method for the analysis of these compounds, and resolution of isomers up to tetramers has been reported [1,7]. However, the resolution of more structurally diverse higher oligomers has not yet been achieved [11]: these compounds co-elute as a large unresolved

"bump" in RP separations [1,7,13]. Promising separation of procyanidins based on molecular weight (MW) has been achieved by normal phase LC (NP-LC), although such methods do not provide resolution of isomers [7,17,18]. Quite recently, the successful application of hydrophilic interaction chromatography (HILIC) for similar MW separation of procyanidins has been reported [4,12]. HILIC is a variant of NP-LC where polar stationary phases are used in combination with aqueous mobile phases to separate analytes according to polarity. The retention mechanism is thought to involve partitioning of analytes between the mobile phase and a water-layer immobilised on the stationary phase [19,20].

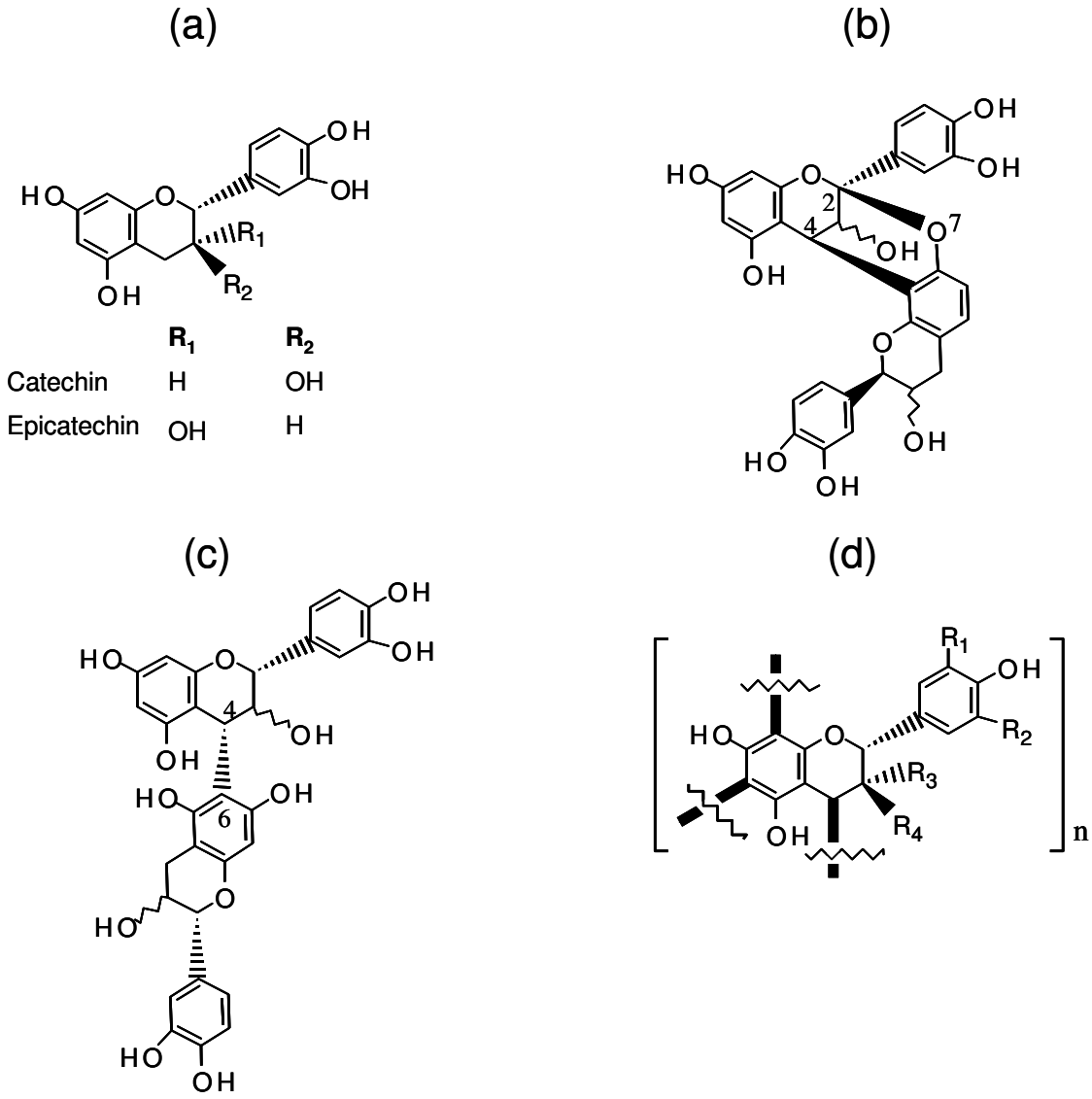

Figure 4.1: Structures of (a) proanthocyanidin monomeric units, (b) an A-type procyanidin dimer, (c) a C4→C6 linked B-type procyanidin dimer, and (d) general polymerisation pattern for proanthocyanidins.

Conventional LC separations offer insufficient resolving power when faced with the analysis of complex procyanidin fractions. For instance, taking into account the four possible types of interflavan bonds, it is theoretically possible to obtain 48 dimeric isomers of catechin and/or epicatechin, while this number increases with the degree of polymerisation [21]. Although not all isomers may be found in a given sample, a large number of isomers have been observed in various natural products. Clearly, the resolution of such large numbers of isomers is not possible with standard 1-dimensional LC methods, which are characterised by maximal theoretical peak capacities not exceeding 200.

Comprehensive 2-D LC techniques offer a powerful approach to increase peak capacity and are ideally suited for the analysis of complex samples, provided the selected separation modes are orthogonal (i.e., based on different separation mechanisms) [22-30]. From this perspective, the combination of HILIC and RP-LC holds significant promise for the comprehensive 2-D LC separations of procyanidins. Several 2-D LC methods have been developed for the analysis of phenolic compounds in a variety of samples [31-39]. However, to the best of our knowledge, no comprehensive 2-dimensional LC method suitable for the analysis of proanthocyanidins has previously been reported. In this paper, an off-line 2-D LC method that allows the separation of procyanidins, as well as additional natural phenolic compounds, is reported. The utility of the developed method is demonstrated for the analysis of cocoa (*Cacao Theobroma*) and apple phenolic extracts.

4.2. Experimental

4.2.1. Reagents and materials

Cocoa beans and apples (Red Starking variety) were purchased from a local supermarket. Standards of (-)-epicatechin and (±)-catechin as well as HPLC grade methanol, acetonitrile, isopropyl alcohol, formic acid and acetone were purchased from Sigma Aldrich (Steinheim, Germany). HPLC grade hexane and acetic acid were purchased from Burdick & Jackson (Muskegon, USA) and Riedel-de Haën (Seelze, Germany), respectively. Dichloromethane (analytical grade) was purchased from ROMIL (Waterbeach Cambridge, England) and ethyl acetate from AnalaR (Midrand, South Africa). Deionised water was obtained using a Milli-Q water purification system (Millipore, Milford, MA, USA). All solutions were filtered through 0.45 μm HVLP membrane filters (Millipore) and degassed in an ultrasonic bath (Branson Model 3510, Danbury, USA) before use.

4.2.2. Instrumentation

4.2.2.1. UPLC-PDA-fluorescence analyses

Analyses were performed on an Acquity UPLC system equipped with a binary pump, autosampler, column oven, photodiode array (PDA) detector (500 nL flow cell, 10 mm path length) and controlled by Waters Empower software (Waters, Milford, MA, USA). The mixing chamber on the UPLC was replaced with a low dead volume union, while the pump was connected to the injection valve using 0.1 mm i.d. tubing (Waters) to reduce the system dead volume. An HP 1046A Programmable Fluorescence detector (5 μL flow chamber, Agilent, Waldbronn, Germany) was connected to the UPLC system downstream of the PDA detector. Fluorescence data were acquired using the DAx 8.0 data acquisition software (Van Mierlo software, Amsterdam, The Netherlands).

4.2.2.2. UPLC–MS analyses

LC–MS analyses were performed on a Waters Acquity UPLC system equipped with a binary solvent manager and autosampler using HILIC and RP-LC conditions as outlined below. The UPLC system was interfaced through an electrospray ionisation (ESI) ion source to a Waters Ultima API quadrupole time-of-flight (Q-TOF) mass spectrometer. The mass spectrometer was operated in a negative ionisation mode with

a capillary voltage of -3.7 kV and a cone voltage of 35 V. The source temperature was 100°C. Masses were scanned from 285 to 2025 amu and data were collected and processed using MassLynx v.4.0 software (Waters). The instrument was calibrated using a NaF solution. Since no lock-spray function was available on this instrument, *m/z* ratios are reported to one decimal place.

For HILIC analyses, a desolvation temperature of 300ºC was applied. The desolvation and cone gas flows (both N_2) were 300 L/h and 50 L/h, respectively. For RP-LC analyses, the desolvation temperature was 350ºC, and desolvation and cone gas flows (both N_2) were 350 L/h and 50 L/h, respectively. The eluent was split 1:7 prior to introduction into the ionisation chamber for RP-LC–ESI-MS analyses.

4.2.3. Chromatographic methods

4.2.3.1. Hydrophilic interaction chromatography (HILIC) analyses

Separations were performed on a Nomura Chemical Develosil Diol-100 column (250 mm × 1 mm i.d., 5 µm d_p, Aichi, Japan) using a method adapted from Kelm *et al* [4]. The binary mobile phase consisted of (A) acetonitrile and acetic acid (99:1, v/v) and (B) methanol, water and acetic acid (94.05: 4.95:1, v/v/v). Separations were effected by a series of linear gradients of B into A as follows: 4–40% B (0–45 min), 40% B isocratic (45–50 min), 40–4% B (50–55 min). The column was re-equilibrated for 15 minutes. The flow rate was 0.050 mL/min. Fluorescence detection was performed with excitation at 276 nm and emission at 316 nm with a photomultiplier (PMT) gain of 5. Separations were performed at ambient temperature. For HILIC-PDA-fluorescence analyses, 10 µL was injected in the 'partial loop with needle overfill' mode using acetonitrile/HOAc (99:1, v/v) as the weak needle wash solvent. For HILIC–ESI-MS analyses, 5 µL was injected under the same conditions.

4.2.3.2. Reversed phase liquid chromatography analyses

The binary mobile phase consisted of acetonitrile (A) and 0.1% formic acid in water (v/v) (B). Injections were performed in the partial loop with needle overfill mode using 0.1% formic acid as the weak needle wash. The column temperature was 50˚C, and UV chromatograms were recorded at 210 nm, 280 nm, 320 nm and 370 nm. Fluorescence detection was performed as for HILIC analyses.

Two gradient methods were developed. For fast RP-LC-PDA-fluorescence analyses, separation was performed using an Agilent Zorbax SB-C18 column (50 mm × 4.6 mm i.d., 1.8 μm) protected with a Phenomenex C18 guard column (4 mm × 3 mm i.d., Torrance, USA). A linear gradient was performed as follows: 2% A (0–0.03 min), 2–18% A (0.03–1.20 min), 18–25% A (1.20–2.00 min), 25–100% A (2.00–2.30 min), 100% A until 2.50 min before returning to the initial conditions at 2.80 min. The column was re-equilibrated for 1.20 minutes before the next analysis. The flow rate was set to 1.8 mL/min and 3 μL was injected.

For high efficiency RP-LC-PDA-fluorescence analyses, separations were performed using two Zorbax SB-C18 columns (each 50 mm × 4.6 mm i.d., 1.8 μm) coupled in series and protected with a guard column as above. A linear gradient was performed as follows: 2% A (0–0.25 min), 2–18% A (0.25–10.70 min), 18–25% A (10.70–18.00 min), 25–100% A (18.00–20.70 min), 100% A until 22.50 min before returning to the initial conditions at 25.20 min. The column was re-equilibrated for 4.80 min before the next analysis. The flow rate was set to 0.8 mL/min and 2 μL was injected.

UPLC–ESI-MS analyses were performed using identical conditions as outlined above for the high efficiency RP-LC gradient analysis, with injections performed in the partial loop mode using water as the weak needle wash. The injection volume was 4 μL and 6 μL, respectively, for the apple and cocoa samples.

4.2.4. Off-line 2-dimensional (HILIC × RP-LC) analyses

One-minute fractions (corresponding to 50 μL each) of the HILIC separations were automatically collected between 2 and 52 minutes using a programmable BIO-RAD Model 2110 fraction collector (Corston, UK). The collected fractions were transferred to 1.5 mL vials containing 250 μL inserts and kept under N_2 until analysed by gradient RP as detailed above. All fractions were analysed within 2 days of collection. Raw fluorescence data for the RP analyses were exported into STATISTICA 8 (Statsoft Inc., US) to create 2-D contour plots.

4.2.5. Sample preparation

Cocoa beans: The sample was prepared using a modified method to that reported by Hammerstone *et al* [11]. Dried cocoa beans were ground in liquid nitrogen using a mortar and pestle. About 2.0 g of the ground material was extracted three times with 9

mL hexane to defat the sample. The remaining solid material was dried under a gentle stream of N_2 to give a final mass of 1.39 g. The dried sample was extracted three times with 3 mL 70% acetone in water (v/v), followed by three times 3 mL 70% methanol in water (v/v). The extracts were combined and centrifuged for 5 min at 5 000 × *g*. The organic solvents were removed by rotary evaporation under reduced pressure at 40˚C to give a final volume of 4 mL. The remaining aqueous extract was filtered through a 0.45 µm hydrophilic PVDF filter membrane (Millipore). The sample was kept under nitrogen at 4˚C and was used for all the RP-LC analyses. For HILIC analyses, the sample was freeze dried and redissolved in 70% acetonitrile and 30% methanol (v/v).

Apple: The apple sample was prepared using a modified method to that of Lazarus *et al* [7]. Half an apple was ground in liquid nitrogen using a mortar and pestle. About 10.0 g of the finely ground material was extracted two times with 20 mL 70% acetone in water (v/v). The suspension was centrifuged for 10 min at 5 000 × *g* after every extraction and the supernatants were combined in a round bottom flask. Acetone was removed by rotary evaporation under reduced pressure at 40˚C, to give a final volume of ~10 mL. The remaining aqueous extract was filtered through a 0.45 µm PVDF filter membrane. The sample was kept under nitrogen at 4˚C and was used for all the RP-LC analyses. For HILIC analyses, the sample was freeze dried and redissolved in acetonitrile, methanol and water in volume ratios of 70:29:1 (v/v/v), respectively.

4.3. Results and discussion

4.3.1. Optimisation of HILIC separation of procyanidins

Fluorescence detection of procyanidins was employed due to the improved selectivity and sensitivity offered by this technique compared to UV detection [1,4,7,40,41]. Initially, four methods adapted from literature [4,8,15,17] were evaluated on four different stationary phases, namely BETASIL diol-100 (Thermo Electron corporation, 250 mm × 4.6 mm i.d., 5 μm d_p), Spherisorb NH_2 (Waters, 250 mm × 4.6 mm i.d., 5 μm d_p), Luna CN (Phenomenex, 250 mm × 4.6 mm i.d., 5 μm d_p) and Develosil Diol-100 (Nomura Chemicals, 250 mm × 1 mm i.d., 5 μm d_p) columns. The goal was to select the column and mobile phase combination that provided the most efficient separation of procyanidins according to DP. Mobile phases based on hexane/acetone [8] and hexane/methanol/ethyl acetate [15] did not provide adequate separation on any of the stationary phases and were not investigated further. Acceptable separation was obtained using the methods of Kelm *et al* [4] and Rigaud *et al* [17] on both diol and Spherisorb NH_2 columns. A mobile phase composition of acetonitrile, methanol, acetic acid and water [4] in combination with the Develosil Diol phase was selected due to improved resolution of especially higher molecular weight procyanidins, as well as the compatibility of these solvents with RP solvents to be used in the second dimension.

Method optimisation was performed using cocoa extracts, and subsequently applied to apple samples. Individual fluorescence chromatograms for these samples are shown in **Figure 4.2**. The method proved to be sufficiently repeatable, as evidenced by the average %RSD for retention times between days (4 days) below 2.9%.

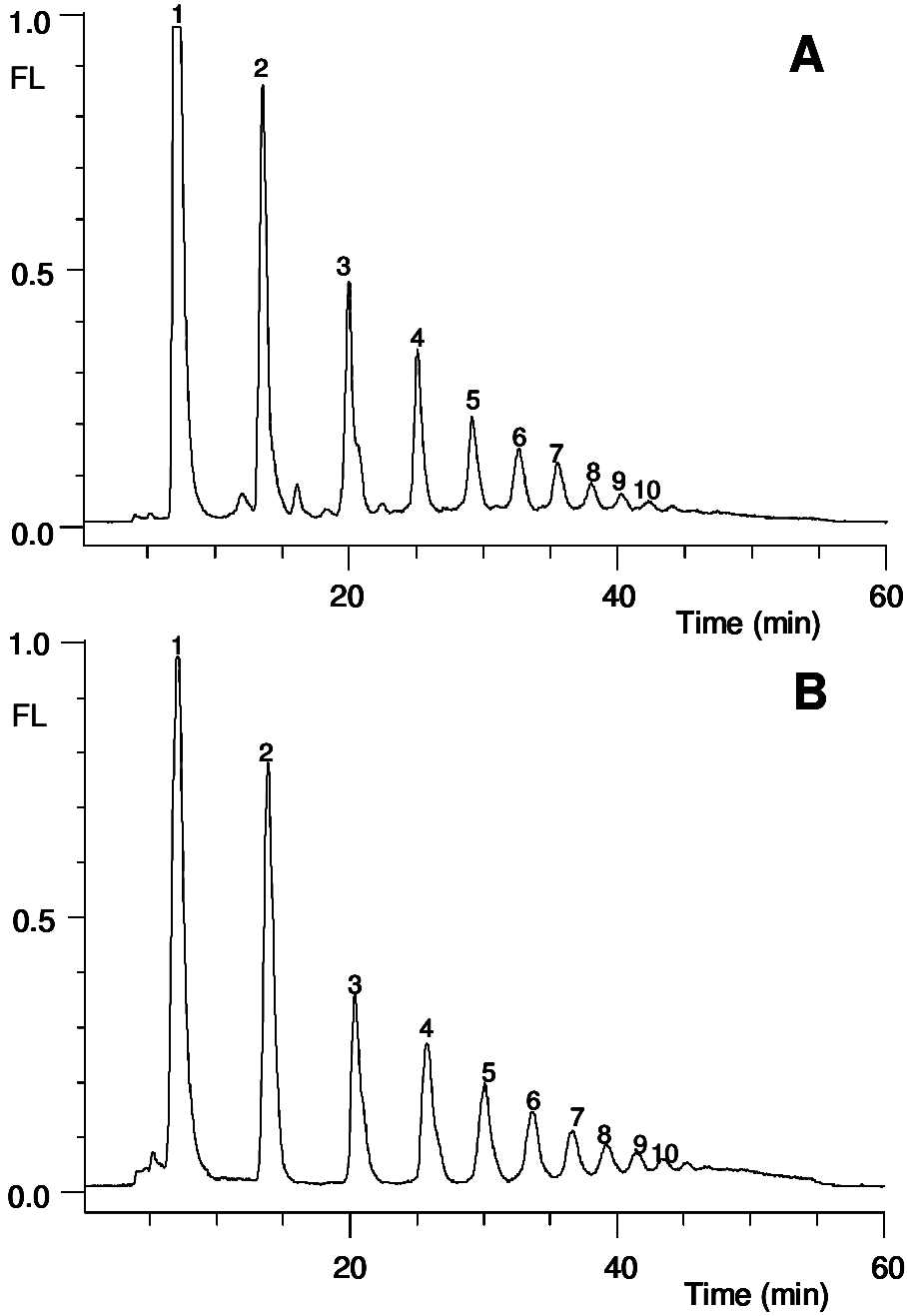

Figure 4.2: Optimised HILIC analysis of the cocoa (**A**) and apple (**B**) procyanidins. Labels 1−10 indicate the DP of procyanidins as identified by HILIC−ESI-MS. Detection: fluorescence; injection volumes: 1 µL and 5 µL for cocoa and apple samples, respectively.

4.3.2. HILIC−ESI-MS analysis of cocoa and apple procyanidins

The optimised HILIC method was coupled to electrospray ionisation mass spectrometry (ESI-MS) in order to identify procyanidins. ESI is the most common atmospheric ionisation technique used for the study of procyanidins, and has been found to be efficient in both positive and negative modes, depending on analysis conditions. In this study, better ionisation was achieved in the negative ionisation

mode (only singly charged ions for DP 1–7 could be detected in the positive ion mode).

Identification was based on mass spectra, including the presence of singly and multiply charged ions, and by comparison of retention times with fluorescence data and literature values. The singly charged molecular ions, $[M-H]^-$, were the most abundant ions for monomers until tetramers at *m/z* 289.1, 577.3/575.3 (B/A-type dimers), 865.5 and 1153.7, respectively. For pentamers and hexamers, the doubly charged ions at *m/z* 720.4 and 864.5 were the predominant ions. In addition, doubly charged ions were the most abundant ions for heptamers through nonamers as well as for dodecamers, while triply charged species were the most intense ions for decamers and undecamers. A summary of the dominant ions corresponding to different procyanidin oligomers as detected in cocoa and apple samples is presented in **Table 4.1**. These data are in accordance with literature values [7,11]. An example of the mass spectrum obtained for trimeric and pentameric procyanidins in the cocoa extract highlighting the principal ions detected is presented in **Figure 4.3**. From the extracted ion chromatograms (EICs) acquired from analysis of the cocoa extract and shown in **Figure 4.4**, it is evident that the procyanidins are indeed separated according to molecular weight using the optimised HILIC method. Also evident from this figure, is that the A-type oligomeric procyanidins, detected at *m/z* $[M_{(B\text{-type})}-2]$ (**Figures 4.3 and 4.4(B)**) are slightly less retained under HILIC conditions, as would be expected due to their lower polarity. Careful examination of mass spectral data indicates the presence of procyanidins up to hexamers containing 1 A-type linkage (data not shown). However, these A-type oligomers are present at much lower levels than their B-type equivalents, and with the exception of a single A-type dimer, are not clearly evident from the fluorescence data. Also of interest is that the major peak corresponding to the B-type trimers displays a significant shoulder at higher retention in both HILIC-fluorescence and HILIC–MS analyses. This might presumably be ascribed to two partially separated trimeric isomers. Since resolution in HILIC decreases with increasing DP, higher MW isomers are not equally resolved.

Two additional compounds were detected at *m/z* 707.4 and 737.4. The former compound partially co-eluted with dimeric procyanidins, while the latter was resolved between dimers and trimers. Mass spectral data and retention times are in agreement

with A-type dimeric glycosides reported in cocoa extracts [11,42]. Porter *et al* [42] identified these compounds as O-β-D-galactopyranosyl-epicatechin-(2α→7,4α→8)-epicatechin and O-L-arabinopyranosyl-epicatechin-(2α→7,4α→8)-epicatechin. It is interesting to note that none of the corresponding B-type glycosides were observed. In addition, similar hexose derivative(s) of epicatechin/catechin were also observed at *m/z* 451 [11], as were hexose and pentose derivatives procyanidin trimers through heptamers. Retention of the higher MW procyanidin-glycosides is in accordance with the procyanidin dimer-glycosides, i.e., slightly higher than the corresponding procyanidin aglycones. Although further work is required to determine the exact structures of these oligomeric procyanidin-glycosides, it seems likely that they are structurally related to the A-type dimeric molecules determined by Porter *et al* [42]. To the best of our knowledge this is the first time that higher molecular weight procyanidin-glycosides are reported in cocoa extracts.

Table 4.1: Summary of the predominant ions detected by HILIC–ESI-MS analysis of procyanidins in cocoa and apple extracts. Base peak ions are highlighted in bold.

DP	$[M–H]^-$	$[2M–H]^-$	$[M–2H]^{2-}/2$	$[M–3H]^{3-}/3$
1	**289.1**	579.3		
2	**575.3**			
	577.3	1155.7		
3	**863.5**			
	865.5			
4	**1151.7**			
	1153.7		576.3	
5	1439.9		**719.4**	
	1441.9		**720.4**	
6	1729.9		**864.5**	
7			**1009.1**	
8			**1152.7**	
9			**1297.3**	
10			1441.9	**960.6**
11			1586.0	**1056.6**
12			**1730.1**	

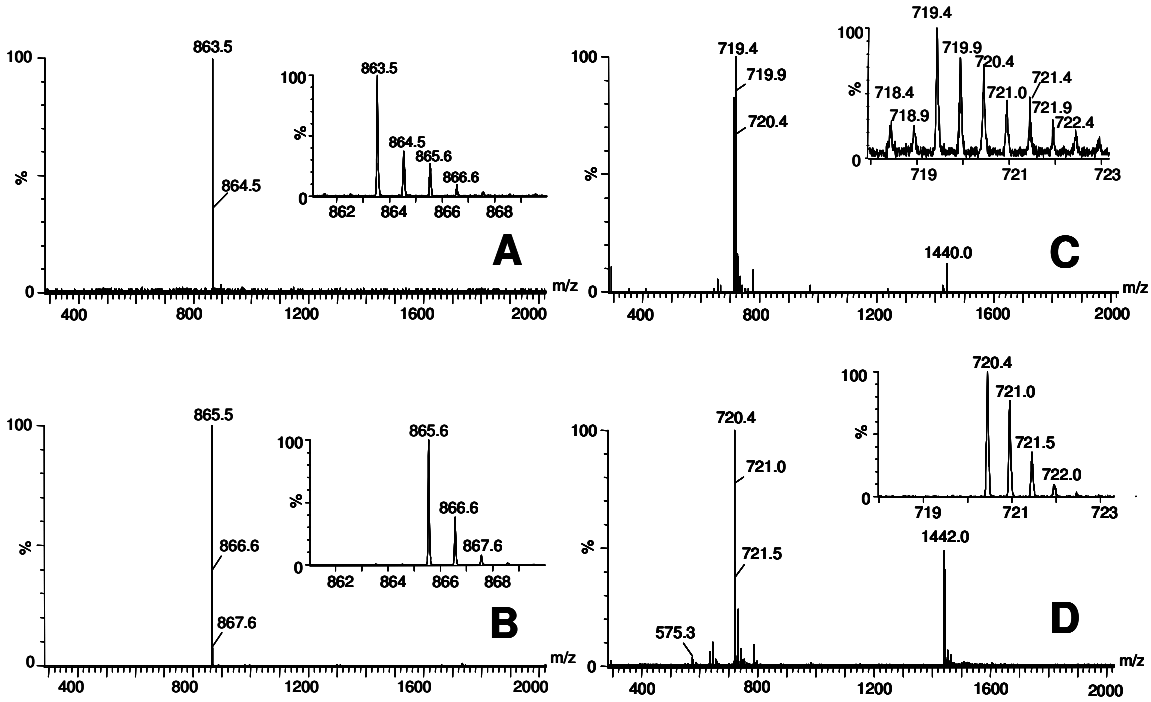

Figure 4.3: Negative ESI mass spectra obtained from the HILIC–MS analysis of oligomeric procyanidins in the cocoa extract: A-type (A) and B-type (B) trimers; and pentamers with a single A-type (C) and only B-type (D) linkages.

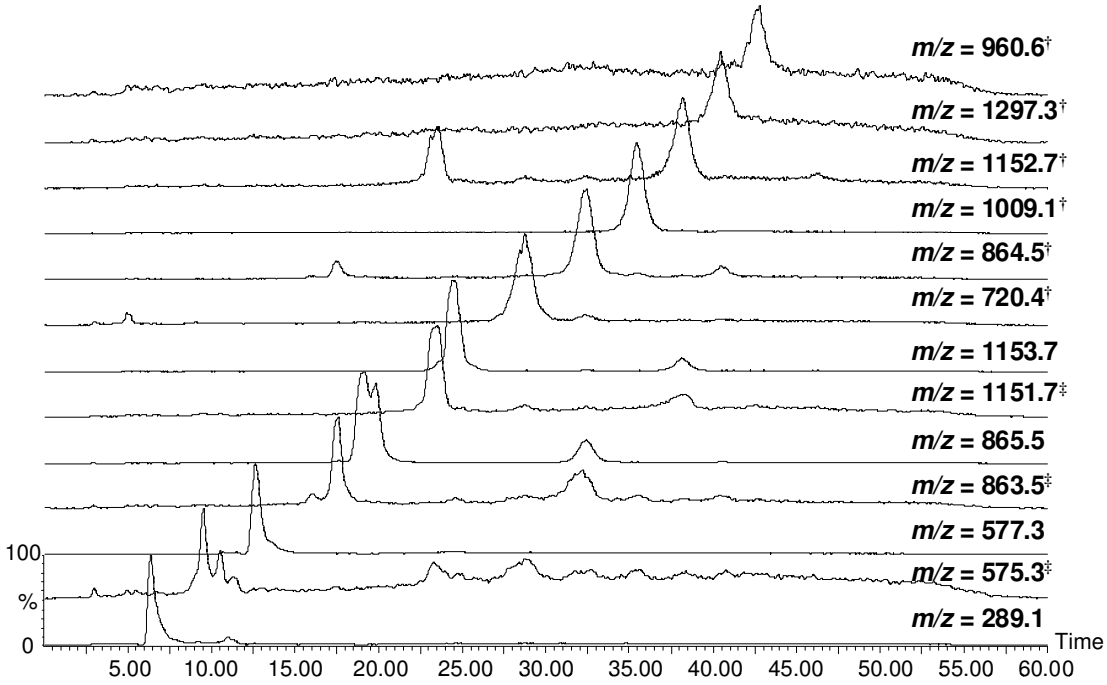

Figure 4.4: Extracted ion chromatograms for individual oligomers obtained by HILIC–ESI-MS analysis of a cocoa extract. Base peak ions were extracted for each DP. (†) Indicates multiply charged species $[M–2H]^{2-}$. (‡) Indicates oligomers containing one A-type linkage (for further discussion, refer to text).

4.3.3. Optimisation of RP-LC separation of procyanidins

In initial studies, three different RP stationary phases and columns formats were evaluated: CN (Phenomenex Luna, 50 mm × 4.6 mm, 5 μm d_p), Acquity BEH C18 (Waters, 50 mm × 2.1 mm, 1.7 μm d_p) and Zorbax SB-C18 (Agilent, 50 mm × 4.6 mm, 1.8 μm d_p). Similar separations were achieved on the Zorbax and UPLC columns, although the former column had a much higher loadability due to the larger internal diameter (i.d.). The CN column offered similar high loadability, although the lower efficiency associated with the larger particle size of this column did not provide satisfactory separation. Therefore, the Zorbax column was selected for further optimisation as this column offered the advantages of fast, efficient separations coupled to higher loadability, which is especially beneficial from a sensitivity point of view in a comprehensive 2-D-LC analysis.

Two approaches were investigated: one employing a fast gradient operating close to maximum pressure for the column (600 bar); and a slower gradient performed on two coupled columns operated at close to optimal linear velocity for procyanidins for maximum efficiency. A column temperature of 50°C was employed to reduce the mobile phase viscosity and allow faster mass transfer of solutes [43], and the gradient was adjusted so as to resolve as many compounds as possible within an acceptable time. Both RP-LC separations provide separation of procyanidin isomers according to hydrophobicity (as confirmed by RP-LC–ESI-MS analyses, see further), and numerous peaks are detected. Typical UV and fluorescence chromatograms for the high efficiency RP-LC analysis of a cocoa extract are shown in **Figure 4.5**. Despite the high chromatographic efficiency offered by the use of two coupled 1.8 μm columns, it is also evident from this figure that complete resolution of especially the higher MW isomers is not possible.

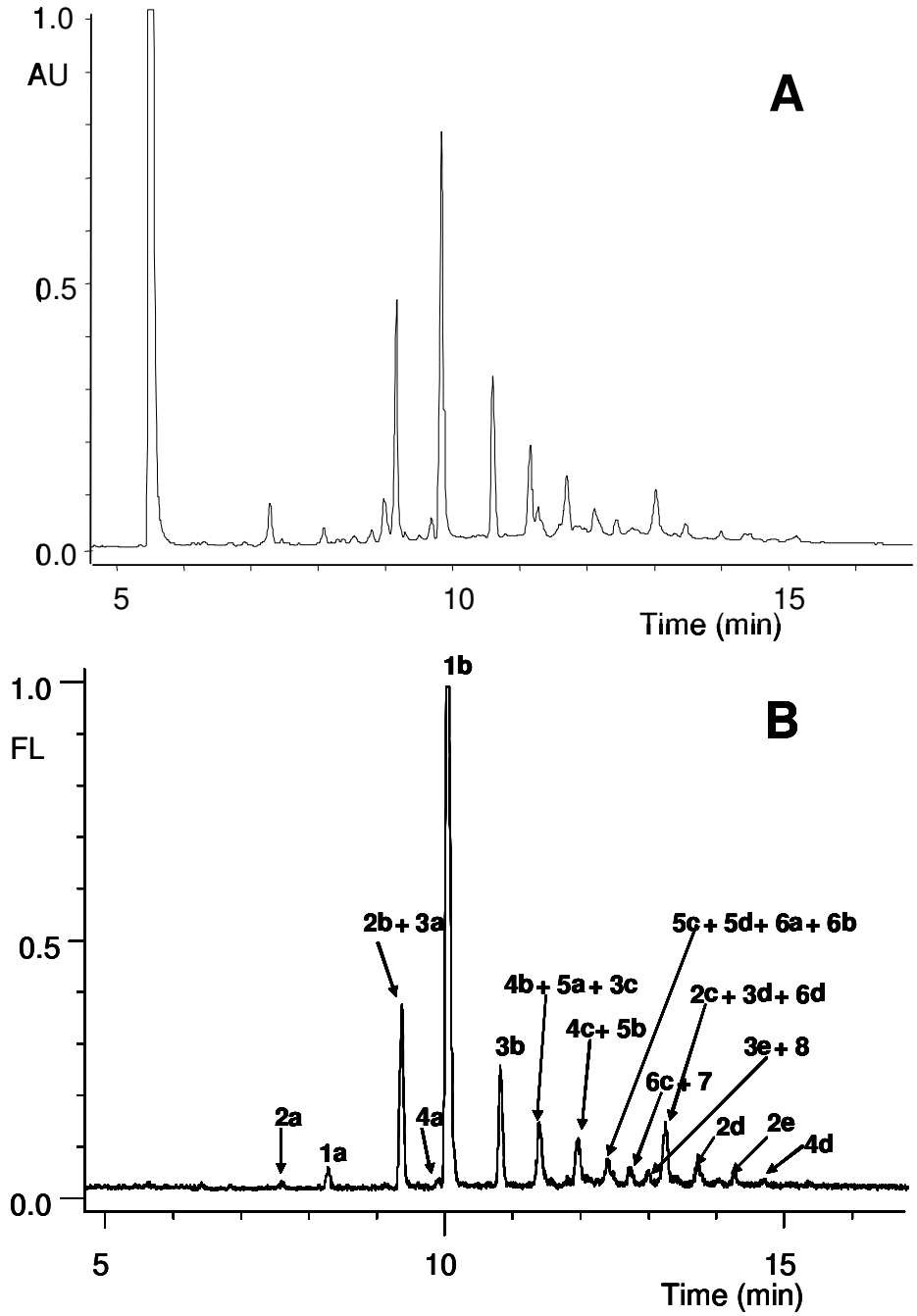

Figure 4.5: UV chromatogram recorded at 280 nm (**A**), and fluorescence chromatogram (**B**) obtained for the optimised high efficiency RP-LC analysis of cocoa procyanidins. Labels indicated the DP of procyanidin isomers as identified by RP-LC–ESI-MS. Columns: 2 × 50 mm × 4.6 mm Zorbax SB-C18 (1.8 µm d_p) columns coupled in series; flow rate: 0.8 mL/min; injection volume: 3 µL; temperature: 50°C.

4.3.4. RP-LC–ESI-MS analysis of procyanidins

The optimised RP-LC method was coupled to ESI-MS in order to identify the major procyanidin isomers. RP-LC–ESI-MS allowed identification of isomeric monomers to

octamers as highlighted in **Figure 4.5**. As anticipated, the elution order in RP-LC is not related to the molecular mass [3,13].

Catechin and epicatechin were identified based on mass spectral data and by comparison of retention times with authentic standards. Tentative identification of additional oligomers is based on mass spectral data and correlation of retention times with fluorescence data, due to lack of suitable standards. For the same reason, exact structure elucidation for individual isomers could not be established.

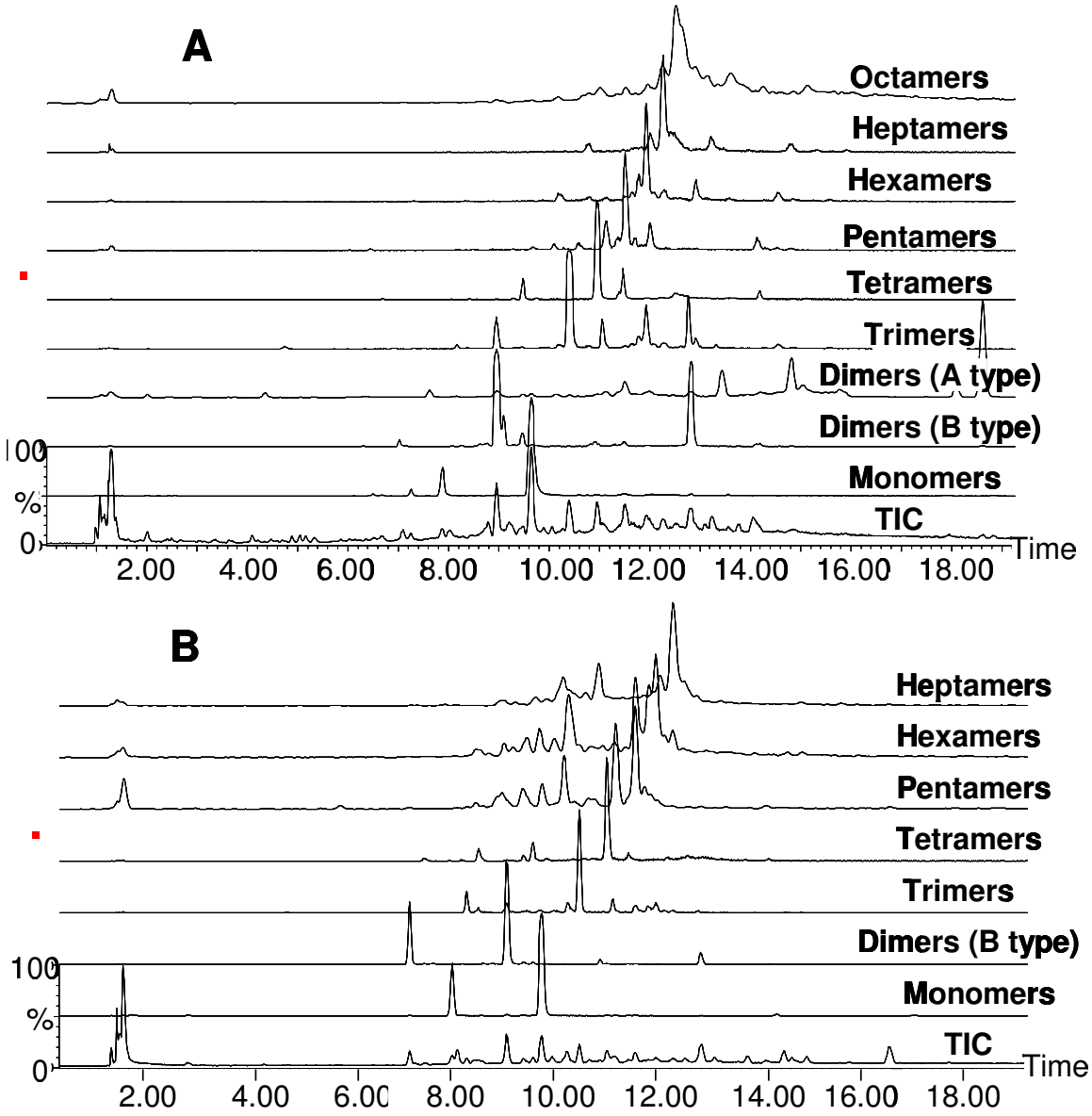

Figure 4.6: Total ion- and extracted ion chromatograms for the procyanidin oligomers detected by RP-LC–ESI-MS analyses of cocoa (**A**) and apple (**B**) extracts. Peak labels indicate the degree of polymerisation of individual isomers and correspond to **Figures 4.8** and **4.10**. Injection volumes: 4 and 6 µL for cocoa and apple samples, respectively. Other conditions as specified in **Figure 4.5**.

Cocoa and apple procyanidin oligomers were found to consist exclusively of catechin and/or epicatechin monomeric units. Three dimeric-, four trimeric- and tetrameric-, five pentameric-, four hexameric-, and one each heptameric- and octameric procyanidin isomers were tentatively identified in cocoa. In contrast, five dimeric-, seven trimeric-, six tetrameric-, pentameric- and hexameric- as well as one heptameric procyanidin isomer(s) were tentatively identified in the apple extract. Although higher order oligomeric isomers could not be detected by fluorescence, oligomers up to dodecamers were observed in MS traces for both cocoa and apple samples. Extracted ion chromatograms highlighting the most important procyanidin oligomers present in cocoa and apple extracts are shown in **Figure 4.6.**

Both A- and B-type procyanidins oligomers were detected in cocoa extracts: four B-type and four A-type dimeric isomers were observed, the latter present at much lower levels. In general, A-type oligomers are characterised by higher retention under RP-LC conditions, as expected. Similar to HILIC–ESI-MS, RP-LC–MS data also indicated the presence of procyanidin oligomers up to hexamers containing 1 A-type linkage, although most of these compounds were present at trace levels and not observed in fluorescence chromatograms. As previously observed by Shoji *et al* [8], only singly linked (B-type) oligomers were found to be present in the apple extract.

No oligomeric phenolics composed exclusively of prodelphinidin or mixed procyanidin/prodelphinidin monomeric units were detected in cocoa and apple. Neither were propelargonidin monomeric units and oligomers or copolymers made up of (epi)afzelechin units detected.

However, UV data recorder at 320 and 370 nm indicated presence of a number of additional non-procyanidin phenolic compounds present in cocoa, and especially apple extracts. By careful correlation of RP-ESI-MS data with the appropriate UV chromatograms and relevant literature reports [11,44,45], some compounds previously reported in these samples were tentatively identified (**Table 4.2**). These include cinnamic acid derivatives, flavonol-glycosides and dihydrochalcones. These compounds all displayed low retention in HILIC mode (results not shown), and were generally well-retained under RP-LC conditions. A typical UV chromatogram recorded at 320 nm and extracted ion chromatograms for the compounds listed in **Table 4.2** are presented in **Figure 4.7**.

Table 4.2: Summary of additional phenolic compounds tentatively identified in cocoa and apple extracts by RP-LC–ESI-MS.

RP-LC Retention time	$[M-H]^-$	Compound	Sample
7.13	337.2	3-*p*-Coumaroylquinic acid	Apple
7.95	353.2	5-Caffeoylquinic acid	Apple [44]
9.33	337.2	*5-p*-Coumaroylquinic acid	Apple
9.46	353.2	4-Caffeoylquinic acid	Apple
9.85	337.2	*4-p*-Coumaroylquinic acid	Apple [44]
11.07	358.2	Clovamide	Cocoa [11]
12.49	609.4	Quercetin-3-O-rhamnoglucoside	Apple [44]
12.82	463.2	Quercetin-3-O-galactoside	Apple [44,45], cocoa [11]
13.07	463.2	Quercetin-3-O-glucoside	Apple [44,45], cocoa [11]
13.73	433.2	Unknown quercetin conjugate	Apple
14.08	433.2	Quercetin-3-O-arabinoside	Apple, cocoa
14.46	433.2	Quercetin-3-O-xyloside	Apple
14.62	567.4	Phloretin-2'-O xyloglucoside	Apple [45]
14.72	433.2	Unknown quercetin conjugate	Apple [45]
14.88	326.2	Dideoxyclovamide	Cocoa [11]
14.91	447.2	Quercetin-3-O-rhamnoside	Apple [44,45]
16.57	435.3	phloretin-2'-O-glucoside (Phloridzin)	Apple [44,45]
19.78	301.1	Quercetin	Apple [44], cocoa [11]

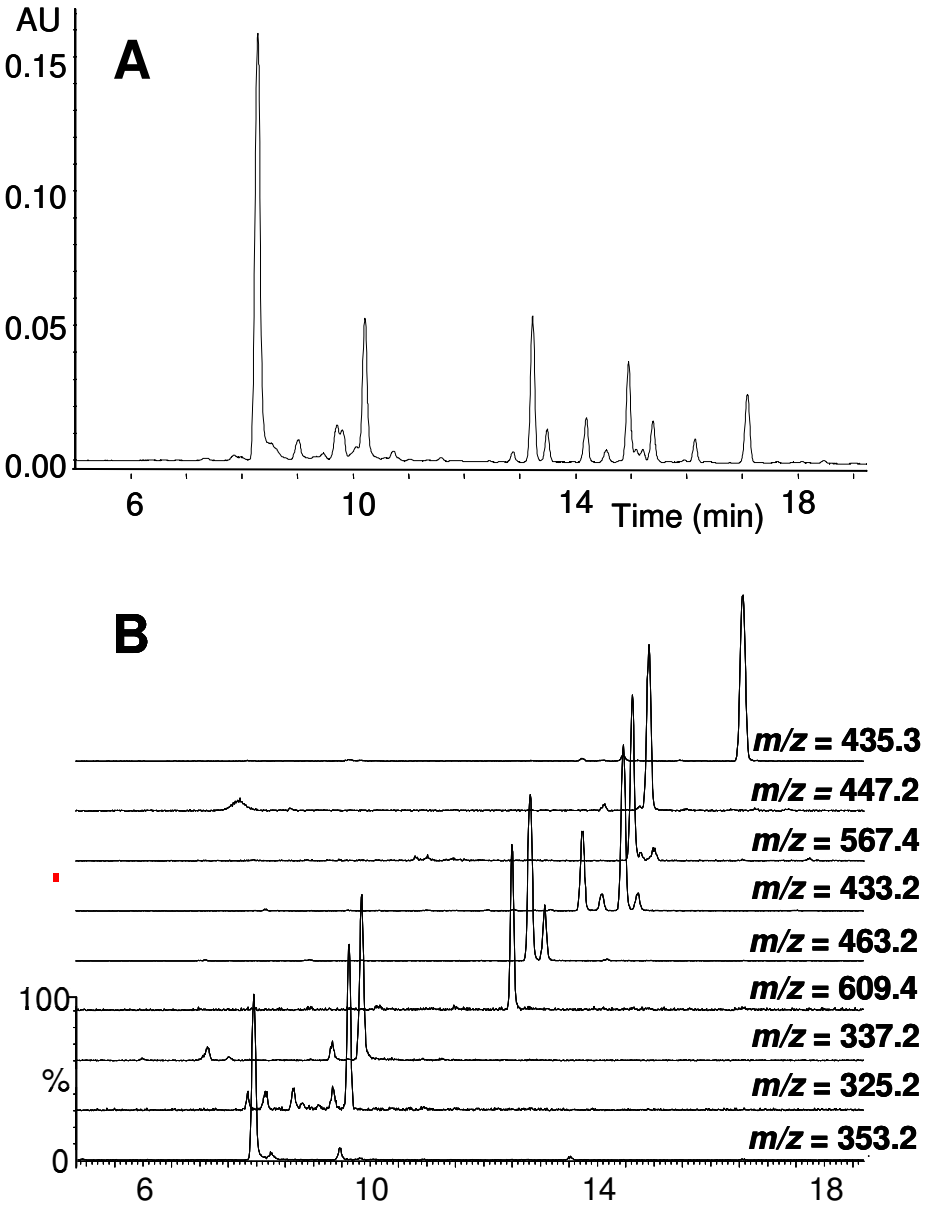

Figure 4.7: (**A**) UV chromatogram recorded at 320 nm for the RP-LC analysis of an apple extract, and (**B**) Extracted ion chromatograms obtained for the RP-LC–ESI-MS analysis of an apple extract, illustrating the detection of compounds listed in **Table 4.2**. Experimental conditions as specified in **Figure 4.5**.

Some of these compounds have not previously been reported in these samples, but were tentatively identified as isomers of previously reported compounds, based on similar fragmentation patterns and absorbance spectra. Isomers have been assigned based on their relative retention times in accordance with literature reports [45-47]. This specifically applies to ions with *m/z* 337.2, 353.2, 433.2 and 463.2. For example, all compounds with *m/z* 433.2 and 463.2 gave a fragment ion at *m/z* 301.1, which corresponds to a quercetin aglycone. Their relative retention was used in peak

assignment: for example, galactoside elutes before glucoside, and arabinoside before xyloside. For *p*-coumaroylquinic and caffeoylquinic acids, the isomers elute in the order of 3', 5' and 4' substitution [46,47]. Clovamide and dideoxyclovamide were assigned according to the elution order described by Sanbongi *et al* [48].

4.3.5. Off-line comprehensive HILIC × RP-LC separation of procyanidins

When designing a comprehensive liquid chromatographic system, orthogonality and solvent compatibility, amongst others, are the main aspects that require careful consideration [49]. This is simply because the first dimension eluent is the second dimension injection solvent [49]. Because HILIC provides different selectivity to RP-LC, the combination of the two modes of separation potentially offers a high degree of orthogonality, as has been demonstrated in several studies [50-52]. Despite the fact that the mobile phases used in HILIC are miscible with RP solvents (in contrast to NP- and RP-LC), interfacing the two separations remains challenging due to the fact that the primary eluent in one mode is a strong solvent in the other. This plays a significant role in on-column focusing of analytes and as a result limits the injection volume if band broadening due to injection is to be avoided in the second dimension.
Both HILIC and RP-LC analyses were optimised independently to maximise resolution in each dimension before their off-line coupling. A 1 mm i.d. column was selected in the first dimension to minimise on-column dilution and avoid the need to evaporate the fractions before analysing them in the second dimension. This could potentially lead to degradation of thermally labile anti-oxidant compounds.

Sample extracts were freeze dried and redissolved in 70/30 (v/v) acetonitrile/methanol to allow higher loadability on the HILIC column and ultimately better sensitivity of the 2-D separation. For the freeze dried apple extracts, 1% water was added to avoid precipitation of the higher molecular weight procyanidins. Maximally 10 µL of these samples could be injected on the HILIC column without noticeable peak distortion.
For RP-LC analyses, various injection volumes utilising HILIC mobile phases as sample solvent were evaluated to maximise loadability, while keeping band broadening to an acceptable level. 3 µL and 2 µL were found to be the maximum allowable injection volumes of these samples for the short and long RP-LC gradients, respectively. For the off-line coupling of HILIC and RP-LC methods, 1 min HILIC

fractions, corresponding to 50 µL, were collected. This is sufficient to provide a minimum of 2 fractions per first dimension peak as required to avoid artificial band broadening due to a too low sampling rate of 1st dimension peaks. This is also made easier by the relatively broad peaks eluting from the HILIC column. Taking into consideration dilution occurring on the first dimension column, this sampling rate effectively implies that 0.4 - 0.6 µL of the extracts were injected onto the second dimension column. The efficiency of the 1.8 µm phase combined with fluorescence detection provides sufficient sensitivity under these conditions. The collected HILIC fractions were immediately transferred to low volume vials (200 µL) and kept under N_2 to minimise the risk of artefact formation.

2-dimensional contour plots for the HILIC × RP-LC analyses of cocoa procyanidins using the short and long RP-LC gradients with fluorescence detection are shown in **Figure 4.8**. Note that throughout the paper contour plots are represented with the second dimensional separation on the x-axis, contrary to common practice. This is done to facilitate visual interpretation of contour plots with references to RP-LC–MS analysis (see **Figure 4.9**).

The resolving power offered by the comprehensive 2D-LC system is clearly evident in **Figure 4.8**: a combination of molecular weight information (y-axis) as well as the isomeric distribution (x-axis) of procyanidins is obtained in a single contour plot. The 2-D separation therefore provides additional information which could not be obtained from any single 1-dimensional separations. In fact, these contour plots display structured patterns reminiscent of comprehensive gas chromatography (GC×GC), where DP for diverse structures is easily deduced by the y-intercept of a particular peak. Especially higher MW isomers are much better resolved in the 2-D space than is possible using even a highly efficient 1-D RP-LC separation. Due to extensive overlap of these isomers, (see for example dimers and trimers in **Figures 4.6** and **4.9**), RP-LC–MS alone could not be used to unambiguously identify higher MW procyanidins.

Comparing **Figure 4.8A and B** it is clear that for procyanidins of DP ≥ 4, extensive overlap of isomers is evident for the shorter RP-LC gradient, highlighting the significant loss of resolution associated with a reduction in the second dimension

analysis time. This has obvious implications for the on-line comprehensive 2-D LC analysis of these samples.

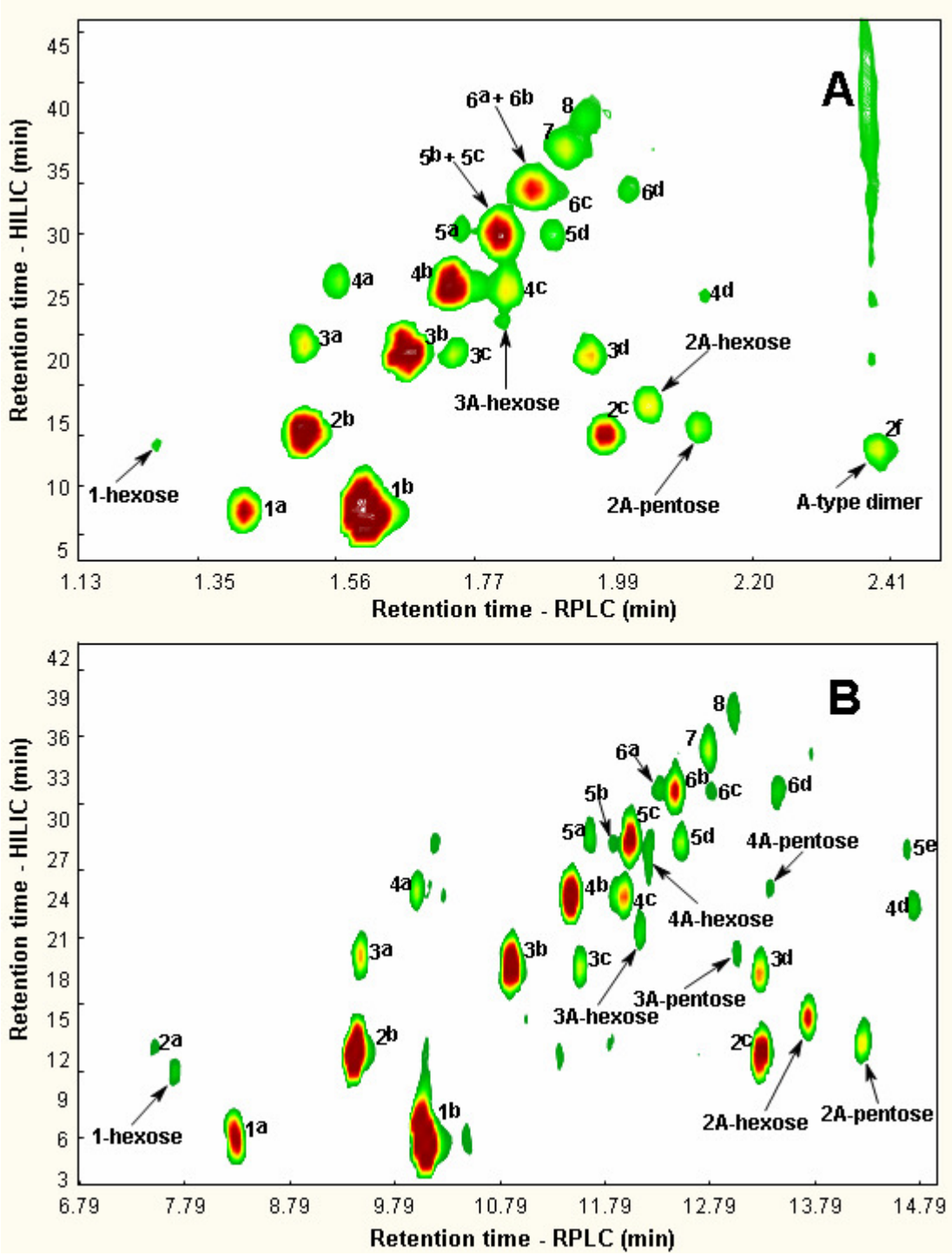

Figure 4.8: Fluorescence contour plots obtained for the HILIC × RP-LC analysis of cocoa procyanidins with the short (**A**) and long (**B**) second dimension RP-LC gradients. Numbers correspond to procyanidin oligomers detected for each degree of polymerisation.

Peaks in the 2-D contour plots were identified by comparison of retention times in both dimensions with 1-dimensional fluorescence and LC–ESI-MS data obtained for

both HILIC and RP separations. This is illustrated in **Figure 4.9**, where extracted ion chromatograms for the RP-LC–MS analysis of B-type dimeric and trimeric procyanidins are aligned with the relevant part of the contour plot. Further confirmation is then achieved by alignment of extracted ion chromatograms obtained by HILIC–MS with the y-axis. Such alignment of MS and fluorescence data with two different separation methods significantly decreases the chances of false identification.

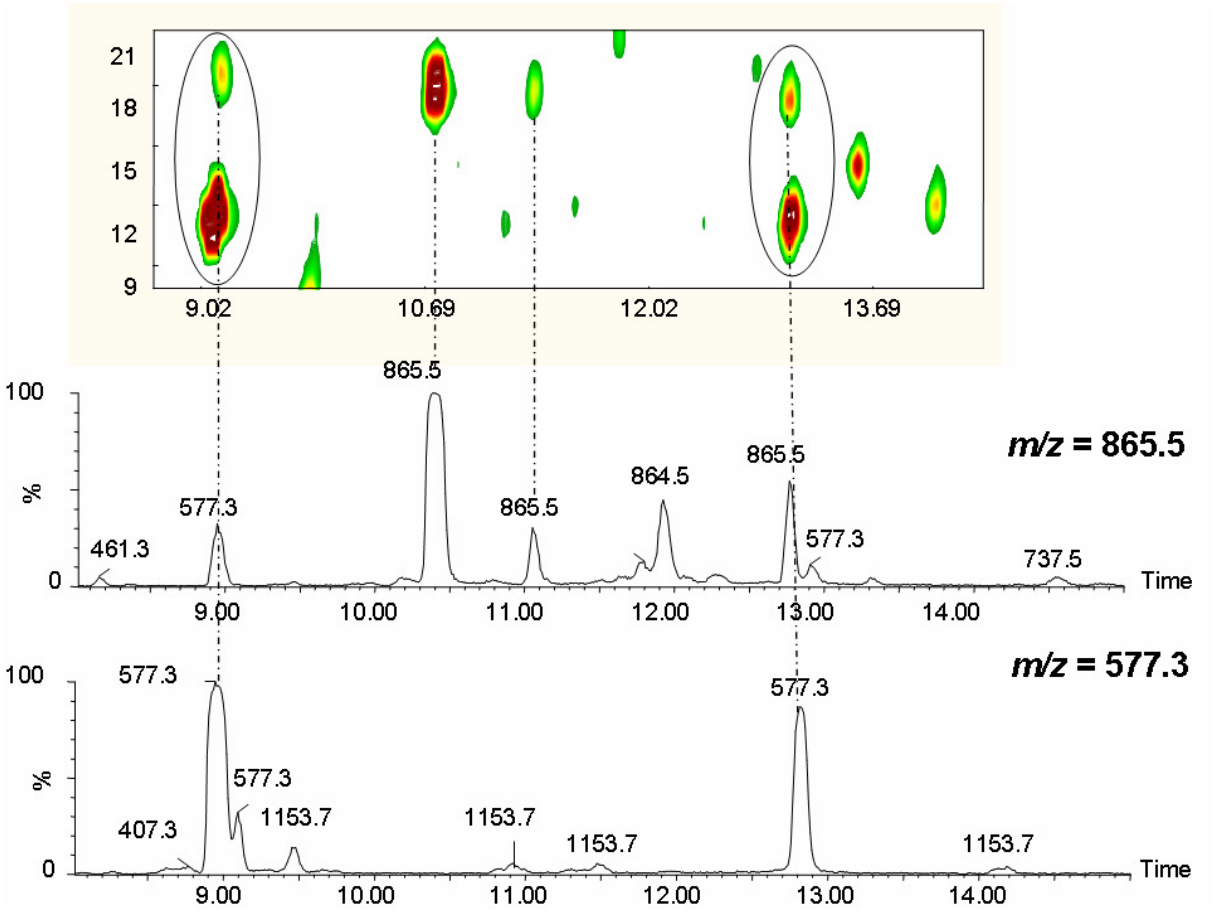

Figure 4.9: Illustration of the identification of dimeric and trimeric procyanidins by alignment of off-line RP-LC–MS extracted ion chromatograms with the relevant section of the fluorescence contour plot.

An additional benefit of the comprehensive HILIC × RP-LC analysis is that the obtained contour plots greatly facilitate the assessment of procyanidin content of different samples by means of visual comparison. This is illustrated in **Figure 4.10**, where contour plots for cocoa and apple extracts are compared. Most strikingly, a larger number of procyanidin isomers of DP 2–5 are detected in the apple sample. Compounds common to both samples are readily identified by their presence in the

same spot in both plots. It is also clear that a number of oligomeric isomers unique to apple are observed in the left of the contour plots, corresponding to lower retention times in RP-LC. This can be attributed to the higher levels of catechin in apple compared to cocoa (peaks labelled $1^{a}/1^{a'}$ and $1^{b}/1^{b'}$ in **Figure 4.10**). This suggests the presence of more isomers of higher DP containing catechin as constituent in the apple sample, and explains their presence at lower RP retention times (catechin is less retained under RP conditions than epicatechin). This illustrates that, even though the exact chemical structure of oligomeric procyanidins cannot be determined by means of mass spectrometry alone, the combination of MS data with chromatographic retention data in two dimensions provides additional information useful for identification purposes. Also evident from **Figure 4.10** is the absence of procyanidin-glycosides in the apple sample, which is related to the lack of A-type procyanidins in this sample.

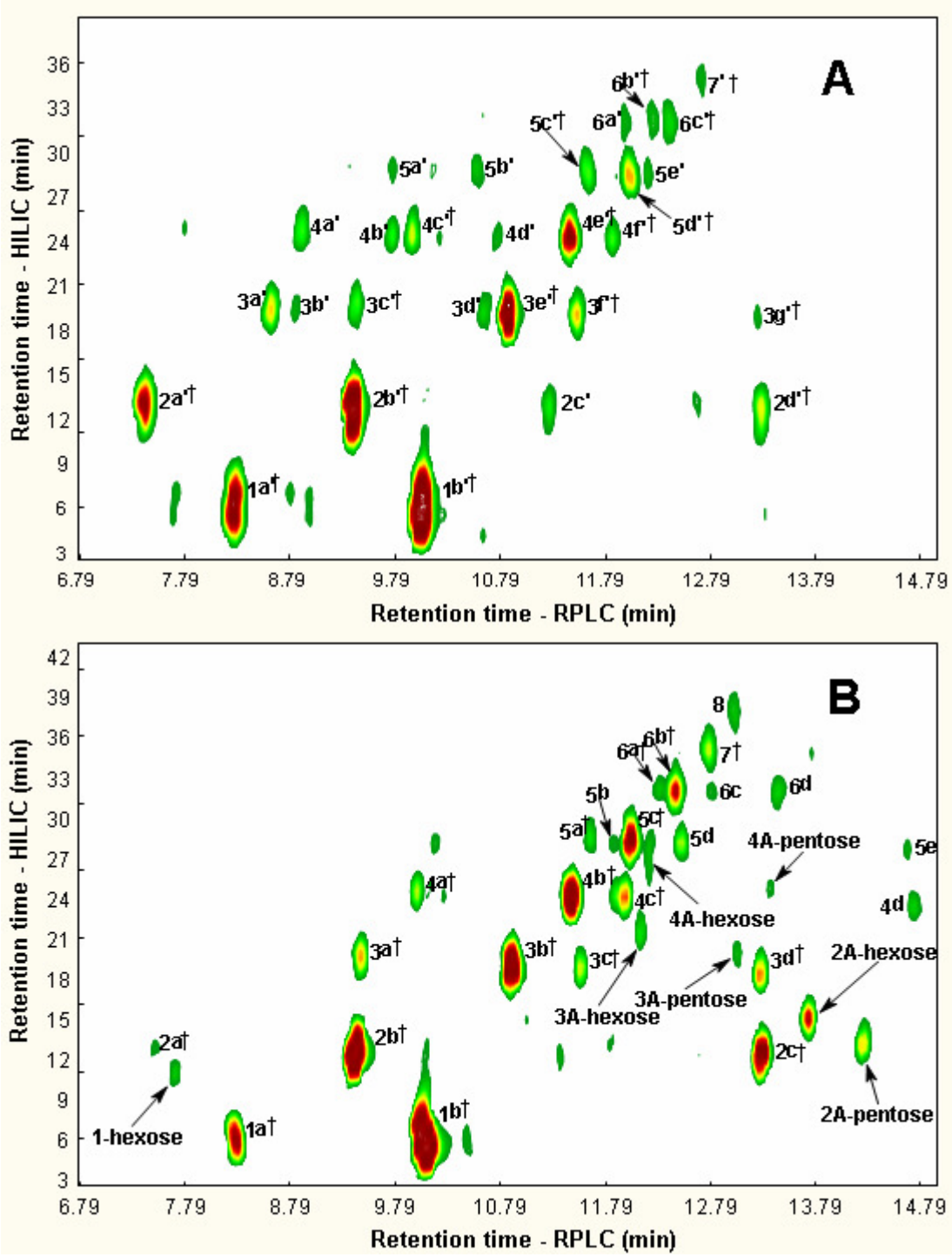

Figure 4.10: Comparison of fluorescence contour plots obtained for the HILIC × RP-LC analysis of apple (**A**) and cocoa (**B**) procyanidins. Numbers correspond to the degree of polymerisation of procyanidin isomers as identified by ESI-MS. Compounds common to both samples are marked with †.

In order to quantitatively evaluate the performance of the 2-D HILIC × RP-LC method, it is informative to determine the practical peak capacity of the 2-D separation in comparison to either 1-D separation. It is known that the maximum

theoretical peak capacity of a 2-dimensional separation is equal to the product of the peak capacities of each of the two dimensions [27,32,53]. However, to benefit from this enhanced resolving power, the separations used in each of the dimensions should be totally uncorrelated (i.e., based on different separation mechanisms) [27,32,53]. Orthogonality may be estimated using the correlation coefficients (r^2) obtained from the range-scaled retention times in each dimension [53]. A summary of the relevant data for procyanidins identified in cocoa and apple samples is presented in **Table 4.3**. The low r^2 values of 0.2092 and 0.1651 signify an exceptionally small degree of correlation between HILIC and RP dimensions, as is indeed evident from **Figure 4.8**. Differences in r^2 values between cocoa and apple may be ascribed to the presence of a higher percentage of high MW procyanidin isomers in the apple extract displaying low RP-LC retention, as discussed above. This leads to a more even distribution of peaks across the separation space.

Correlation coefficients may be used to calculate the practical peak capacity of the 2-D separation according to the method of Liu *et al* [53]. This method essentially uses the correlation coefficient to estimate the effective area of the total 2-dimensional space (i.e., $n_1 \times n_2$) being utilised. High orthogonality implies effective usage of this space, and should therefore provide a practical peak capacity value close to the theoretical value obtained by the multiplication of peak capacities in each dimension. Practical peak capacities of 3512 and 2493 (calculated according to [53]) obtained for HILIC × RP-LC separations compare relatively well with the theoretical maximum values of 4384 and 3024 for cocoa and apple, respectively. A summary of the experimental values used to calculate peak capacities is presented in **Table 4.3**.

Table 4.3: Summary of the parameters used to calculate the practical peak capacity of the off-line HILIC × RP-LC methods.

Parameter	Value		
	Cocoa (4 min)	**Cocoa (30 min)**	**Apple (30 min)**
[a]HILIC peak capacity, n_1	32	32	27
[a]RP peak capacity, n_2	54	137	112
[b]Correlation coefficient, r^2	0.0876	0.2092	0.1651
[c]Theoretical peak capacity, n_T	1728	4384	3024
[b]Practical peak capacity, n_p	1475	3512	2493
[d]Practical peak capacity, n_p	1237	3137	2334

[a] Calculated according to Neue [54].
[b] Calculated according to Liu *et al* [53].
[c] $n_T = n_1 \times n_2$.
[d] Calculated according to Li *et al* [58].

One shortcoming of precedent method of calculating effective peak capacity is the failure to take into account the effect of under-sampling of 1st dimension peaks. Especially in on-line comprehensive 2-D LC separations, excessive modulation times are often used due to practical constraints. Long modulation times, relative to the peak widths in the first dimension, lead to a significant decrease in the apparent 1st dimension peak capacity, and therefore of the 2-D system [54]. This aspect may quantitatively be evaluated using the peak broadening factor, β, according to [55]:

$$\beta = \sqrt{1 + 0.214\left(\frac{t_s}{\sigma_1}\right)^2} \qquad (\mathbf{4.1})$$

where t_s is the sampling time and σ_1 the standard deviation of peaks eluting from the first dimension column. Peak widths in the HILIC separation varied between 1.1–3.9 min and 1.5–5.5 min for the cocoa and apple samples, respectively (average peak widths 2.3 and 3.0 min, respectively). For a sampling time of 1 minute as used on the off-line HILIC × RP-LC analyses, β-values varying between 1.1–1.9 and 1.1–1.6 are calculated according to **Equation 4.1** (average βs are 1.4 and 1.3).

According to Davis *et al* [55], and in accordance with the work of other authors [56,57], the sampling rate used in comprehensive 2-D separations should obey the inequality $t_s/^1\sigma \leq 2$. This requisite translates into a β-value of 1.4. From this it may be concluded that the effect of under-sampling only plays a minor role by contributing to the effective band broadening of the later-eluting procyanidins: only for DP ≥ 7 does β increase above 1.4.

Recently, Li *et al* [58] further developed this approach to estimate the practical 2-D peak capacity according to:

$$n'_{2-D} = \frac{n_1 n_2}{\sqrt{1 + 3.35\left(\frac{^2t_c n_1}{^1t_g}\right)^2}} \qquad (\mathbf{4.2})$$

where n'_{2D} is the effective 2-D peak capacity, n_1 and n_2 the peak capacities in first and second dimensions, respectively, ^2t_c the second dimension cycle time and ^1t_g the first dimension gradient time. The fraction collection time, 1 minute, is substituted for the second dimension cycle time (^2t_c) since in our case off-line 2-D analyses were performed. Using 60 minutes for ^1t_g and 137 and 112 for second dimension peak capacities for cocoa and apple samples, respectively, this provides effective peak capacities of 3137 and 2334 for the off-line HILIC × RP-LC analyses of cocoa and apple samples (**Table 4.3**). These values are indeed commensurate with those obtained using the method of Liu *et al.* for the same analyses.

Considering that two different models, one focussing on orthogonality and second on under-sampling, provide similar results, we suggest that the practical peak capacities shown in **Table 4.3** represent an accurate reflection of the resolving power of the off-line HILIC × RP-LC method. This is indeed corroborated by the contour plots in **Figures 4.8** and **4.10.**

Clearly, the use of an off-line 2-D-LC approach places fewer restrictions on the 1st dimension sampling time: in an on-line system, the sampling rate is equal to the 2nd dimension analysis time, or at the best, half the second dimension analysis time [59]. The practical limitations encountered in achieving fast second dimension analyses therefore often result in under-sampling of first dimension peaks. In contrast, for off-line comprehensive analyses, very high sampling rates are in theory possible, the limiting factor in fact being the maximum total analysis time considered feasible. Moreover, since the off-line approach places no restrictions on analysis times, and especially flow rates, in each dimension, the resolving power of each of the two dimensions is maximally utilised. The use of relatively long gradients and optimal flow rates are therefore responsible for the exceptionally high practical peak capacities achieved here.

The effective peak capacity of the 2-dimensional separation also clearly illustrates the considerable benefit of off-line comprehensive 2-D LC analysis, when compared to

the peak capacities measured for each 1-dimensional separation. A comparison of comprehensive analyses using short and long RP-LC gradients in the second dimension (**Table 4.3**), shows that the practical peak capacity measured using the short gradient is less than half that achieved for the long gradient. The total time required for each of these analyses is ~4.5 and 26.5 hours, respectively. Despite these long analysis times, the gain in separation power provided by the off-line comprehensive LC method cannot be matched by any single dimensional LC analysis. Depending on the complexity of the sample of interest, on-line comprehensive 2-D LC combining similar 1-D separations may present a promising alternative for the fast analysis of procyanidins. It is clear from the precedent discussion that the associated reduction in second dimension analysis times, coupled to the challenges associated with achieving sufficient sampling rates, would result in much lower resolving power. However, an on-line system would provide the advantages of automation, faster analysis and less risk of analyte loss. Another option is to perform stop-and-go 2-D analysis, where the flow from the first dimension column is stopped while each fraction is analysed in the second dimension [60]. Analysis times for such methods are comparable to off-line comprehensive LC methods, although the approach also offers the advantage of automation and reduced risk of analyte loss. Current research in our laboratory is aimed at investigating these alternative methodologies.

In principle, the same approach should be equally suitable for analysis of non-procyanidin oligomeric phenolics. It should be noted that in the case of procyanidins, identification was simplified by the selectivity of fluorescence detection coupled to off-line MS analysis, whereas compounds lacking fluorescence properties might not be identified with the same ease.

4.4. Conclusions

An off-line comprehensive 2-dimensional LC method for the analysis of procyanidins has been developed. Oligomeric procyanidins were separated according to molecular weight using HILIC in the first dimension. In the second dimension, procyanidin isomers were separated using reversed phase LC. Contour plots were constructed using selective fluorescence detection.

Mass spectral data indicated that cocoa and apple procyanidins consist exclusively of catechin and epicatechin monomeric units. Oligomeric procyanidins up to dodecamers were detected in both apple and cocoa extracts using HILIC–ESI-MS, while isomers up to octamers were tentatively identified by RP-LC–ESI-MS analysis. In addition, A-type oligomers up to DP 6 and procyanidin-glycosides up to DP 7 were detected in cocoa samples.

The combination of two complementary separation mechanisms proved to be particularly effective due to the significantly improved resolution of oligomeric procyanidin isomers provided by the pre-separation according to degree of polymerisation in the HILIC mode. Visual interpretation of procyanidin content of the analysed samples is facilitated by the structured nature of contour plots, with molecular weight- and isomeric information easily ascertained from the 1-D and 2-D axes, respectively. HILIC and RP-LC separations were shown to provide high orthogonality ($r^2 < 0.2$), and the 2-dimensional system is characterised by exceptionally high practical peak capacities. Moreover, for the off-line approach utilised here, it is shown that virtually no additional band broadening results from under-sampling of first dimensional peaks.

The off-line HILIC × RP-LC method therefore represents an exceptionally powerful separation strategy for the detailed investigation of complex phenolic fractions. The developed methodology should be equally suitable for the analysis of other complex proanthocyanidin fractions, and could essentially be extended to other phenolic compounds. The on-line coupling of HILIC × RP-LC–MS, not attempted in the current study, would further enhance the applicability of the method.

4.5. References

[1] G.E. Adamson, S.A. Lazarus, A.E. Mitchell, R.L. Prior, G. Cao, P.H. Jacobs, B.G. Kremers, J.F. Hammerstone, R.B. Rucker, K.A. Ritter, H.H. Schmitz, J. Agric. Food Chem. 47 (1999) 4184.

[2] Y.J. Hong, F.A. Tomas-Barberan, A.A. Kader, A.E. Mitchell, J. Agric. Food Chem. 54 (2006) 2405.

[3] M. Karonen, J. Loponen, V. Ossipov, K. Pihlaja, Anal. Chim. Acta 522 (2004) 105.

[4] M.A. Kelm, J.C. Johnson, R.J. Robbins, J.F. Hammerstone, H.H. Schmitz, J. Agric. Food Chem. 54 (2006) 1571.

[5] L.Gu, M.A. Kelm, J.F. Hammerstone, Z. Zhang, G. Beecher, J. Holden, D. Haytowitz, R.L. Prior, J. Mass Spectrom. 38 (2003) 1272.

[6] L. Gu, M. Kelm, J.F. Hammerstone, G. Beecher, D. Cunningham, S. Vannozzi, R.L. Prior, J. Agric. Food Chem. 50 (2002) 4852.

[7] S.A. Lazarus, G.E. Adamson, J.F. Hammerstone, H.H. Schmitz, J. Agric. Food Chem. 47 (1999) 3693.

[8] T. Shoji, S. Masumoto, N. Moriichi, T. Kanda, Y. Ohtake, J. Chromatogr. A 1102 (2006) 206.

[9] L. Gu, M.A. Kelm, J.F. Hammerstone, G. Beecher, J. Holden, D. Haytowitz, R.L. Prior, J. Agric. Food Chem. 51 (2003) 7513.

[10] H.J. Li, M.L. Deinzer, Anal. Chem. 79 (2007) 1739.

[11] J.F. Hammerstone, S.A. Lazarus, A.E. Mitchell, R. Rucker, H.H. Schmitz, J. Agric. Food Chem. 47 (1999) 490.

[12] A. Yanagida, H. Murao, M. Ohnishi-Kameyama, Y. Yamakawa, A. Shoji, M. Tagashira, T. Kanda, H. Shindo, Y. Shibusawa, J. Chromatogr. A 1143 (2007) 153.

[13] J. Wollgast, L. Pallaroni, M.-E. Agazzi, E. Anklam, J. Chromatogr. A 926 (2001) 211.

[14] A. Yanagida, T. Kanda, T. Shoji, M. Ohnishi-Kameyama, T. Nagata, J. Chromatogr. A 855 (1999) 181.

[15] A. Yanagida, T. Kanda, T. Takahashi, A. Kamimura, T. Hamazono, S. Honda, J. Chromatogr. A 890 (2000) 251.

[16] S. Pati, I. Losito, G. Gambacorta, E.L. Notte, F. Palmisano, P.G. Zambonin, J. Mass Spectrom. 41 (2006) 861.

[17] J. Rigaud, M.T. Escribano-Bailon, C. Prieur, J.M. Souquet, V. Cheynier, J. Chromatogr. A 654 (1993) 255.

[18] R.L. Prior, S.A. Lazarus, G. Cao, H. Muccitelli, J.F. Hammerstone, J. Agric. Food Chem. 49 (2001) 1270.

[19] D.V. McCalley, U.D. Neue, J.Chromatogr. A 1192 (2008) 225.

[20] U. D. Neue, HPLC Columns, Theory, Technology and Practice, Wiley-VCH, New York, 1997, p217-223

[21] R. Mayer, G. Stecher, R. Wuerzner, R.C. Silva, T. Sultana, L. Trojer, I. Feuerstein, C. Krieg, G. Abel, M. Popp, O. Bobleter, G.K. Bonn, J. Agric. Food Chem. 56 (2008) 6959.

[22] D.R. Stoll, X. Li, X. Wang, P.W. Carr, S.E.G. Porter, S.C. Rutan, J. Chromatogr. A 1168 (2007) 3.

[23] P. Dugo, F. Cacciola, T. Kumm, G. Dugo, L. Mondello, J. Chromatogr. A 1184 (2008) 353.

[24] P. Jandera, J. Fischer, H. Lahovská, K. Novotná, P. Cesla, L. Kolárová, J. Chromatogr. A 1119 (2006) 3.

[25] P.Q. Tranchida, P. Dugo, G. Dugo, L. Mondello, J. Chromatogr. A 1054 (2004) 3.
[26] P. Dugo, V. Skerikova, T. Kumm, A. Trozzi, P. Jandera, L. Mondello, Anal. Chem. 78 (2006) 7743.
[27] S.P. Dixon, I.D. Pitfield, D. Perrett, Biomed. Chromatogr. 20 (2006) 508.
[28] I. François, A. de Villiers, P. Sandra, J. Sep. Sci. 29 (2006) 492.
[29] P.E. Toups, M.J. Gray, G.R. Dennis, N. Reddy, M.A. Wilson, R.A. Shalliker, J. Sep. Sci. 29 (2006) 481.
[30] C.J. Venkatramani, A. Patel, J. Sep. Sci. 29 (2006) 510.
[31] E. Blahová, P. Jandera, F. Cacciola, L. Mondello, J. Sep. Sci. 29 (2006) 555.
[32] F. Cacciola, P. Jandera, E. Blahová, L. Mondello, J. Sep. Sci. 29 (2006) 2500.
[33] F. Cacciola, P. Jandera, L. Mondello, J. Sep. Sci. 30 (2007) 462.
[34] P. Dugo, F. Cacciola, M. Herrero, P. Donato, L. Mondello, J. Sep. Sci. 31 (2008) 3297.
[35] T. Hájek, V. Skeríková, P. Cesla, K. Vynuchalová, P. Jandera, J. Sep. Sci. 31 (2008) 3309.
[36] P. Jandera, K. Vynuchalová, T. Hájek, P. Cesla, G. Vohralík, J. Chemometrics 22 (2008) 203.
[37] M. Kivilompolo, T. Hyötyläinen, J. Sep. Sci. 31 (2008) 3466.
[38] M. Kivilompolo, T. Hyötyläinen, J. Chromatogr. A 1145 (2007) 155.
[39] M. Kivilompolo, V. Oburka, T. Hyotylainen, Anal. Bioanal. Chem. 391 (2008) 373.
[40] S. Gómez-Alonso, E. García-Romero, I. Hermosín-Gutiérrez, J. Food Compos. Anal. 20 (2007) 618.
[41] J. Wollgast, E. Anklam, Food Res. Int. 33 (2000) 423.
[42] L.J. Porter, Z. Ma, B.G. Chan, Phytochemistry 30 (1991) 1657.
[43] H. Tanaka, X. Zhou, O. Masayoshi, J. Chromatogr. A 987 (2003) 119.
[44] R.M. Alonso-Salces, K. Ndjoko, E.F. Queiroz, J.R. Ioset, K. Hostettmann, L.A. Berrueta, B. Gallo, F. Vicente, J. Chromatogr. A 1046 (2004) 89.
[45] J.-S. Xiao, L. Liu, H. Wu, B.-J. Xie, E.-N. Yang, Z.-D. Sun, J. Agric. Food Chem. 56 (2008) 2096.
[46] D. Del Rio, A.J. Stewart, W. Mullen, J. Burns, M.E.J. Lean, F. Brighenti, A. Crozier, J. Agric. Food Chem. 52 (2004) 2807.
[47] L.-Z. Lin, P. Chen, J.M. Harnly, J. Agric. Food Chem. 56 (2008) 8130.
[48] C. Sanbongi, N. Osakabe, N. Midori, T. Takizawa, S. Gomi, T. Osawa, J. Agric. Food Chem. 46 (1998) 454.
[49] P.J. Schoenmakers, G. Vivo-Truyols, W.M.C. Decrop, J. Chromatogr. A 1120 (2006) 282.
[50] X. Wang, W. Li, H.T. Rasmussen, J. Chromatogr. A 1083 (2005) 58.
[51] Y. Liu, X. Xue, Z. Guo, Q. Xu, F. Zhang, X. Liang, J. Chromatogr. A 1208 (2008) 133.
[52] R. t'Kindt, M. Storme, D. Deforce, J. Van Bocxlaer, J. Sep. Sci 31 (2008) 1609.
[53] Z. Liu, D.G. Patterson, M.L. Lee, Anal. Chem. 67 (1995) 3840.
[54] U.D. Neue, J. Chromatogr. A 1079 (2005) 153.
[55] J.M. Davis, D.R. Stoll, P.W. Carr, Anal. Chem. 80 (2008) 461.
[56] J.V. Seeley, J. Chromatogr. A 962 (2002) 21.
[57] R.E. Murphy, M.R. Schure, J.P. Foley, Anal. Chem. 70 (1998) 1585.
[58] X. Li, D.R. Stoll, P.W. Carr, Anal. Chem. 81 (2009) 845.

[59] I. François, A. de Villiers, B. Tienpont, F. David, P. Sandra, J. Chromatogr. A 1178 (2008) 33.
[60] J.N. Fairchild, K. Horváth, G. Guiochon, J. Chromatogr. A 1216 (2009) 1363.

Chapter 5

Comprehensive Hydrophilic Interaction × Reversed Phase Liquid Chromatographic Analysis of Green tea Phenolics

5.1. Introduction

Tea, *Camellia sinensis*, is an evergreen plant species belonging to the Theaceae family which is grown throughout the world [1]. Tea is one of the most highly consumed beverages in the world [1-8]. The culture of tea drinking was adopted long ago in China (around 2700 B.C.) following its accidental discovery by the then Chinese emperor, Shen Nung [1]. Initially, tea was consumed as a refreshing and mood enhancing drink and for its pleasant taste and aroma [9]. However, much of the current increased consumption of tea is associated with the wide range of health benefits that tea is known to possess [9-12]. This knowledge is ancient considering that tea has long been used in China as a fluid supply for people suffering from infectious diseases [1,13]. However, detailed investigation of these supposed beneficial properties has only been carried out recently.

Tea has a very complex chemical composition comprising diverse groups of polyphenols, purine alkaloids, polysacharrides, amino acids, vitamins, lipids and volatiles [4,14]. Different processing methods, in addition to other factors such as climate, agronomic and horticultural practices, are responsible for the unique sensory characteristics (such as colour, taste and aroma) and chemical composition of each tea [8,12-17]. Tea can be categorised into green, oolong or black tea depending on the processing method following harvesting.

The enzyme polyphenol oxidase is responsible for the oxidative polymerisation of monomeric polyphenols into higher molecular weight (MW) phenolics [13]. The enzyme remains inactive until such time that the leaves are chopped, and only then does enzymatic oxidation of polyphenols take place [1]. In the preparation of green tea, fresh tea leaves are rolled and steamed or dried immediately after harvesting to inactivate the enzyme [1,8,11,14,18]. This prevents oxidation of monomeric units into higher oligomers, and as a result, green tea is composed mainly of catechins, which account for 30% of the dry weight [1,2,7,8,11,13,16,18,19]. For oolong tea, the leaves are allowed to stand for less than an hour (this process is referred to as fermentation) before the enzyme is inactivated, which allows for partial oxidation of monomers into higher oligomers [1,8,11,17]. In the case of black tea, the leaves are fermented for 3-6 hours before inactivation and this leads to oxidation of monomers into higher oligomers, mainly theaflavins and thearugibins, which constitute about 10% of black

tea dry weight [1,8,11,17]. In general, the sensory characteristics and chemical complexity becomes more pronounced with the degree of fermentation. Green and black teas are considered as the most potent teas, with catechins and theaflavins being the most biologically active components [17].

Tea catechins include (+) catechin (C), (-) epicatechin (EC), (+) gallocatechin (GC), (-) epigallocatechin (EGC), (-) epicatechin gallate (ECG) and (-) epigallocatechin gallate (EGCG) (**Figure 5.1**). EGCG is the most abundant catechin in green tea, accounting for 65% of the total catechin content, while catechin and gallocatechin are present at the lowest concentrations [11,15,18]. In addition to catechins, other compounds such as proanthocyanidins [20-22], phenolic acids, flavones, flavonols and their derivatives [8,23] are also present in green tea. Flavonols and phenolic acids contribute about 13% and 10% of green tea total phenolic constituents, respectively [8]. Proanthocyanidins are subdivided into various groups including procyanidins, which are polymers of catechin and epicatechin subunits, prodelphinidins, which are made up of gallocatechin and epigallocatechin units and propelargonidins, which are made up of afzelechin and epiafzelechin monomeric units. In addition, galloylated proanthocyanidin monomeric units also occur.

(a) Catechins

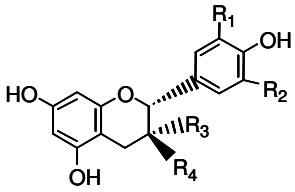

Flavan-3-ol	R1	R2	R3	R4
Catechin	H	OH	H	OH
Epicatechin	H	OH	OH	H
Gallocatechin	OH	OH	H	OH
Epigallocatechin	OH	OH	OH	H
Afzelechin	H	H	H	OH
Epiafzelechin	H	H	OH	H
Epiafzelechin gallate	H	H	Gallic acid ester	H
Epicatechin gallate	H	OH	Gallic acid ester	H
Epigallocatechin gallate	OH	OH	Gallic acid ester	H

(b) Proanthocyanidins

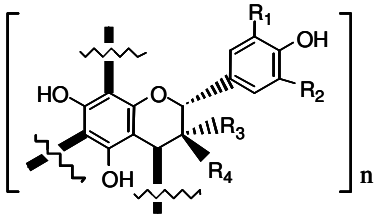

(c) Phenolic acids

Hydroxybenzoic acids

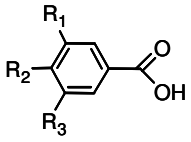

Hydroxycinnamic acids

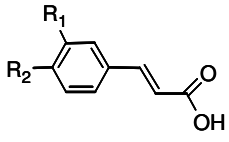

(d) Flavonols

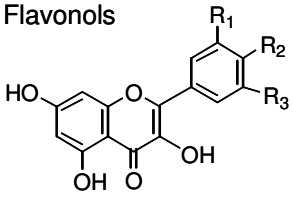

(e) Flavones

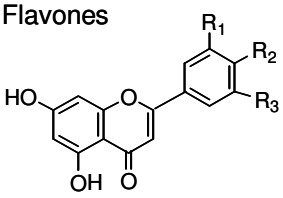

Figure 5.1: General structures of the principal green tea phenolics.

Green tea polyphenols, especially catechins, have been studied quite substantially, with emphasis mostly on their disease preventative aspects. Tea is associated with various health benefits including antibacterial, antioxidant, anti-cancer, anti-atherosclerotic, anti-aging, anti-HIV, anti-diabetic, anti-hypertensive and anti-inflammatory activities [7,14,17,24-33]. In addition, catechins contribute to the organoleptic properties of green tea such as astringency and bitterness [12,16]. Caffeine, which makes up about 4% of green tea, acts as a nervous system stimulant improving alertness and alleviating tiredness [12]. While these bioactive roles are well recognised *in vitro*, the underlying mechanisms for beneficial roles *in vivo* are yet to be fully established [11]. This is of particular importance considering the increased worldwide consumption of green tea as well as the increased use of green tea extracts in food-, pharmaceutical- and cosmetic additives [11]. However, to be able to do this, reliable analytical techniques for accurate determination and quantification of these compounds in foods and various biological systems are required.

High performance liquid chromatography (HPLC) and capillary electrophoresis (CE) are the most commonly used separation techniques for the analysis of green tea polyphenols. Reversed-phase (RP) LC coupled with UV- and mass spectrometric (MS) detection is frequently used, while UV and electrochemical detection (EC) are the most popular detection modes in CE. Both HPLC and CE allow good quantitation of the major phenolics in tea. However, complete separation of most phenolic compounds in tea, including minor components and especially the oligomeric and polymeric compounds, cannot be achieved using conventional HPLC and CE methods. RP-LC is the method of choice, but does not provide sufficient resolving power to enable complete resolution of all diverse phenolics in tea. For example, conventional C18 columns do not provide complete resolution of all tea phenolics in a single analysis [20,34,35], and often multiple methods are used to quantify proanthocyanidins, flavonols and phenolic acids [8,32]. The efficiency of a chromatographic separation can be improved by increasing the column length, decreasing the stationary phase particle size or by using multidimensional separation techniques to increase the separation space [36]. Given the finite peak capacity of 1-D LC methods, we investigated comprehensive 2-dimensional (2-D) LC using a small particle-packed column in the second dimension as a means of providing improved separation of tea phenolics. We have previously demonstrated that off-line comprehensive 2-D-LC coupling hydrophilic interaction chromatography (HILIC) with RP-LC provides a particularly powerful method for improved resolution of procyanidins in cocoa and apple extracts [37]. In the present report, this methodology is extended for the separation of green tea phenolics.

5.2. Experimental

5.2.1. Reagents and materials

Green tea (Freshpak brand) was purchased from a local supermarket. Standards of (-)-epicatechin and (±)-catechin as well as HPLC grade methanol, acetonitrile, formic acid and acetone were purchased from Sigma Aldrich (Steinheim, Germany). HPLC grade acetic acid was purchased from Riedel-de Haën (Seelze, Germany). Deionised water was obtained using a Milli-Q water purification system (Millipore, Milford, MA, USA). All solutions were filtered through 0.45 μm HVLP membrane filters (Millipore) and degassed in an ultrasonic bath (Branson Model 3510, Danbury, USA) before use.

5.2.2. Sample preparation

The sample was prepared using a modified method to that of Lazarus *et al* [38]. About 1.45 g (one teabag) of the finely ground material was extracted 3 times with 5 mL of 70% acetone in water (v/v). The suspension was centrifuged for 5 min at 5 000 *g* after every extraction and the supernatants were combined in a round bottom flask. Acetone was removed by rotary evaporation under reduced pressure at 40˚C, to give a final volume of ~4 mL. The remaining aqueous extract was filtered through a 0.45 μm PVDF filter membrane (Millipore). This sample was kept under nitrogen at 4˚C and was used for all the RP-LC analyses. For HILIC analyses, the sample was freeze dried and redissolved in 80% acetonitrile and 20% methanol (v/v).

5.2.3. Instrumentation

5.2.3.1. UPLC-PDA-fluorescence analyses

Analyses were performed on an Acquity UPLC system equipped with a binary pump, autosampler, column oven, photodiode array (PDA) detector (500 nL flow cell, 10 mm path length) and controlled by Waters Empower software (Waters, Milford, MA, USA). The UPLC mixing chamber was replaced with a low dead volume union, while the pump was connected to the injection valve using 0.1 mm ID tubing (Waters) to reduce the system dead volume. An HP 1046A programmable fluorescence detector (5 μL flow chamber, Agilent, Waldbronn, Germany) was connected to the UPLC

system downstream of the PDA detector. Fluorescence data were acquired using DAx 8.0 data acquisition software (Van Mierlo software, Amsterdam, The Netherlands).

5.2.3.2. UPLC-MS and MS^2 analyses

LC-MS and LC-MS^2 analyses were performed on a Waters Acquity UPLC system equipped with a binary solvent manager and autosampler. The UPLC system was interfaced through an electrospray ionisation (ESI) ion source to a Waters Ultima API quadrupole time-of-flight (Q-TOF) mass spectrometer. The mass spectrometer was operated in negative ionization mode with a capillary voltage of -3.7 kV and a cone voltage of 35 V. The source temperature was 100°C. Masses were scanned from 285 – 2025 amu and data were collected and processed using MassLynx v.4.0 software (Waters). The instrument was calibrated using a NaF solution. Since no lock-spray function was available on this instrument, *m/z* ratios are reported to one decimal place. For HILIC analyses, a desolvation temperature of 300ºC was used. The desolvation and cone gas flows (both N_2) were 300 L/h and 50 L/h, respectively. Collision energies of 20 or 25 V were used for MS^2 analyses. For RP-LC analyses, the desolvation temperature was 350ºC, and desolvation and cone gas flows (both N_2) were 350 L/h and 50 L/h, respectively. The eluent was split 1:7 prior to introduction into the ionisation chamber for RP-LC-ESI-MS analyses.

5.2.4. Chromatographic methods

5.2.4.1. Hydrophilic interaction chromatography (HILIC) analyses

Separations were performed on a Nomura Chemical Develosil Diol-100 column (250 × 1 mm i.d., 5 µm d_p, Aichi, Japan) using a method adapted from Kelm *et al* [39]. The binary mobile phase consisted of (A) acetonitrile and acetic acid (99:1, v/v) and (B) methanol, water and acetic acid (94.05: 4.95:1, %v/v/v). Separations were effected by a series of linear gradients of B into A as follows: 4-20% B (0-45 min), 20-40% B (45-50 min), 40-4% B (50-55 min). The column was re-equilibrated for 15 minutes. The flow rate was 0.050 mL/min. UV spectra were recorded between 200 – 500 nm with selective wavelength monitoring at 210 nm, 280 nm, 320 nm and 370 nm at an acquisition rate of 10 points/sec. Fluorescence detection was performed with

excitation at 276 nm and emission at 316 nm and a photomultiplier (PMT) gain of 5. Separations were performed at ambient temperature. For HILIC-PDA analyses, 10 µL was injected in the 'partial loop with needle overfill' mode using acetonitrile/HOAc (99:1, v/v) as the weak needle wash solvent. For HILIC-ESI-MS analyses, 4 µL was injected under the same conditions.

5.2.4.2. Reversed phase liquid chromatography analyses

RP-LC-PDA-fluorescence analysis was performed using two Zorbax SB-C18 columns (each 50 × 4.6 mm i.d., 1.8 µm, Agilent, Waldbronn, Germany) coupled in series and protected with a Phenomenex C18 guard column (4 × 3 mm i.d., Torrance, USA). The binary mobile phase consisted of 0.1% formic acid in water (v/v) (A) and acetonitrile (B). A linear gradient was performed as follows: 2% B (0-0.25 min), 2-18% B (0.25-10.70 min), 18-25% B (10.70-18.00 min), 25-100% B (18.00-20.70 min), 100% B until 22.50 min before returning to the initial conditions at 25.20 min. The column was re-equilibrated for 4.80 minutes before the next analysis. The flow rate was set to 0.8 mL/min and 2 µL was injected. Injections were performed in the partial loop with needle overfill mode using 0.1% formic acid as the weak needle wash. The column temperature was 50˚C. Fluorescence and UV detection was performed as for HILIC analyses. UPLC-ESI-MS analyses were performed using identical conditions as outlined above, with injection volumes of 4 µL using water as the weak needle wash.

5.2.5. Off-line 2-dimensional HILIC × RP-LC analyses

One-minute fractions (corresponding to 50 µL each) of the HILIC separations were automatically collected between 2 and 52 minutes using a programmable BIO-RAD Model 2110 fraction collector (Corston, UK). The collected fractions were transferred to 1.5 mL vials containing 250 µL inserts and kept under N_2 until analysed by gradient RP as detailed above. All fractions were analysed within 2 days of collection. Raw fluorescence and UV data for the RP analyses were exported into STATISTICA 8 (Statsoft Inc, US) to create 2-D contour plots.

5.3. Results and discussion

5.3.1. Method optimisation

Based on previous results for the analysis of cocoa and apple procyanidins presented in chapter 4, the combination of HILIC × RP-LC was investigated in the current study for the analysis of green tea phenolics. Individual 1-D LC methods used initially were the same as those used for the analysis of cocoa procyanidins [37]. However, because green tea does not contain high MW procyanidins, the HILIC gradient was slightly modified for better separation of catechins and catechin gallates which were poorly resolved under the optimal HILIC conditions for procyanidins. Under the new gradient conditions, not only were the compounds better resolved but a larger portion of the retention window was used, while keeping the analysis times the same. Individual fluorescence and UV chromatograms for the optimised HILIC and RP-LC separation of green tea phenolics are shown in **Figure 5.2 and 5.3**.

Various groups of phenolic compounds have been detected by UV at different wavelengths in both HILIC and RP-LC analyses. Since HILIC separation is based on differences in polarity, weakly-polar compounds eluted before highly-polar compounds. For instance, the gallocatechins were more retained than the catechins under these conditions. An elution sequence in order of increasing polarity was also observed for flavonols in HILIC. For example, kaempferol glycosides eluted before myricetin glycosides and flavonol monoglycosides were eluted before the corresponding diglycosides of the same parent aglycone.
Compounds which exhibited low retention in HILIC were generally spread across the entire separation window in RP-LC. In contrast, (epi)gallocatechins eluted before (epi)catechins, while their galloylated derivatives eluted later in RP-LC. For flavonol glycosides, the order of elution was reversed in RP-LC, with retention time decreasing with the number of sugars attached. The elution order in RP-LC is consistent with the elution sequence for these compounds reported by Santos-Buelga *et al* [40].

The employment of small particles and high temperature in the second dimension resulted in a highly efficient RP-LC separation. Numerous peaks were separated within 20 minutes, as evident in **Figure 5.3**. Both methods demonstrated good

repeatability with average %RSD for retention times between days (3 days) of 1.28% and 0.99% for HILIC and RP-LC, respectively.

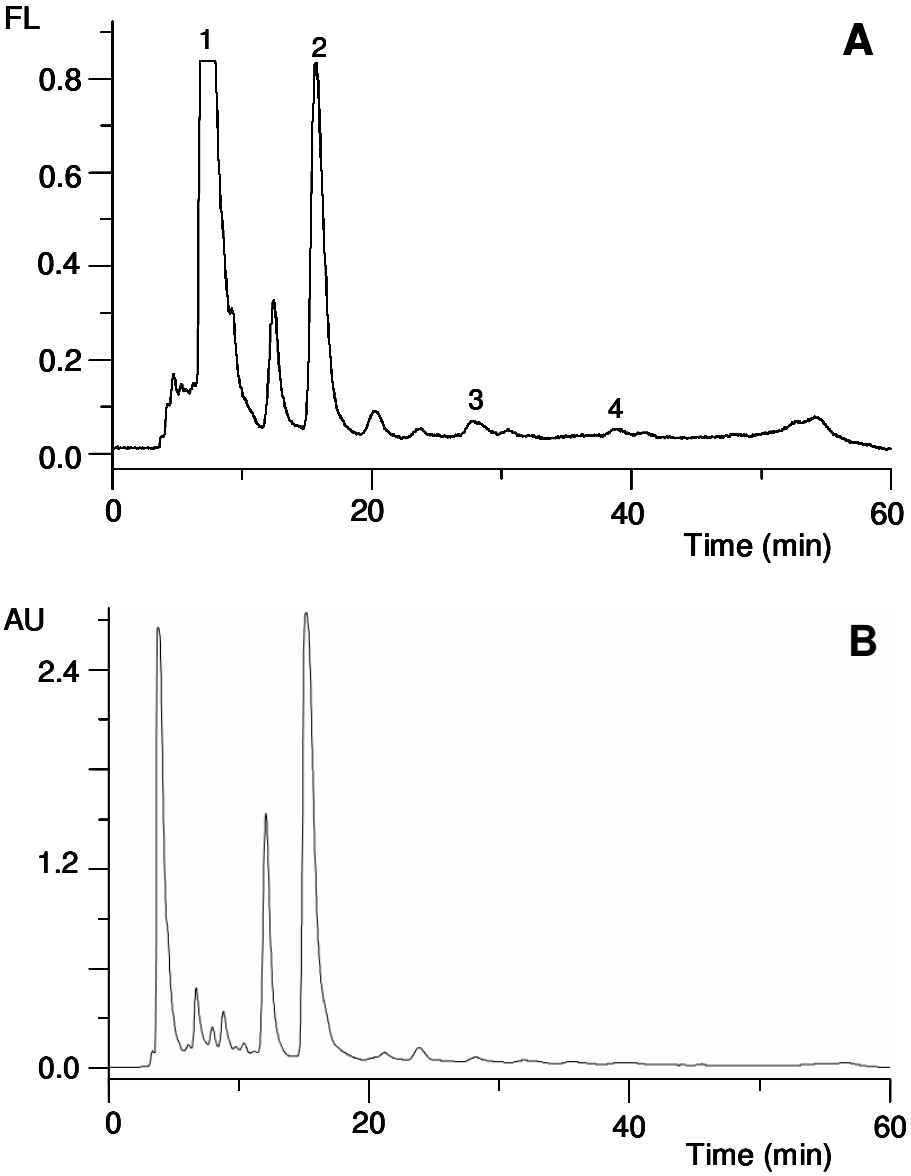

Figure 5.2: Fluorescence (A) and UV (280 nm) (B) chromatograms for the HILIC separation of the green tea extract. Injection volumes = 0.5 µL. Labels 1-4 indicate the DP of procyanidins identified by HILIC-ESI-MS.

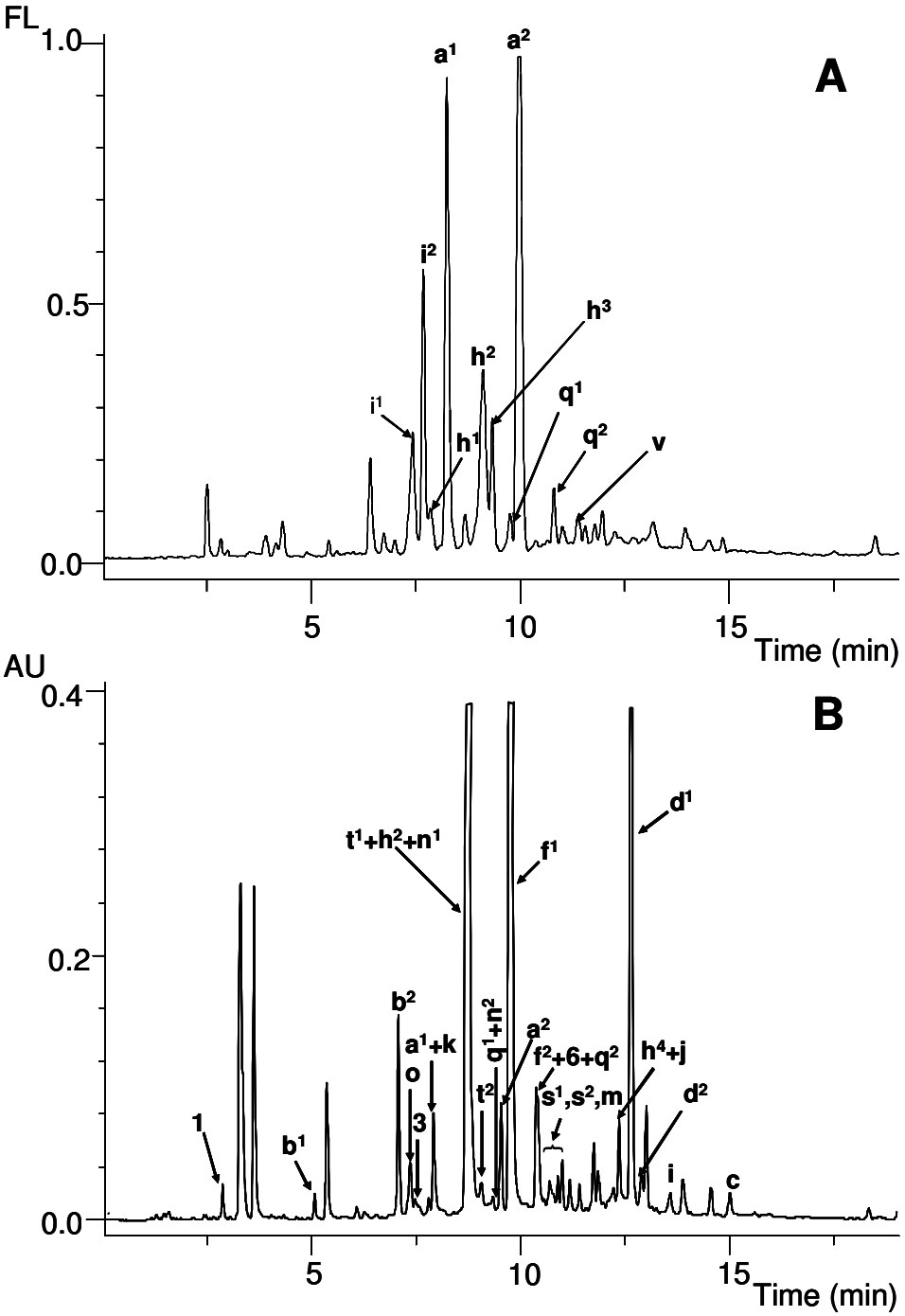

Figure 5.3: Fluorescence (A) and UV (280 nm) (B) chromatograms for the RP-LC separation of the green tea extract. Injection volumes = 4 µL for fluorescence and 0.5 µL for UV. See tables 1 and 2 for peak identification. Isomers with the same letters are differentiated by numbers in superscript fonts.

5.3.2. LC-ESI-MS analysis of green tea phenolics

Individual HILIC and RP-LC methods were combined with ESI-MS detection for tentative identification of compounds. Individual compounds were identified based on their singly and/or multiply charged ions, fragmentation patterns, correlation of the retention times to UV and/or fluorescence data, absorbance spectra as well as by comparison to literature data [8,20-22,32,34,35,38,41]. Catechin and epicatechin were identified by means of mass spectrometry and by comparison of retention times with authentic standards.

The mass spectral data indicated that green tea contains a very complex mixture of proanthocyanidins, in addition to other compounds. B-type procyanidin oligomers up to octamers could be identified, but no A-type oligomers were detected. Although several isomers of the higher procyanidin oligomers were detected, it should be noted that these compounds were present in relatively low concentrations and only oligomers up to tetramers were present in appreciable amounts. This is unsurprising considering that the processing method for green tea does not allow for polymerisation of monomeric units into higher oligomers.

As previously reported, a certain degree of heterogeneity exists in green tea [35,38]. Low MW oligomeric (up to DP = 3) prodelphinidins, propelargonidins, prodelphinidin/procyanidin copolymers and/or their galloylated derivatives were detected (**Table 5.1**), and in fact were found to be present in higher concentrations than procyanidins. It was also noted that galloylated oligomers were present in higher concentrations than their non-galloylated counterparts. This is consistent with previous observations [38]. (Epi)afzelechin gallate (*m/z* 425.2) and its methoxylated derivative (*m/z* 455.3) were the only ions detected from the propelargonidin class. The presence/absence of (epi)afzelechin monomeric units (*m/z* 273) could not be confirmed due to the mass scan range used (285 – 2025 amu), although these compounds have been reported in green tea previously [35]. The extracted ion chromatograms (EICs) for proanthocyanidin oligomers detected in the green tea extract by RP-LC-ESI-MS are shown in **Figure 5.4.** A summary of the predominant ions for each oligomer is presented in **Table 5.1**. Note that unambiguous

identification of individual isomers could not be established using mass spectral data alone.

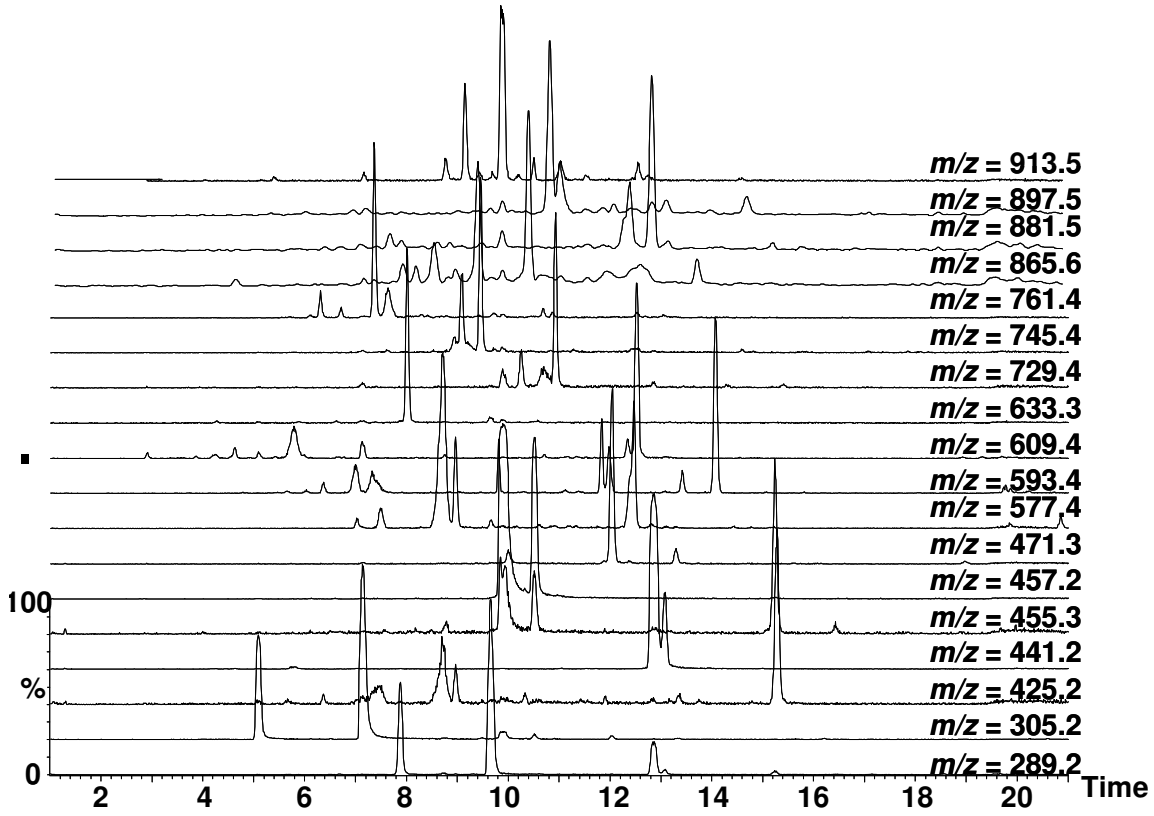

Figure 5.4: Stack plots of the individual extracted ion chromatograms for the proanthocyanidin oligomers detected in the RP-LC-ESI-MS analysis of the green tea extract. For identity of compounds, refer to **Table 5.1**.

In addition to proanthocyanidins, other phenolic compounds which were detected by UV at 320 nm and 370 nm, were tentatively identified by correlating their HILIC and RP-LC retention times, fragmentation patterns and by comparison with literature values [8,35,42] and are listed in **Table 5.2**. These included phenolic acids (caffeoylquinic acids, coumaroylquinic acids and galloylquinic acids), flavones (apigenin and derivatives) as well as flavonols (kaempferol, quercetin, myricetin and/or derivatives). However, some compounds presented in **Table 5.2** were detected by MS but were present in too low concentrations to be detected by UV, thus their absence in the contour plots (see further).

Table 5.1: A summary of the procyanidins, galloylated procyanidins, prodelphinidins, propelargonidins and copolymers detected in green tea

Peak label	$[M-H]^-$	Identity	Fragment ions (*m/z*)
a	289.2	(epi)catechin [8,32,34,35,38]	245, 205, 179
b	305.2	(epi)gallocatechin [8,32,34,35,38]	261, 221, 219, 179, 125
c	425.2	(epi)afzelechin gallate [35]	273, 255, 169
d	441.2	(epi)catechin gallate [8,32,34,35,38]	331, 289, 245, 169, 125
e	455.3	Methoxyepiafzelechin gallate [35]	289, 125
f	457.2	(epi)gallocatechin gallate [8,32,34,35,38]	331, 305, 169, 125
g	471.3	methylated (epi)gallocatechin gallate [41]	305, 183, 169, 125
h	577.4	(epi)catechin dimer [35,38]	451, 425, 299, 289
i	593.4	(epi)catechin-(epi)gallocatechin gallate [20] or (epi)catechin-(epi)gallocatechin	467, 441, 425, 289
j	609.4	(epi)gallocatechin dimer [20,35,38]	305
k	633.3	methyl (epi)gallocatechin gallate [35]	441, 289, 169
l	720.4[#]	(epi)catechin pentamer	577, 575, 289
m	729.4	(epi)catechin- (epi)catechin gallate [20,38]	577, 559, 451, 407, 289, 287, 169, 125
n	745.4	(epi)gallocatechin-(epi)catechin gallate or (epi)gallocatechin gallate-(epi)catechin [20,21,35,38]	289, 169, 125
o	761.4	(epi)gallocatechin gallate-(epi)gallocatechin* [20,22,38]	609, 457, 305, 169
p	864.6[#]	(epi)catechin hexamer	865, 720, 577, 575, 289
q	865.6	(epi)catechin trimer [20,35]	577, 407, 289
r	881.5	(epi)catechin gallate-(epi)catechin gallate [20] or (epi)catechin-(epi)catechin-(epi)gallocatechin*	593, 591, 577
s	897.5	(epi)gallocatechin-(epi)gallocatechin-(epi)catechin* [20,35,38]	289
t	913.5	(epi)gallocatechin trimer [38] or (epi)gallocatechin gallate – (epi)gallocatechin gallate [20]	716,743,591,573,423
u	1009.6[#]	(epi)catechin heptamer	577, 289
v	1153.8	(epi)catechin tetramer	1027, 1001, 983, 865, 863, 577, 575, 289

[#]Doubly charged ions, *exact sequences could not be established from MS data alone

Table 5.2: A summary of additional phenolic compounds tentatively identified in the green tea extract by RP-LC-ESI-MS.

Peak label	RP-LC Retention time	$[M-H]^-$	Compound	Fragment ions (*m/z*)
14	2.86	331.2	galloylglucose [35]	169, 125
13[a]	3.21	343.2	3-galloylquinic acid [8,35]	191, 169
13[b]	3.61	343.2	5-galloylquinic acid [8,35]	191, 169
8	7.42	483.3	1,6-digalloylglucose [35]	331, 169
1[a]	7.55	337.2	3-*p*-coumaroylquinic acid [8,35]	191, 173, 163
2	8.28	353.2	5-caffeoylquinic acid [8,35]	191, 179, 135
1[b]	9.36	337.2	5-*p*-coumaroylquinic acid [8,35]	191, 173, 163
10	10.58	635.3	1,2,6-trigalloylglucose [35]	483, 169
9[a]	11.01	563.4	apigenin glucosylarabinoside [35]	545, 473, 443, 353
9[b]	11.12	563.4	apigenin arabinosylglucoside [35]	545, 473, 443, 353
7[a]	11.16	479.3	myricetin galactoside [35]	316, 179
7[b]	11.35	479.3	myricetin glucoside [35]	316, 179
12[a]	11.57	771.5	quercetin galactosylrutinoside [35]	301
12[b]	11.91	771.5	quercetin glucosylrutinoside [35]	301
11[c]	12.14	755.5	quercetin dirhamnosylglucoside [35]	301
11[d]	12.25	755.5	quercetin dirhamnosylglucoside [35]	301
3[a]	12.34	609.4	quercetin-3-O-rhamnosylgalactoside [8,35]	301
3[b]	12.52	609.4	quercetin-3-rutinoside [8,35]	301
11[a]	12.53	755.5	kaempferol galactosylrutinoside [35]	285
16	12.58	533.3	apigenin dipentoside [35]	497
19	12.68	431.3	kaempferol-3-O-rhamnoside [35]	285
4[a]	12.83	463.3	quercetin-3-O-galactoside [35]	301
4[b]	13.11	463.3	quercetin-3-O-glucoside [35]	301
15[a]	13.16	739.5	unknown kaempferol conjugate	285
11[b]	13.19	755.5	kaempferol glucosylrutinoside [35]	285
17	13.42	593.4	kaempferol-3-O-rhamnosylgalactoside [35]	285
15[b]	13.76	739.5	kaempferol xylosylrutinoside [35]	285
17	14.07	593.4	kaempferol rutinoside [8,35]	285
5[a]	14.15	447.3	kaempferol galactoside [8,35]	285
5[b]	14.78	447.3	kaempferol glucoside [8,35]	285
18	18.55	1049.7	quercetin-3-O-acylglycoside [35]	301
18	19.43	1049.7	quercetin-3-O-acylglycoside [35]	301
6	19.79	301.1	quercetin [35]	273, 257, 179, 151, 107

5.3.3. Off-line HILIC × RP-LC analysis of green tea

The availability of a wide range of separation techniques with different selectivities in HPLC, suggests a large number of orthogonal combinations for 2-D LC systems [43]. However, some combinations, though orthogonal, are not feasible due to solvent immiscibility and mobile/stationary phase incompatibility [43,44]. Therefore, careful consideration is required in the design of 2-D LC systems, taking into account the fact that the first dimension eluent is the second dimension injection solvent [44]. Because HILIC and RP-LC are based on different separation mechanisms, the combination of

the two LC methods offers a highly orthogonal 2-D separation system [37,45-47]. Despite the compatibility of the solvents used in the two modes, the combination of these two methods is still problematic given that the primary eluent in either mode is a strong injection solvent in the secondary mode. Injection of a strong sample solvent results in peak distortion, and injection volumes on the second dimension column have to be limited due to this phenomenon.

Considering this limitation, different volumes of samples dissolved in HILIC mobile phases were injected onto the RP-LC columns in order to determine the highest volume that could be injected before peak distortion becomes apparent. 2 µL was found to be the maximum injection volume. The tea extract was freeze dried and redissolved in 80% acetonitrile and 20% methanol to allow relatively large injection volumes on the HILIC column for sufficient sensitivity in the second dimension. A 1 mm internal diameter (i.d.) column was employed in the first dimension so as to minimise on-column dilution. 4.6 mm i.d. columns were used in the second dimension for higher loadability. One-minute fractions (50 µL each) were collected into 1.5 mL vials with 250 µL inserts and kept under N_2 until analysed by RP-LC. Regardless of the small volumes injected in the second dimension, compounds were still detected with sufficient sensitivity by UV and fluorescence.

The fluorescence and UV contour plots for the HILIC × RP-LC analysis are presented in **Figure 5.5**. Given the structural relatedness of the catechin compounds, it is apparent from the 2-D plots that even in the absence of high molecular weight compounds, it was not possible to separate all the monomeric and dimeric compounds by either 1-dimensional LC method alone.

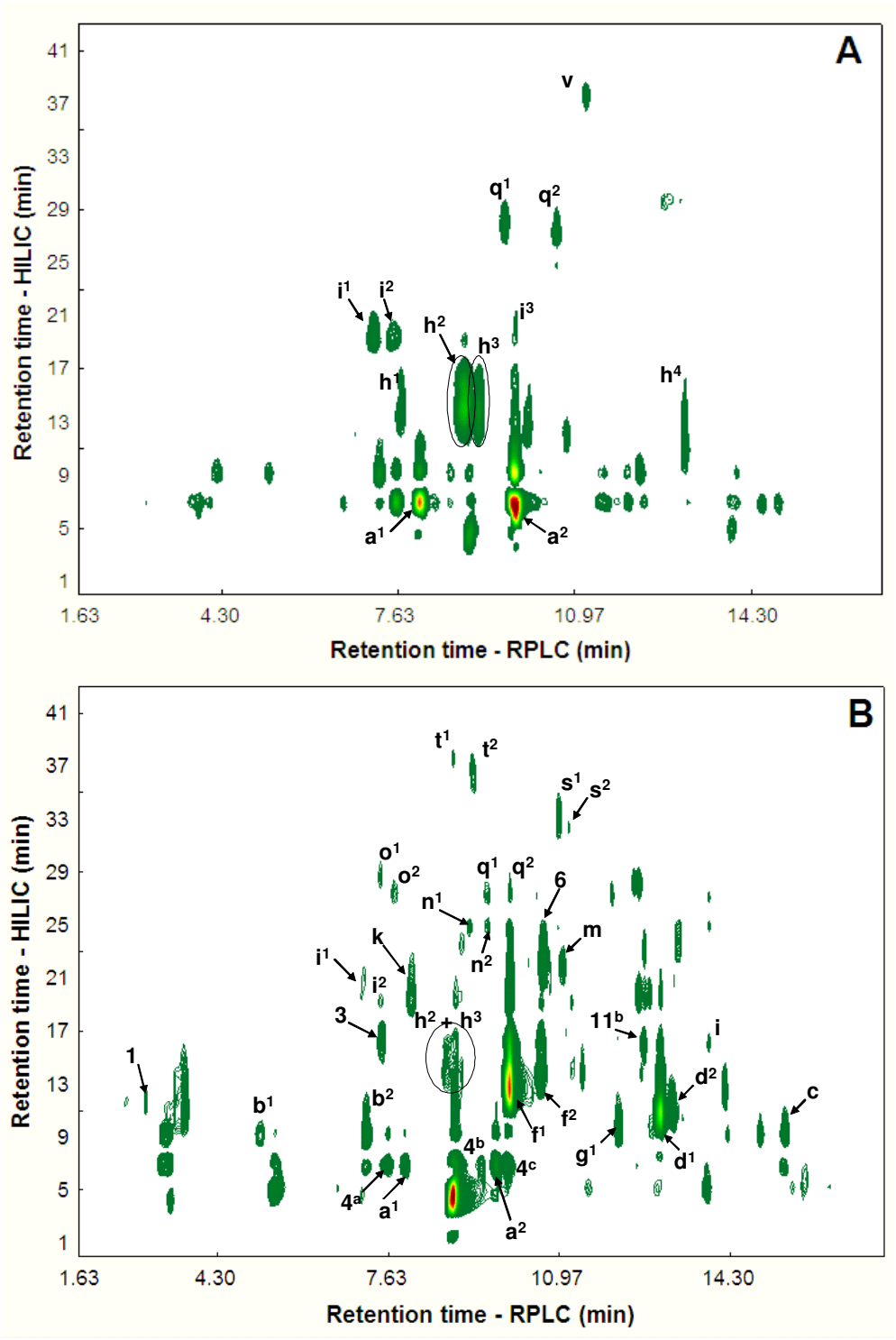

Figure 5.5: Fluorescence (A) and UV (280 nm) (B) contour plots of the HILIC × RP-LC analysis of the green tea extract. Refer to **Tables 5.1 and 5.2** for peak identification. Isomers with the same letters are distinguished by numbers in superscript fonts.

For example, it was not possible to separate all the compounds with similar letters (e.g. a^1 and a^2) by HILIC, but these are clearly resolved by RP-LC. On the other hand, compounds such as (epi)gallocatechin (f^2) and 1,2,6-trigalloylglucose (10),

(epi)gallocatechin gallate (f^1) and (epi)catechin trimer (q^2), (epi)catechin- (epi)catechin gallate (m) and (epi)gallocatechin-(epi)gallocatechin-(epi)catechin (s^1), (epi)catechin trimer (q^1) and (epi)gallocatechin-(epi)catechin gallate (n^2), (epi)gallocatechin trimer (t^1), (epi)catechin dimer (h^1) and (epi)gallocatechin-(epi)catechin gallate (n^1) as well as (epi)catechin dimer (h^2) and (epi)gallocatechin dimer (j), all co-elute in RP-LC, but are well resolved based on differences in polarity in HILIC. Similarly, contour plots of UV data at 320 nm and 370 nm as presented in **Figure 5.6** revealed the same occurrence. This indicates that the resolving power of 1-D LC techniques is not sufficient for complete resolution of green tea compounds, as peak overlap is inevitable.

Galloylated proanthocyanidins were found not to exhibit fluorescence properties as noted from the absence (or poor detection) of these compounds in the fluorescence 2-D plot. A similar observation was made by Gomez-Alonso *et al* [48] for (+)-catechin and (-) epicatechin gallates. Identification of proanthocyanidins based on UV data at 280 nm was hampered by the presence of other non-proanthocyanidin compounds which absorb at the same wavelength. However, the use of a diode-array detector further enhanced the system as it allowed simultaneous detection of all analytes at different wavelengths. Other compounds including cinnamic acids, flavonols and their glycosylated derivatives were detected using UV at 320 nm and 370 nm. However, unambiguous identity of each peak in **Figure 5.6** could not be established due to lack of reference standards.

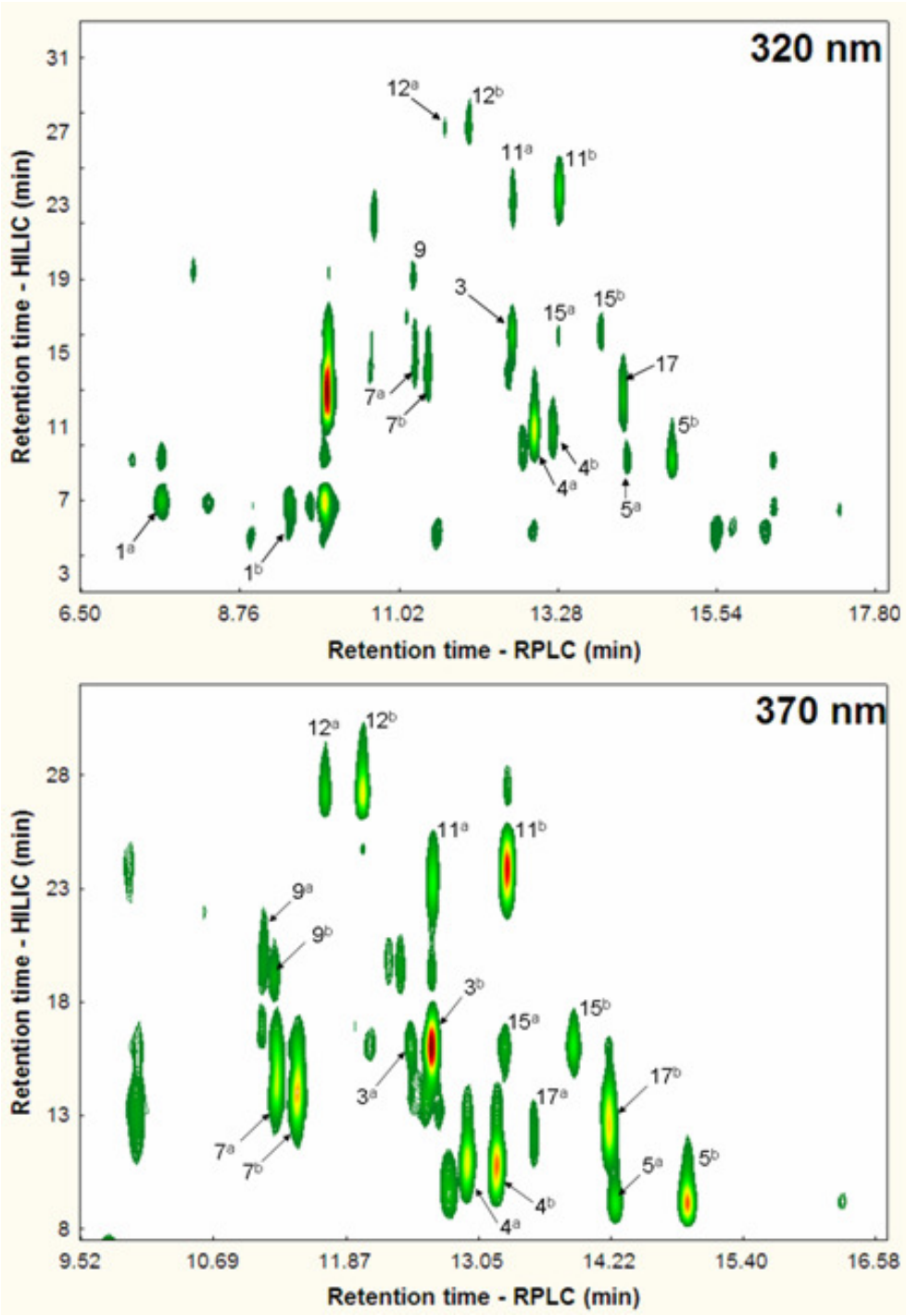

Figure 5.6: Contour plots of the HILIC × RP-LC analysis of the green tea extract, UV data at 320 nm and 370 nm. Refer to **Table 5.2** for tentative identification. Isomers with the same number are differentiated by letters in superscript fonts.

One of the benefits of multidimensional separations is the increased peak capacities offered by these systems. Ideally, the theoretical peak capacity of a comprehensive 2-dimensional separation is equal to the product of the peak capacities in each dimension [36,49,50]. However, it is required that the selected modes of separation be

uncorrelated (i.e. orthogonal) if this benefit is to be realised [36,49,50]. A correlation coefficient (r^2) obtained from the range-scaled retention times in the two dimensions may be used to assess the orthogonality of a 2-D system [49]. A plot of the scaled retention factors is shown in **Figure 5.7**.

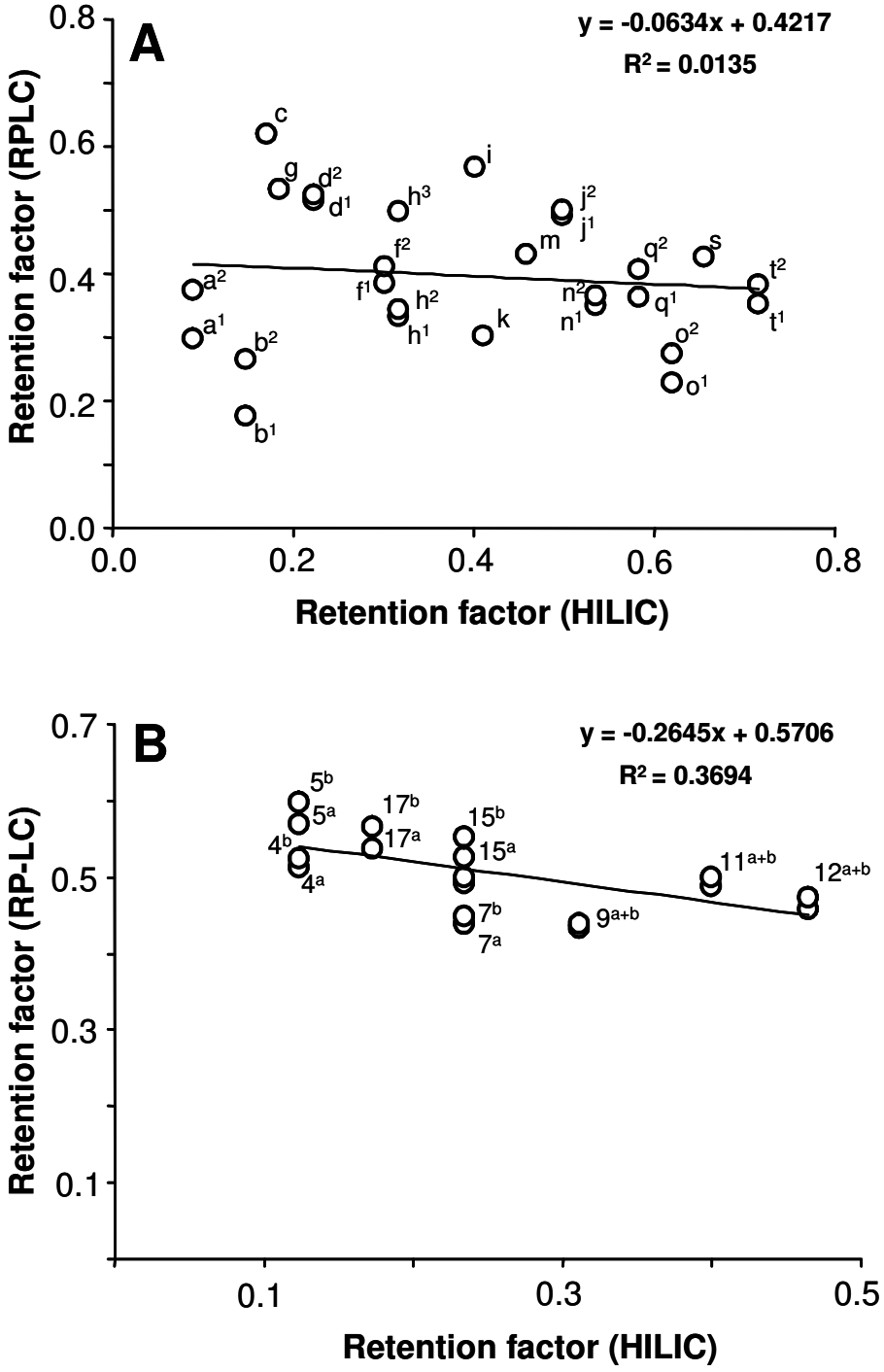

Figure 5.7: Plots of the scaled retention factors for the proanthocyanidin oligomers (A) and flavonols (B) tentatively identified by HILIC × RP-LC in the green tea extract.

For the proanthocyanidin 2-D system, an r^2 value of 0.0135 was obtained, which signifies high orthogonality. A practical peak capacity of 3556 was obtained using the method of Liu *et al* [49], implying an effective usage of the 2-D space which has a theoretical peak capacity of 3751. Peak widths in the HILIC separation ranged between 2.54 and 5.39 min (average peak width = 4.29 min), indicating sampling rates of 3 or more per first dimension peak for a fraction collection time of 1 min used here. This sampling rate is generally sufficient to avoid artificial band broadening due to first dimension under-sampling.

To further assess this phenomenon the peak capacities calculated according to the method of Liu *et al* [49] were compared to those obtained with the method of Li *et al* [51], which takes under-sampling, although not orthogonality into account. Although the method of Liu *et al* [49] does not account for under-sampling, no loss of peak capacity is expected to have resulted based on the sampling rate used in this analysis. Therefore, the peak capacities computed using the two methods are expected to be comparable. However, this was not the case: a lower value was obtained with the method of Li *et al* [51], which seems to indicate that some degree of under-sampling existed. A conclusive deduction could not be made in terms of which approach provides a more accurate estimation, considering that the two methods account for different parameters, which are both relevant in the determination of a 2-D peak capacity. A method taking both parameters into consideration would provide a better approximation. A summary of the peak capacities and related parameters is presented in **Table 5.3**.

Table 5.3: A summary of the parameters used to calculate the practical peak capacity

Parameter	Value		
	280 nm	**320 and 370 nm**	**Average**
[a]HILIC peak capacity, n_1	31	28	30
[a]RP peak capacity, n_2	121	125	123
[b]Correlation coefficient, r^2	0.0135	0.3694	0.1915
[c]Theoretical peak capacity, n_T	3751	3500	3626
[b]Practical peak capacity, n_p	3568	2535	3052
[d]Practical peak capacity, n_p	2725	2186	2456

[a] Calculated according to Neue [52].
[b] Calculated according to Liu *et al* [49].
[c] $n_T = n_1 \times n_2$.
[d] Calculated according to Li *et al* [51].

5.4. Conclusions

Green tea phenolics have been studied by comprehensive 2-dimensional liquid chromatography. The method reported herein allowed simultaneous detection of various classes of phenolic compounds, demonstrating the wide applicability of comprehensive HILIC × RP-LC analysis for phenolic compounds. Diode-array detection was found to provide a powerful qualitative tool, as it allowed simultaneous detection of mixtures of compounds at different wavelengths. Fluorescence detection could not be used for selective detection of compounds lacking fluorescent properties. Off-line HILIC × RP-LC analysis showed that green tea contains a complex composition of low molecular weight proanthocyanidins, with galloylated oligomers present in higher concentrations than non-galloylated oligomers. Even in the absence of high molecular weight compounds, complete resolution of all phenolics could not be achieved using either 1-D method alone, due to the structural similarity of the compounds present in green tea. The low correlation between the selected separation mechanisms afforded a 2-D system with an enhanced peak capacity. This illustrates that 2-D-LC offers an effective alternative approach to improve the resolving power of 1-D-LC for the analysis of complex phenolic fractions in natural products.

5.5. References

[1] J.H. Weisburger, Cancer Lett. 114 (1997) 315.
[2] N. Khan, H. Mukhtar, Life Sciences 81 (2007) 519.
[3] H. Wang, G.J. Provan, K. Helliwell, Trends Food Sci. Technol. 11 (2000) 152.
[4] C.D. Wu, G.-X. Wei, Nutrition 18 (2002) 443.
[5] D.A. Balentine, in Chi-Tang Ho, Chang. Y. Lee, M.-T. Huang (Editors), Phenolic compounds in food and their effects on health I, American Chemical Society, Washington DC, 1992, p. 102.
[6] J.H. Weisburger, F.-L. Chung, Food Chem. Toxicol. 40 (2002) 1145.
[7] D.S. Barbosa, J. Consum. Protect. Food Safety 2 (2007) 407
[8] D. Del Rio, A.J. Stewart, W. Mullen, J. Burns, M.E.J. Lean, F. Brighenti, A. Crozier, J. Agric. Food Chem. 52 (2004) 2807.
[9] S.M. Lee, S.-J. Chung, O.-H. Lee, H.-S. Lee, Y.-K. Kim, K.-O. Kim, J. Sens. Stud. 23 (2008) 450.
[10] Y. Yoshida, M. Kiso, T. Goto, Food Chem. 67 (1999) 429.
[11] N.T. Zaveri, Life Sciences 78 (2006) 2073.
[12] U.D. Uysal, Z. Aturki, M.A. Raggi, S. Fanali, J. Sep. Sci. 32 (2009) 1002.
[13] Y.-S. Lin, Y.-J. Tsai, J.-S. Tsay, J.-K. Lin, J. Agric. Food Chem. 51 (2003) 1864.
[14] A.B. Sharangi, Food Res. Int. 42 (2009) 529.
[15] L. Yao, N. Caffin, B. D'Arcy, Y. Jiang, J. Shi, R. Singanusong, X. Liu, N. Datta, Y. Kakuda, Y. Xu, J. Agric. Food Chem. 53 (2005) 6477.
[16] J.-K. Lin, C.-L. Lin, Y.-C. Liang, S.-Y. Lin-Shiau, I.M. Juan, J. Agric. Food Chem. 46 (1998) 3635.
[17] J.A. Vinson, Y.A. Dabbagh, Nutr. Res. 18 (1998) 1067.
[18] M.W.L. Koo, C.H. Cho, Eur. J. Pharmacol. 500 (2004) 177.
[19] C.J. Dufresne, E.R. Farnworth, J. Nutr. Biochem. 12 (2001) 404.
[20] A. Kiehne, C. Lakenbrink, U.H. Engelhardt, Z Lebensm Unters Forsch A 205 (1997) 153.
[21] G.-I. Nonaka, R. Sakai, I. Nishioka, Phytochemistry 23 (1984) 1753.
[22] C. Lakenbrink, U.H. Engelhardt, V. Wray, J. Agric. Food Chem. 47 (1999) 4621.
[23] K.R. Price, M.J.C. Rhodes, K.A. Barnes, J. Agric. Food Chem. 46 (1998) 2517.
[24] M.P. Williamson, T.G. McCormick, C.L. Nance, W.T. Shearer, J. Allergy Clin. Immunol. 118 (2006) 1369.
[25] C.L. Nance, W.T. Shearer, J. Allergy Clin. Immunol. 112 (2003) 851.
[26] C.L. Nance, E.B. Siwak, W.T. Shearer, J. Allergy Clin. Immunol. 123 (2009) 459.
[27] C.L. Nance, A. Victores, S. Ali, W.T. Shearer, J. Allergy Clin. Immunol. 121 (2008) S229.
[28] C.L. Nance, M.P. Williamson, T.G. McCormick, S.M. Paulson, W.T. Shearer, J. Allergy Clin. Immunol. 117 (2006) S325.
[29] K. Kawai, N.H. Tsuno, J. Kitayama, Y. Okaji, K. Yazawa, M. Asakage, N. Hori, T. Watanabe, K. Takahashi, H. Nagawa, J. Allergy Clin. Immunol. 112 (2003) 951.
[30] M. Zhang, C. Holman, J. D'Arcy, J.-p. Huang, X. Xie, Carcinogenesis 28 (2007) 1074.

[31] H. Negishi, J.-W. Xu, K. Ikeda, M. Njelekela, Y. Nara, Y. Yamori, J. Nutr. 134 (2004) 38.
[32] A.J. Stewart, W. Mullen, A. Crozier, Mol. Nutr. Food Res. 49 (2005) 52.
[33] E. Blahova, E. Brandsteterova, A. Fabulova, J. Liq. Chromatogr. Relat. Technol. 27 (2004) 31.
[34] P. Miketova, K.H. Schram, J. Whitney, M. Li, R. Huang, E. Kerns, S. Valcic, B.N. Timmermann, R. Rourick, S. Klohr, J. Mass Spectrom. 35 (2000) 860.
[35] L.-Z. Lin, P. Chen, J.M. Harnly, J. Agric. Food Chem. 56 (2008) 8130.
[36] S.P. Dixon, I.D. Pitfield, D. Perrett, Biomed. Chromatogr. 20 (2006) 508.
[37] K.M. Kalili, A. de Villiers, J. Chromatogr. A 1216 (2009) 6274.
[38] S.A. Lazarus, G.E. Adamson, J.F. Hammerstone, H.H. Schmitz, J. Agric. Food Chem. 47 (1999) 3693.
[39] M.A. Kelm, J.C. Johnson, R.J. Robbins, J.F. Hammerstone, H.H. Schmitz, J. Agric. Food Chem. 54 (2006) 1571.
[40] C. Santos-Buelga, C. Garcia-viguera, F.A. Tomas-Barberan, in C. Santos-Buelga, G. Williamson (Editors), Methods in polyphenol analysis, The Royal Society of Chemistry, Cambridge, 2003, p. 102.
[41] R. Amarowicz, F. Shahidi, Food 47 (2003) 21.
[42] M.N. Clifford, K.L. Johnston, S. Knight, N. Kuhnert, J. Agric. Food Chem. 51 (2003) 2900.
[43] P.Q. Tranchida, P. Dugo, G. Dugo, L. Mondello, J. Chromatogr. A 1054 (2004) 3.
[44] P.J. Schoenmakers, G. Vivo-Truyols, W.M.C. Decrop, J. Chromatogr. A 1120 (2006) 282.
[45] X. Wang, W. Li, H.T. Rasmussen, J. Chromatogr. A 1083 (2005) 58.
[46] Y. Liu, X. Xue, Z. Guo, Q. Xu, F. Zhang, X. Liang, J. Chromatogr. A 1208 (2008) 133.
[47] R. t'Kindt, M. Storme, D. Deforce, J. Van Bocxlaer, J. Sep. Sci. 31 (2008) 1609.
[48] S. Gómez-Alonso, E. García-Romero, I. Hermosín-Gutiérrez, J. Food Comp. Anal. 20 (2007) 618.
[49] Z. Liu, D.G. Patterson, M.L. Lee, Anal. Chem. 67 (1995) 3840.
[50] F. Cacciola, P. Jandera, E. Blahová, L. Mondello, J. Sep. Sci. 29 (2006) 2500.
[51] X. Li, D.R. Stoll, P.W. Carr, Anal. Chem. 81 (2009) 845.
[52] U.D. Neue, J. Chromatogr. A 1079 (2005) 153.

Chapter 6

On-line Comprehensive 2-Dimensional Hydrophilic Interaction × Reversed Phase Liquid Chromatography Analysis of Cocoa and Apple Procyanidins

6.1. Introduction

Since its first application in 1978 [1], two dimensional liquid chromatography (2-D LC) has increasingly been used as a tool for the analysis of complex samples. This development was prompted by the greater need for high resolving power required for the separation of complex samples [2]. By combining orthogonal separations, 2-D LC techniques offer much higher peak capacities than can be achieved by 1-dimensional LC [1,3]. Because these techniques are able to combine uncorrelated information in a single 2-D separation space, the peak capacities of such systems are in ideal cases multiplicative [2-4]. Although truly orthogonal separation mechanisms are hard to achieve in practice because of unavoidable retention correlations between dimensions [2,4,5], the combination of less correlated separation mechanisms often results in peak capacities comparable to the ideal.

2-D-LC may be performed in either heart-cutting or comprehensive modes. In the heart-cutting approach, only certain fractions of the first dimension effluent are re-analysed in the second dimension [4,6,7]. Although this allows detailed characterisation of specific parts of the sample, information on the rest of the sample is lost [6,7]. In comprehensive 2-D separations, the entire sample is subjected to two independent separation mechanisms, either in an on-line or off-line manner [2-5,8]. Off-line comprehensive LC involves the collection of fractions from the first dimension before their re-injection on the second dimension column. Although these systems are often preferred due to simplicity and high peak capacities [6], they can be time consuming, difficult to automate, prone to artefact formation and reproducibility may be low [1,4,6-8]. In on-line comprehensive separations, fractions from the first dimension are subjected to a secondary separation in a continuous manner, usually achieved by means of a high pressure switching valve [2,4,5,8]. While this offers advantages of ease of automation and high analytical reproducibility, these systems often require specific interfaces that are difficult to design and operate [4,5,8].

Quite a large number of comprehensive 2-D LC systems have been developed for the analysis of complex real-life samples, particularly in the areas of biomedical research and pharmaceuticals [4]. Phenolic compounds have also received attention in this regard, but only recently. These compounds have been studied quite considerably

over the years because of their well-recognised beneficial health roles. However, phenolic analysis is a daunting analytical challenge due to the diversity and complexity of their structures [9,10]. Therefore, there is still a demand for high resolution analytical techniques for polyphenol analysis. Various 2-D systems utilising reversed phase LC (RP-LC) × RP-LC [11-15], RP-LC × high temperature RP-LC [16,17], RP-LC × ion-pair chromatography [18,19] as well as RP-LC × ion-exchange chromatography using both solvent and temperature programming [16,20] have been developed for the analysis of phenolic and flavone antioxidants in a variety of samples. However, most of this work focussed on phenolic acids and flavonols only. No comprehensive on-line LC × LC method for the analysis of procyanidins has been reported to date. We have successfully developed an off-line hydrophilic interaction chromatography (HILIC) × RP-LC method for procyanidin analysis [21]. While this method offers advantages of exceptionally high peak capacities and ease of operation, it is relatively time-consuming and laborious. Therefore, the development of an on-line system may be beneficial to allow automation, faster analysis and better reproducibility. This chapter presents initial results for the development of an on-line HILIC × RP-LC method for procyanidin analysis.

6.2. Materials and Methods

All reagents and materials used in this experiment are the same as those outlined in chapter 4. Apple and cocoa samples were prepared using the same procedures described in chapter 4.

6.2.1. Experimental conditions

In the first dimension (HILIC), analyses were performed on a Waters Acquity UPLC system equipped with a binary pump, autosampler, column oven, photodiode array (PDA) detector (500 nL flow cell, 10 mm path length) and controlled by Waters Empower software (Waters, Milford, MA, USA). The UPLC mixing chamber was replaced with a low dead volume union and the pump outlet tubing was replaced with a 0.1 mm i.d. tubing (Waters) to reduce the system dead volume. Separations were performed on a Nomura Chemical Develosil Diol-100 column (250 mm × 1 mm i.d., 5μm d_p, Aichi, Japan) at ambient temperature using a method adapted from Kelm *et al* [22]. The binary mobile phase consisted of (A) acetonitrile and acetic acid (99:1, v/v) and (B) methanol, water and acetic acid (94.05: 4.95:1, v/v/v). Separations were performed using the following gradient conditions: 4-40% B (0–425 min), 40 % B isocratic (425-473 min), 40–4% B (473–520 min). The flow rate was 0.005 mL/min and 5 μL of the cocoa and apple extracts were injected.

An HP 1090 Liquid Chromatograph equipped with a binary pump, a fan oven compartment, a UV detector and controlled by Agilent Chemstation software (Agilent, Waldbronn, Germany) was used in the second dimension. Data were acquired on an HP 1046A programmable fluorescence detector (5 μL flow chamber) using DAx 8.0 data acquisition software (Van Mierlo software, Amsterdam, The Netherlands). Separations were performed on an Agilent Zorbax SB-C18 column (50 mm × 4.6 mm i.d., 1.8 μm) protected with a Phenomenex C18 guard column (4 mm × 3 mm i.d., Torrance, USA) using an isocratic mobile phase consisting of 20% acetonitrile/80% 0.1% formic acid. The flow rate was 1.00 mL/min and the column temperature was 50 °C.

The two instruments were interfaced through two 6-port switching valves (Spark Holland Prospekt-SDU Model 795/796, Emmen, The Netherlands) with two identical

sample loops (50 µL each) as shown in **Figure 6.1**. 0.13 mm i.d. connection tubing of minimal length was used to minimise extra-column volume. A make-up flow of 20 µL/min deionised H_2O provided by a syringe pump (Harvard Apparatus, South Natick, USA) was added to the 1st dimension effluent prior to injection onto the 2nd dimension column, resulting in a total injection volume of 50 µL. The switching valves were manually started at the beginning of each 1st dimension gradient. Fractions from the first dimension were alternately trapped in the sampling loops and valves were automatically switched every 2nd minute. Two-minute chromatograms were acquired through a remote start signal from the switching valves. The data were exported into STATISTICA 8 (Statsoft Inc, US) to create 2-D or 3-D plots.

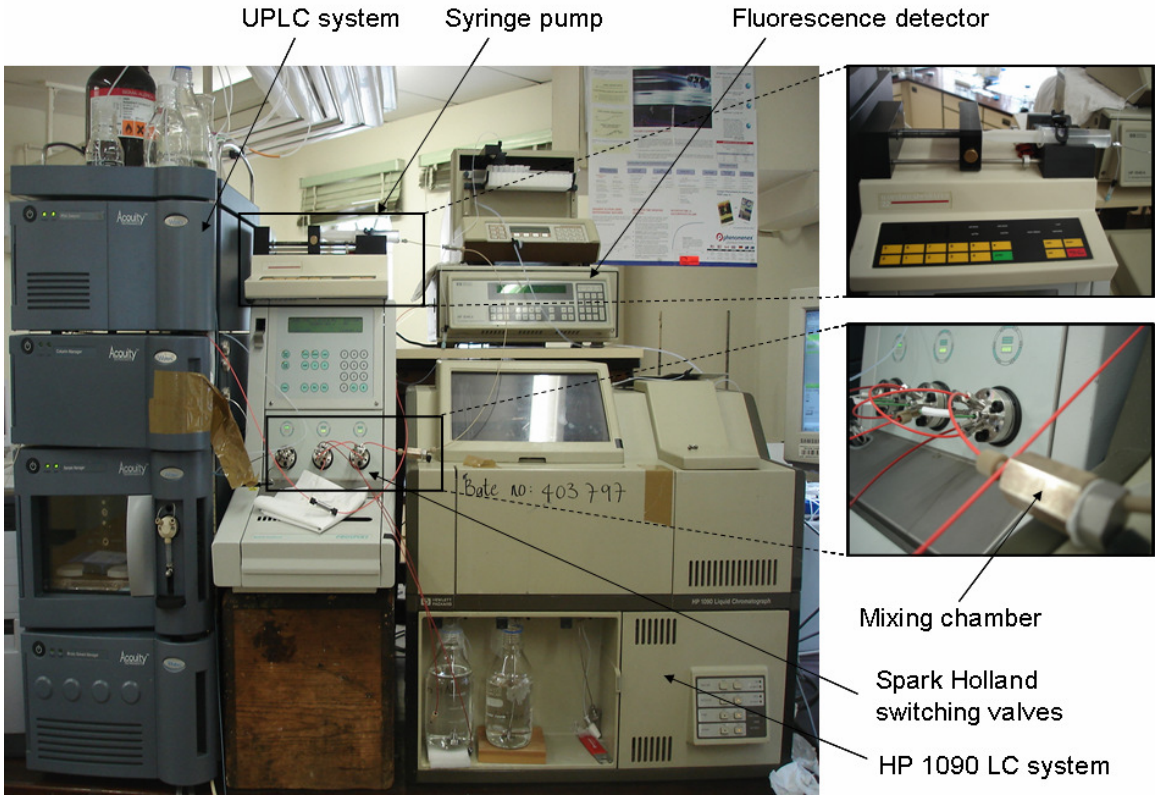

Figure 6.1: Instrumental setup for the online 2-D system.

6.3. Results and discussion

6.3.1. Method optimisation

The design of a comprehensive 2-D LC method involves selection of well-matched column dimensions, flow rates, injection volumes, mobile phase compositions as well as elution modes to be used in the two dimensions. Following successful off-line coupling of the two separation methods, an on-line coupling was investigated as a means of automating the system for better reproducibility and operation reliability as well as minimising the risk of analyte degradation associated with off-line analysis. Before on-line coupling of the two methods, each method was optimised independently so as to maximize peak capacities in each 1-D separation.

For on-line 2-D analysis, the second dimension separation needs to be carried out relatively fast to enable sufficient sampling of the first dimension peaks. This can be achieved using short columns and high flow rates, although at the cost of peak capacity. Reduction in the stationary phase particle size results in high efficiency but at the expense of increased pressure. Since the maximum operating pressure for this system was 400 bar (for the switching valves and the HP 1090 LC system), acetonitrile was selected for its low viscosity. A column temperature of 50°C was used to reduce the mobile phase viscosity further to allow higher flow rates and to benefit from faster mass transfer of solutes [23,24]. A short, conventional bore column packed with small particles was employed in the second dimension for high efficiency, loadability and faster separations because it permits the use of higher flow rates.

An isocratic elution presented a straightforward starting point for the second dimension, because of ease of execution and since no column equilibration is required before fraction transfer, as is the case with gradient analysis. Column re-equilibration was found to reduce the available separation time to less than 30 sec for a 2 min collection time under gradient conditions. With this in mind, it was imperative to determine the best mobile phase composition and flow rate that provides a reasonable separation and allows for elution of all compounds within the sampling period. Elution of all compounds within the sampling period is necessary to avoid the "wraparound" effect, which could hamper the interpretation of contour plots. 20%

acetonitrile/80% 0.1% formic acid provided a reasonable separation in 2 minutes at a flow rate of 1 mL/min under 400 bar. A chromatogram for the cocoa extract under these conditions is presented in **Figure 6.2A**.

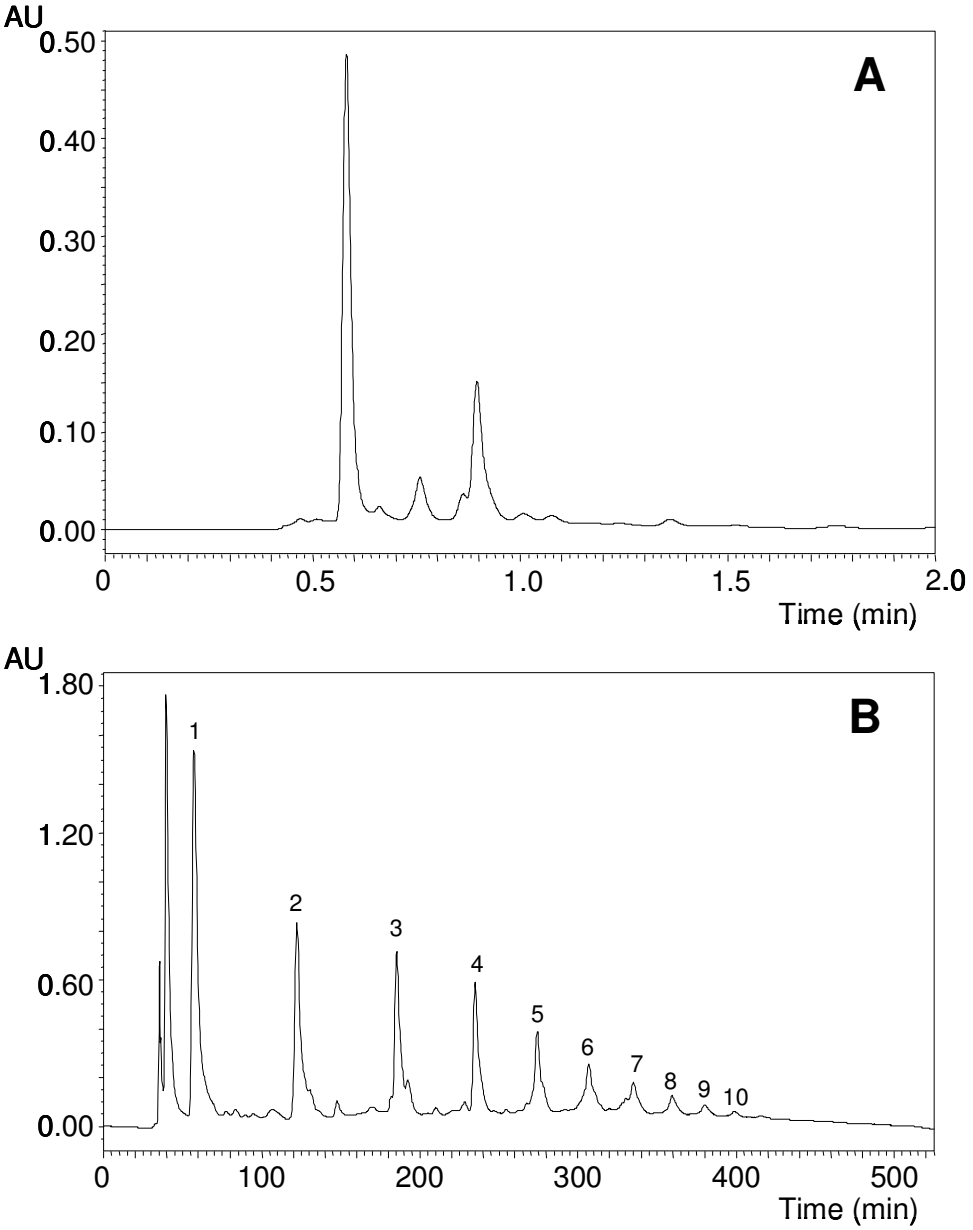

Figure 6.2: UV chromatograms of the cocoa separation under optimal isocratic RP conditions, 0.1 µL injection (A) and HILIC conditions at 5 µL/min, 2 µL injection (B). The numbers indicate degree of polymerisation (DP).

Subsequently, different volumes of samples dissolved in HILIC solvents were injected onto the RP column in order to establish the highest volume that could be injected without compromising chromatographic performance. 2 µL was found to be the maximum. However, an injection of 2 µL for a 2 minute analysis implied a flow

rate of 1 µL/min in the first dimension, which translates into an unreasonable analysis time of 43.3 hours. This is also significantly below the optimal linear velocity and would lead to loss of efficiency and resolution in the first dimension. A flow rate of 5 µL/min was therefore selected in the first dimension, resulting in a more practical (although still very long) analysis time (8.7 hrs) and better efficiency on the 1 mm i.d. column used here. In order to avoid band broadening associated with injection of 5 µL of HILIC solvents onto a RP column, water was added post-column to the HILIC effluent (20 µL/min). This ensured that the final injection solvent was similar to the RP-LC mobile phase (i.e. 80% water) and 50 µL could be injected without any apparent band broadening. The dilution caused by this approach was still acceptable in terms of overall sensitivity of the 2-D analysis.

For the HILIC analysis, the gradient previously optimised in the off-line analysis was adapted to a flow rate of 5 µL/min. The same separation was maintained, except that peak widths were in the order of 5-20 min for cocoa and 4.5-24 min for apple (**Figure 6.2B**). This is however beneficial for comprehensive 2-D analysis, since it allowed sufficient sampling of the first dimension peaks.

6.3.2. Evaluation of the on-line HILIC × RP-LC system

Initial results of the off-line analysis indicated that the resolution of procyanidin isomers is greatly reduced under short gradient conditions. Considering the fact that resolution of complex samples is generally poor under isocratic conditions, complete separation of these complex samples within the specified time frame was not anticipated. Nevertheless, complete separation is not required due to the pre-separation in the first dimension. The contour plots for the online analysis of cocoa and apple extracts are shown in **Figure 6.3**. As evident from the contour plots, poor separation was achieved in the second dimension. However, this is only partly due to the isocratic elution: partial separation is obscured by detector saturation and therefore resulted in very broad peaks in the second dimension. This greatly affected the peak capacity in the second dimension. From **Figure 6.3A**, it can clearly be seen that the HILIC separation was maintained and different DP oligomers are distinguishable. For example, the monomeric units are separated from the A type dimers, which elute just before the dimeric oligomers, followed by dimeric glycosides, etc. A small degree of

resolution has also been achieved in the second dimension, at least two distinct peaks (although not so obvious from the contour plot) could be seen for the monomers and dimers. Undoubtedly, a small injection volume in the first dimension would give better results. However, this could not be remedied in this study due to instrumental breakdown.

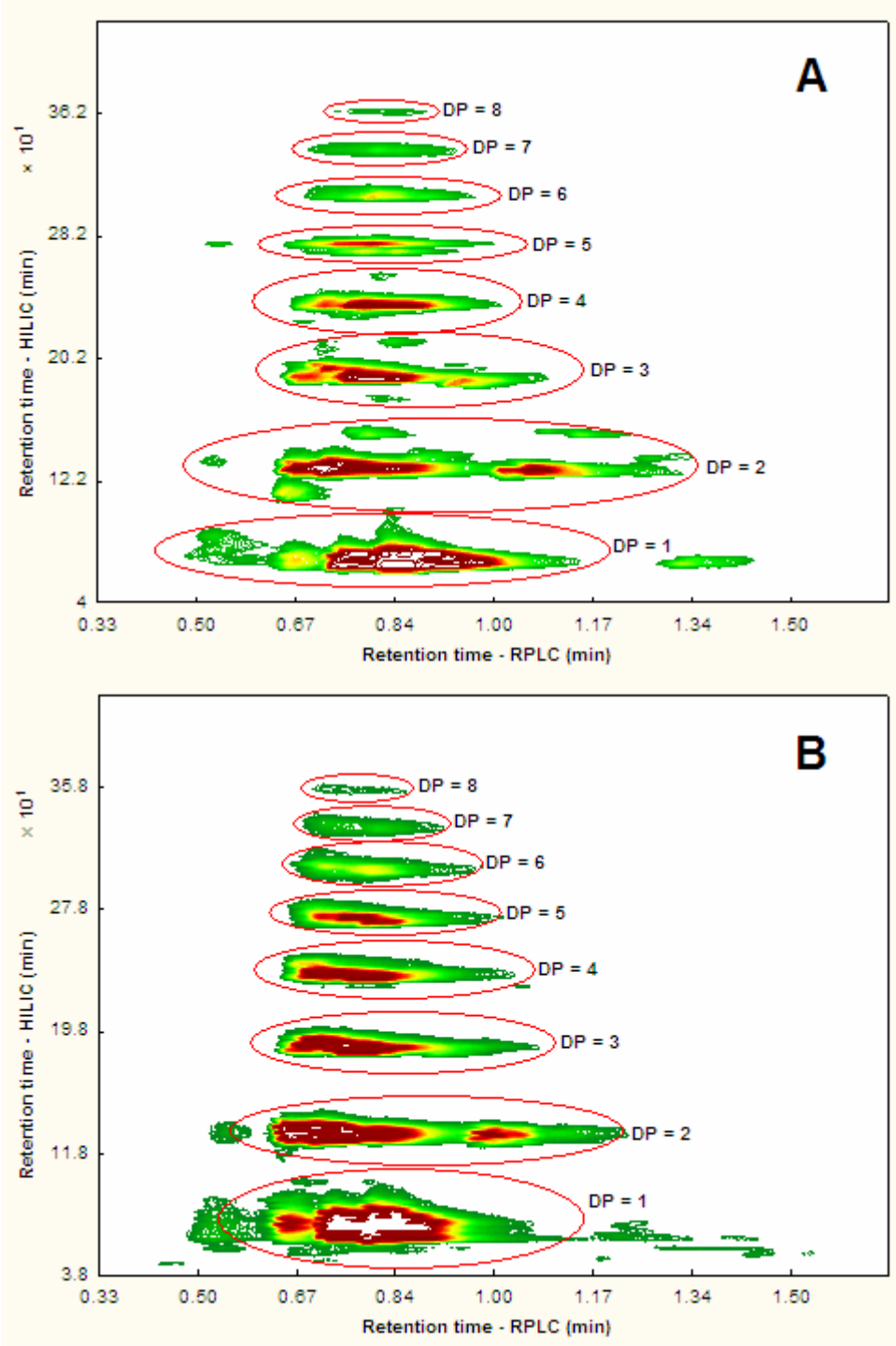

Figure 6.3: Fluorescence contour plots for the on-line HILIC × RP-LC analysis of cocoa (**A**) and apple (**B**) procyanidins.

Peak capacity is commonly used to evaluate the quality of chromatographic separations [24-26]. It is well known that in order to maximally utilise the separation space of a 2-D separation, highly orthogonal separation mechanisms must be selected [4-6,8,27-31] and a balance between the sampling rate of the first dimension peaks and the second dimension analysis time must be ensured [32]. The combination of HILIC and RP-LC as an orthogonal system for 2-D separations has been demonstrated in the off-line analysis (chapter 4). This is also evident from the low correlation coefficient (r^2) values of 0.0231 and 0.0182 obtained in this study for cocoa and apple, respectively (**Table 6.1**). These values were obtained from the plots of the scaled retention factors for the procyanidin oligomers identified by on-line HILIC × RP-LC in cocoa and apple extracts.

In general, the sampling rate of a 2-D chromatographic technique is considered sufficient to avoid under-sampling when at least three fractions per first dimension peak are collected [32-36]. Sampling rates of three or more per peak imply fairly fast analysis times in the second dimension and usually results in limited separation times in the second dimension and a resultant loss of peak capacity. Therefore, in order for the benefit of 2D separations to be realised, there should be a balance between the first dimension sampling rate and the second dimension analysis time [32]. This is generally achieved through the use of a microbore column in the first dimension which is operated at a low flow rate to enable sufficient sampling and at the same time allow adequate analysis time in the second dimension. A microbore column also provides volumes compatible for injecting onto the second dimension column and has small dilution factors [2,5,6].

This same approach was adopted in our on-line system and resulted in the first dimension peak widths in the ranges of 5.31-20.42 (average = 13.29) and 4.49-23.77 (average = 16.19) for cocoa and apple samples, respectively. This did not only allow sufficient sampling of the first dimension peaks, but reasonable separation times were also allowed in the second dimension to maximise the total peak capacity of the system. Since all peaks were sampled at least 3 times, no major loss of first dimension peak capacity is expected. To evaluate this phenomenon, peak capacities were computed using two methods, one which accounts for under-sampling [35] and

another, which does not take under-sampling into account but is based on orthogonality [37]. These two methods were also compared with the recently reported method of Li *et al* [38], which is assumed to provide a more accurate estimation of the 2D separation peak capacity. A summary of the peak capacities is shown in **Table 6.1.** In these calculations, a value of 20 for peak capacity in the second dimension was used, as calculated for the chromatogram in **Figure 6.2A.** This represents the ideal case where detector saturation in the second dimension does not affect overall separation (as is the case in **Figure 6.3**).

No major differences were obtained in the peak capacities obtained using the two calculation methods. However, the trend that can be drawn from the peak capacities obtained using the two methods is that, the method of Liu *et al* [37] seems to overrate the practical peak capacity when a certain degree of under-sampling exists, and underrate the peak capacity in the absence of under-sampling. A method accounting for both effects (orthogonality and under-sampling) would provide a much more accurate approximation, given that the peak capacities of 2-D separations are highly dependent on both parameters.

Table 6.1: Summary of the parameters used to calculate the practical peak capacity of the on-line HILIC × RP-LC methods.

Parameter	**Value**	
	Cocoa	**Apple**
[a]HILIC peak capacity, n_1	40	33
[a]RP peak capacity, n_2	20	20
[b]Correlation coefficient, r^2	0.0231	0.0182
[c]Theoretical peak capacity, n_T	800	660
[b]Practical peak capacity, n_p	742	617
[d]Practical peak capacity, n_p	772	648
[e]Practical peak capacity, n_p	770	642

[a] Calculated according to Neue [39].
[b] Calculated according to Liu *et al* [37].
[c] $n_T = n_1 \times n_2$.
[d] Calculated according to Davis *et al* [35].
[e] Calculated according to Li *et al* [38].

6.4. Conclusions

An on-line 2-D LC method using HILIC and RP-LC was developed for the analysis of cocoa and apple procyanidins. This was achieved using 2 × 6-port valves, a 1 mm i.d. column in the first dimension operated at low flow rates and a short 1.8 µm column run in isocratic mode in the second dimension. This approach ensured sufficient sampling times and high practical peak capacities. Practical realisation of the on-line separation was hampered by detector saturation, and further optimisation was not possible due to instrumental constraints. However, further optimisation of this system would allow analyses to be performed in an automated fashion, and also guarantee better reliability of operation and reproducibility [1]. Taking into consideration the pressure limits within which this work was performed, the system could undoubtedly significantly be improved by performing the second dimension analysis at higher pressures. On the other hand, the method is suitable for use with conventional LC instruments.

In addition, performing a gradient analysis at higher pressures in the second dimension would result in significantly improved results. Nevertheless, the total peak capacities achieved on this system are still high and could not be achieved using either 1-dimensional method alone. In addition, the method offers an added advantage of automation and less risk of analyte loss and /or degradation. On-line coupling to MS detection would further enhance the utility of the method as it would allow detection of compounds as they elute from the second dimension column, which would facilitate identification. This will be attempted in future work.

Two-dimensional separations hold significant promise as far as the analysis of complex samples is concerned. In spite of lengthy method development, long analysis times and complex data analysis associated with 2D separations, the high resolving power and amount of information obtainable with such systems cannot be matched by conventional LC methods. However, it should be stressed that parameters such as separation mechanisms for the two dimensions, sampling rate of the first dimension peaks and speed of analysis in the second dimension need to be carefully considered for this benefit to be realised.

6.5. References

[1] F. Erni, R.W. Frei, J. Chromatogr. A 149 (1978) 561.
[2] M.M. Bushey, J.W. Jorgenson, Anal. Chem. 62 (1990) 161.
[3] P.J. Schoenmakers, G. Vivo-Truyols, W.M.C. Decrop, J. Chromatogr. A 1120 (2006) 282.
[4] S.P. Dixon, I.D. Pitfield, D. Perrett, Biomed. Chromatogr. 20 (2006) 508.
[5] P. Dugo, F. Cacciola, T. Kumm, G. Dugo, L. Mondello, J. Chromatogr. A 1184 (2008) 353.
[6] I. François, A. de Villiers, P. Sandra, J. Sep. Sci. 29 (2006) 492.
[7] P. Dugo, O. Favoino, R. Luppino, G. Dugo, L. Mondello, Anal. Chem. 76 (2004) 2525.
[8] P.Q. Tranchida, P. Dugo, G. Dugo, L. Mondello, J. Chromatogr. A 1054 (2004) 3.
[9] A. Schieber, P. Keller, R. Carle, J. Chromatogr. A 910 (2001) 265.
[10] B. Sun, M.C. Leandro, V. de Freitas, M.I. Spranger, J. Chromatogr. A 1128 (2006) 27.
[11] M. Kivilompolo, T. Hyotylainen, J. Chromatogr. A 1145 (2007) 155.
[12] E. Blahová, P. Jandera, F. Cacciola, L. Mondello, J. Sep. Sci. 29 (2006) 555.
[13] F. Cacciola, P. Jandera, E. Blahová, L. Mondello, J. Sep. Sci. 29 (2006) 2500.
[14] F. Cacciola, P. Jandera, Z. Hajdu, P. Cesla, L. Mondello, J. Chromatogr. A 1149 (2007) 73.
[15] T. Hájek, V. Skeríková, P. Cesla, K. Vynuchalová, P. Jandera, J. Sep. Sci. 31 (2008) 3309.
[16] F. Cacciola, P. Jandera, L. Mondello, J. Sep. Sci. 30 (2007) 462.
[17] P. Dugo, F. Cacciola, M. Herrero, P. Donato, L. Mondello, J. Sep. Sci. 31 (2008) 3297.
[18] M. Kivilompolo, V. Oburka, T. Hyotylainen, Anal. Bioanal. Chem. 391 (2008) 373.
[19] M. Kivilompolo, T. Hyötyläinen, J. Sep. Sci. 31 (2008) 3466.
[20] F. Cacciola, P. Jandera, L. Mondello, Chromatographia 66 (2007) 661.
[21] K.M. Kalili, A. de Villiers, J. Chromatogr. A 1216 (2009) 6274.
[22] M.A. Kelm, J.C. Johnson, R.J. Robbins, J.F. Hammerstone, H.H. Schmitz, J. Agric. Food Chem. 54 (2006) 1571.
[23] H. Tanaka, X. Zhou, O. Masayoshi, J. Chromatogr. A 987 (2003) 119.
[24] U.D. Neue, J. Chromatogr. A 1184 (2008) 107.
[25] S. Pous-Torres, J.J. Baeza-Baeza, J.R. Torres-Lapasió, M.C. García-Álvarez-Coque, J. Chromatogr. A 1205 (2008) 78.
[26] J.C. Giddings, Anal. Chem. 56 (1984) 1258A.
[27] D.R. Stoll, X. Li, X. Wang, P.W. Carr, S.E.G. Porter, S.C. Rutan, J. Chromatogr. A 1168 (2007) 3.
[28] P. Jandera, J. Fischer, H. Lahovská, K. Novotná, P. Cesla, L. Kolárová, J. Chromatogr. A 1119 (2006) 3.
[29] P. Dugo, V. Skerikova, T. Kumm, A. Trozzi, P. Jandera, L. Mondello, Anal. Chem. 78 (2006) 7743.
[30] P.E. Toups, M.J. Gray, G.R. Dennis, N. Reddy, M.A. Wilson, R.A. Shalliker, J. Sep. Sci. 29 (2006) 481.
[31] C.J. Venkatramani, A. Patel, J. Sep. Sci. 29 (2006) 510.
[32] D.R. Stoll, X. Wang, P.W. Carr, Anal. Chem. 80 (2008) 268.

[33] K. Horie, H. Kimura, T. Ikegami, A. Iwatsuka, N. Saad, O. Fiehn, N. Tanaka, Anal. Chem. 79 (2007) 3764.
[34] R.E. Murphy, M.R. Schure, J.P. Foley, Anal. Chem. 70 (1998) 1585.
[35] J.M. Davis, D.R. Stoll, P.W. Carr, Anal. Chem. 80 (2008) 461.
[36] C.V. McNeff, B. Yan, D.R. Stoll, R.A. Henry, J. Sep. Sci. 30 (2007) 1672.
[37] Z. Liu, D.G. Patterson, M.L. Lee, Anal. Chem. 67 (1995) 3840.
[38] X. Li, D.R. Stoll, P.W. Carr, Anal. Chem. 81 (2009) 845.
[39] U.D. Neue, J. Chromatogr. A 1079 (2005) 153.

Chapter 7

General Conclusions and Future Work

For complete resolution of complex samples, multidimensional separations are necessary. In this study, off-line and on-line comprehensive 2-D LC methods combining hydrophilic interaction chromatography (HILIC) and reversed phase liquid chromatography (RP-LC) have been developed. These methods allowed simultaneous separation of diverse groups of phenolic compounds including proanthocyanidins, flavonols and their glycosylated derivatives, chalcones and phenolic acids. Given the difficulty of analysis for phenolic compounds, these methods offered improved separation for these compounds. Therefore, this study has provided insight into potentially powerful separation strategies which may in future be used to enable complete characterisation of samples containing complex phenolic fractions.

The combination of HILIC and RP-LC has been shown to provide a highly orthogonal combination for 2-D LC separation of phenolics. A comparison of the off-line and on-line comprehensive 2-D LC approaches indicated that the high resolving power offered by 2-D LC systems is better demonstrated in the off-line approach. While the on-line approach provides automation and minimises chances of analyte loss, contamination and/or degradation, the peak capacities of such systems are greatly sacrificed to balance the first dimension sampling rate and the second dimension analysis times. However, both approaches offer peak capacities an order of magnitude higher than those that could be achieved even by extensively optimised 1-dimensional LC methods. This demonstrates the power of 2-dimensional separations as promising tools towards resolving complex samples.

While other 2-D techniques such as LC-MS and GC-MS provide very powerful analytical tools and a wealth of information on complex samples, their resolving power is not comparable to 2-D separations [1]. Because subjecting a sample to multiple separation techniques reduces component overlap [2,3], not only do 2-D separations result in highly purified components, but they also facilitate component identification and exclude false identification since two independent retention times are obtained for each compound [1]. In addition, 2-D separations offer the benefit of data presentation in the form of contour or 3-D plots. This provides a platform where quick inferences can be made regarding different sample profiles by means of visual inspection.

The availability of powerful detection systems in HPLC is a benefit widely enjoyed by chromatographers. The use of fluorescence detection in this study allowed selective detection of procyanidins in various samples, which offers a quick screening tool for the presence of procyanidins in samples. In addition, fluorescence detection offers the option of selective, quantitative determination of procyanidins in various samples. The ability of the diode-array detector to monitor mixtures of compounds greatly enhanced the robustness of the system and facilitated the identification of the compounds. Moreover, the combination of LC with mass spectrometry provided a powerful detection system for identification of compounds.

In future, improvement of the on-line system developed in this study needs to be carried out. Other approaches such as performing a gradient analysis in the second dimension could also provide better separation of compounds. In addition, performing a stop-flow comprehensive 2-D separation is also worth investigating given that most of these compounds have high molecular weights, and would therefore diffuse slowly, ruling out the possibility of excessive band broadening. Combinations of the 1-D separation methods used in this study with other separation techniques such as capillary electrophoresis (CE) could also provide powerful separation systems worth investigating. Evaluation of other separation mechanisms or the use of alternative stationary phases could also provide different selectivities to these two LC methods, potentially resulting in better separation.

References

[1] M.M. Bushey, J.W. Jorgenson, Anal. Chem. 62 (1990) 161.
[2] J.M. Davis, J.C. Giddings, Anal. Chem. 57 (1985) 2168.
[3] J.M. Davis, J.C. Giddings, Anal. Chem. 57 (1985) 2178.

Appendix A

Repeatability Data

Repeatability data between days for the HILIC and RP-LC analysis of apple, cocoa and green tea extracts. The numbers 1-15 represent compounds and RT stands for retention time.

Table 1A: Repeatability data between days for the optimized HILIC analysis of the cocoa extract on a Develosil diol column.

RT	1	2	3	4	5	6	7	8	9	10	11	12	13	14	
RT1	4.015	7.501	13.617	16.192	18.267	20.000	22.492	25.142	29.217	32.675	35.580	38.067	40.350	42.350	
RT2	4.217	7.508	13.900	16.533	18.583	20.130	22.833	25.183	29.342	32.717	35.670	38.092	40.260	42.130	
RT3	3.858	6.867	13.167	15.817	18.017	19.430	22.125	24.675	28.967	32.608	35.810	38.450	40.820	42.760	
RT4	3.992	7.183	13.592	16.192	18.400	19.880	22.600	25.125	29.325	32.842	35.850	38.442	40.780	42.730	
Average	4.021	7.265	13.569	16.184	18.317	19.860	22.513	25.031	29.213	32.711	35.730	38.263	40.550	42.490	
Standard Deviation	0.148	0.305	0.302	0.292	0.238	0.304	0.295	0.239	0.173	0.099	0.124	0.212	0.289	0.305	
%RSD	3.69	4.20	2.22	1.81	1.30	1.53	1.31	0.95	0.59	0.30	0.35	0.55	0.71	0.72	**1.45**

Table 2A: Repeatability data between days for the optimized HILIC analysis of the apple extract on a Develosil diol column.

RT	1	2	3	4	5	6	7	8	9	10	
RT1	4.967	6.308	12.617	18.850	24.250	28.750	32.450	35.625	38.283	40.683	
RT2	4.542	6.325	13.667	19.925	25.933	29.192	32.767	35.742	38.417	40.600	
RT3	5.033	6.634	14.083	20.425	25.542	29.833	33.392	36.425	39.008	41.000	
RT4	4.025	6.509	13.458	19.867	25.033	29.583	32.925	36.183	38.633	41.067	
Average	4.642	6.444	13.456	19.767	25.190	29.340	32.884	35.994	38.585	40.838	
Standard Deviation	0.465	0.156	0.617	0.661	0.727	0.473	0.392	0.375	0.317	0.230	
%RSD	10.02	2.42	4.58	3.34	2.88	1.61	1.19	1.04	0.82	0.56	**2.85**

Table 3A: Repeatability data between days for the optimized HILIC analysis of the green tea extract on a Develosil diol column.

RT	**1**	**2**	**3**	**4**	**5**	**6**	**7**	**8**	**9**	
RT1	6.875	9.967	12.075	14.483	16.317	18.475	23.817	28.292	31.450	
RT2	7.342	10.317	12.442	14.683	16.417	18.483	23.567	27.717	31.342	
RT3	7.325	10.100	12.508	14.642	16.350	18.542	23.683	27.942	31.400	
RT4	7.167	10.175	12.267	14.708	16.483	18.617	23.767	28.075	31.508	
RT5	7.608	10.125	12.242	14.592	16.258	18.433	23.783	27.108	31.308	
Average	7.263	10.137	12.307	14.622	16.365	18.510	23.723	27.827	31.402	
Standard Deviation	0.269	0.127	0.172	0.089	0.087	0.071	0.100	0.453	0.081	
%RSD	3.70	1.25	1.40	0.61	0.53	0.39	0.42	1.63	0.26	**1.13**

Table 4A: Repeatability data between days for the optimized RP-LC analysis of the cocoa extract on a 50 mm Zorbax C18 column.

RT	**1**	**2**	**3**	**4**	**5**	**6**	**7**	**8**	**9**	**10**	**11**	**12**	**13**	**14**	**15**	**16**	
RT1	0.605	0.773	1.265	1.4	1.493	1.595	1.652	1.720	1.797	1.852	1.893	1.968	2.040	2.078	2.380	2.822	
RT2	0.617	0.768	1.262	1.388	1.483	1.583	1.640	1.710	1.783	1.828	1.885	1.957	2.023	2.082	2.378	2.817	
RT3	0.598	0.780	1.27	1.407	1.500	1.600	1.657	1.732	1.810	1.862	1.907	1.977	2.042	2.092	2.380	2.823	
RT4	0.598	0.775	1.273	1.413	1.503	1.603	1.660	1.738	1.817	1.868	1.912	1.982	2.048	2.095	2.385	2.830	
Average	0.605	0.774	1.268	1.402	1.495	1.595	1.652	1.725	1.802	1.853	1.899	1.971	2.038	2.087	2.381	2.823	
Standard Deviation	0.009	0.005	0.005	0.011	0.009	0.009	0.009	0.012	0.015	0.018	0.012	0.011	0.011	0.008	0.003	0.005	
%RSD	1.48	0.64	0.39	0.77	0.59	0.55	0.53	0.72	0.830	0.95	0.66	0.56	0.53	0.39	0.13	0.19	**0.62**

Table 5A: Repeatability data between days for the optimized RP-LC analysis of the cocoa extract on 2 × 50 mm Zorbax C18 columns.

RT	**1**	**2**	**3**	**4**	**5**	**6**	**7**	**8**	**9**	**10**	**11**	**12**	**13**	**14**	**15**	
RT1	2.413	2.547	3.485	7.512	8.155	9.228	9.940	10.680	11.240	11.792	12.210	12.538	13.100	13.550	14.068	
RT2	2.408	2.542	3.467	7.490	8.138	9.215	9.918	10.655	11.208	11.765	12.210	12.510	13.070	13.520	14.052	
RT3	2.423	2.543	3.470	7.487	8.115	9.200	9.912	10.643	11.195	11.757	12.170	12.500	13.060	13.520	14.038	
RT4	2.438	2.560	3.515	7.592	8.268	9.357	10.048	10.807	11.375	11.945	12.380	12.685	13.210	13.700	14.202	
Average	2.421	2.548	3.484	7.520	8.169	9.250	9.955	10.696	11.255	11.815	12.240	12.558	13.110	13.570	14.09	
Standard Deviation	0.013	0.008	0.022	0.049	0.068	0.072	0.064	0.075	0.083	0.088	0.092	0.086	0.070	0.085	0.0757	
%RSD	0.55	0.33	0.63	0.65	0.83	0.78	0.64	0.71	0.73	0.75	0.753	0.68	0.53	0.63	0.537	**0.65**

Table 6A: Repeatability data between days for the optimized RP-LC analysis of the apple extract on 2 × 50 mm Zorbax C18 columns.

RT	**1**	**2**	**3**	**4**	**5**	**6**	**7**	**8**	**9**	**10**	**11**	**12**	**13**	**14**	**15**	
RT1	7.380	7.730	8.280	8.567	8.808	9.377	9.705	10.083	10.830	11.405	11.823	11.965	12.385	12.713	13.263	
RT2	7.442	7.797	8.343	8.622	8.890	9.428	9.778	10.118	10.878	11.458	11.858	12.033	12.418	12.805	13.297	
RT3	7.363	7.700	8.217	8.533	8.795	9.320	9.848	10.002	10.772	11.340	11.873	12.183	12.312	12.853	13.208	
Average	7.395	7.742	8.280	8.574	8.831	9.375	9.777	10.068	10.827	11.401	11.851	12.060	12.372	12.790	13.256	
Standard Deviation	0.042	0.050	0.063	0.045	0.052	0.054	0.072	0.060	0.053	0.059	0.026	0.112	0.054	0.071	0.045	
%RSD	0.56	0.64	0.76	0.52	0.58	0.58	0.73	0.59	0.49	0.52	0.22	0.92	0.44	0.56	0.34	**0.53**

Table 7A: Repeatability data between days for the optimized RP-LC analysis of the green tea extract on 2 × 50 mm Zorbax C18 columns.

RT	**1**	**2**	**3**	**4**	**5**	**6**	**7**	**8**	**9**	
RT1	6.550	7.610	7.750	8.010	8.4	9.210	9.470	10.150	10.920	
RT2	6.417	7.443	7.690	7.867	8.24	9.083	9.320	9.973	10.770	
RT3	6.737	7.453	7.677	7.877	8.265	9.108	9.342	10.033	10.800	
RT4	6.422	7.435	7.663	7.845	8.238	9.073	9.327	10.008	10.770	
RT5	6.410	7.443	7.657	7.843	8.23	9.000	9.310	10.000	10.777	
Average	6.507	7.477	7.687	7.888	8.275	9.111	9.354	10.033	10.807	
Standard Deviation	0.141	0.075	0.037	0.069	0.071	0.057	0.066	0.069	0.064	
%RSD	2.17	1.00	0.48	0.88	0.86	0.63	0.71	0.69	0.59	**0.89**

Appendix B

Additional Correlation Coefficient Plots, Retention Data and Calculations of the Peak Capacities

Table 1B: Retention times, peak widths and scaled retention factors for the off-line HILIC and RP-LC analysis of the cocoa extract.

Compound	HILIC			RP-LC (Short gradient)		
	Retention time (min)	**Peak width (min)**	**Scaled retention factor**	**Retention time (min)**	**Peak width (min)**	**Scaled retention factor**
Catechin (1)	7.26	3.21	0.079	1.42	0.05	0.350
Epicatechin (1')	7.26	3.21	0.079	1.62	0.05	0.436
B-type dimer1(2')	13.62	2.45	0.238	1.51	0.07	0.390
B-type dimer2(2'')	13.62	2.45	0.238	1.99	0.07	0.600
A-type dimer3(2''')	13.62	2.45	0.238	2.06	0.07	0.630
A-type dimer(2'''')	16.19	1.1	0.302	2.38	0.07	0.772
Trimer 1(3')	20.00	2.44	0.398	1.67	0.04	0.459
Trimer2(3'')	20.00	2.44	0.398	1.75	0.08	0.493
Trimer3(3''')	20.00	2.44	0.398	1.99	0.07	0.600
Tetramer1(4)	25.14	2.73	0.527	1.62	0.05	0.436
Tetramer2(4')	25.14	2.73	0.527	1.75	0.08	0.493
Tetramer3(4'')	25.14	2.73	0.527	1.82	0.05	0.526
Pentamer1(5')	29.22	2.34	0.629	1.75	0.08	0.493
Pentamer2(5'')	29.22	2.34	0.629	1.82	0.05	0.526
Hexamer1(6)	32.68	2.05	0.715	1.99	0.07	0.600
Heptamer(7)	35.58	2.05	0.788	1.99	0.07	0.600
Octamer(8)	38.07	1.46	0.850	1.99	0.07	0.600
Unretained compound (t_0)	4.11	0.82		0.63	0.07	
Last eluting compound (t_l)	44.06	1.37		2.90	0.04	
	Average	**2.39**		**Average**	**0.06**	

Table 2B: Retention times, peak widths, peak broadening factors and scaled retention factors for the off-line HILIC and RP-LC analysis of the cocoa extract.

Compound	HILIC				RP-LC (Long gradient)		
	Retention time (min)	**Peak width (min)**	**Peak broadening factor (<β>)**	**Scaled retention factor**	**Retention time (min)**	**Peak width (min)**	**Scaled retention factor**
Catechin (1)	7.26	3.21	1.15	0.079	8.27	0.11	0.294
Epicatechin (1)	7.26	3.21	1.15	0.079	10.05	0.22	0.383
B-type dimer1(2)	13.62	2.45	1.25	0.238	6.42	0.13	0.201
B-type dimer2(2')	13.62	2.45	1.25	0.238	9.36	0.18	0.348
B-type dimer3(2'')	13.62	2.45	1.25	0.238	13.21	0.22	0.542
B-type dimer4 (2'''')	13.62	2.45	1.25	0.238	14.20	0.22	0.592
A-type dimer(2''')	16.19	1.1	1.96	0.302	13.70	0.20	0.567
Trimer1(3)	20.00	2.44	1.26	0.398	9.36	0.18	0.348
Trimer 2(3')	20.00	2.44	1.26	0.398	10.81	0.18	0.421
Trimer3(3'')	20.00	2.44	1.26	0.398	11.38	0.18	0.450
Trimer4(3''')	20.00	2.44	1.26	0.398	13.21	0.22	0.542
Tetramer1(4)	25.14	2.73	1.21	0.527	9.91	0.09	0.376
Tetramer2(4')	25.14	2.73	1.21	0.527	11.38	0.18	0.450
Tetramer3(4'')	25.14	2.73	1.21	0.527	11.95	0.19	0.479
Tetramer4(4''')	25.14	2.73	1.21	0.527	14.68	0.14	0.616
Pentamer1(5')	29.22	2.34	1.27	0.629	11.38	0.18	0.450
Pentamer2(5'')	29.22	2.34	1.27	0.629	11.95	0.19	0.479
Pentamer3 (5''')	29.22	2.34	1.27	0.629	12.38	0.20	0.500
Pentamer4 (5'''')	29.22	2.34	1.27	0.629	12.38	0.20	0.500
Hexamer1(6)	32.68	2.05	1.35	0.715	12.38	0.20	0.500
Hexamer2(6')	32.68	2.05	1.35	0.715	12.38	0.20	0.500
Hexamer3(6'')	32.68	2.05	1.35	0.715	12.72	0.14	0.518
Hexamer4 (6''')	32.68	2.05	1.35	0.715	13.21	0.22	0.542
Heptamer(7)	35.58	2.05	1.35	0.788	12.72	0.14	0.518
Octamer(8)	38.07	1.46	1.61	0.850	12.97	0.14	0.530
Unretained compound (t_0)	4.11	0.82			2.44	0.08	
Last eluting compound (t_l)	44.06	1.37			22.30	0.24	
	Average	**2.36**	**1.30**		**Average**	**0.178**	

Table 3B: Retention times, peak widths, peak broadening factors and scaled retention factors for the off-line HILIC and RP-LC (long gradient) analysis of the apple extract.

Compound	HILIC				RP-LC (Long gradient)		
	Retention time (min)	**Peak width (min)**	**Peak broadening factor (<β>)**	**Scaled retention factor**	**Retention time (min)**	**Peak width (min)**	**Scaled retention factor**
Catechin (1)	7.08	2.75	1.21	0.046	8.22	0.19	0.059
Epicatechin (1')	7.08	2.75	1.21	0.046	10.00	0.26	0.174
B-type dimer1(2)	13.83	2.58	1.23	0.209	7.31	0.2	0.000
B-type dimer2(2')	13.83	2.58	1.23	0.209	9.32	0.23	0.130
B-type dimer3(2'')	13.83	2.58	1.23	0.209	11.34	0.29	0.260
B-type dimer4(2''')	13.83	2.58	1.23	0.209	13.19	0.17	0.379
Trimer 1(3)	20.36	2.67	1.22	0.366	8.51	0.2	0.077
Trimer2(3')	20.36	2.67	1.22	0.366	8.76	0.21	0.093
Trimer3(3'')	20.36	2.67	1.22	0.366	9.32	0.23	0.130
Trimer5 (3'''')	20.36	2.67	1.22	0.366	10.77	0.21	0.223
Trimer6(3''''')	20.36	2.67	1.22	0.366	11.34	0.29	0.260
Trimer7 (3'''''')	20.36	2.67	1.22	0.366	13.19	0.17	0.379
Tetramer2(4')	25.75	3.17	1.16	0.496	8.76	0.21	0.093
Tetramer3(4'')	25.75	3.17	1.16	0.496	9.66	0.12	0.152
Tetramer4(4''')	25.75	3.17	1.16	0.496	9.66	0.12	0.152
Tetramer5(4'''')	25.75	3.17	1.16	0.496	11.34	0.29	0.260
Tetramer6(4''''')	25.75	3.17	1.16	0.496	11.88	0.14	0.295
Pentamer1(5)	30.14	2.84	1.19	0.602	9.66	0.12	0.152
Pentamer2(5')	30.14	2.84	1.19	0.602	10.00	0.26	0.174
Pentamer4 (5''')	30.14	2.84	1.19	0.602	11.34	0.29	0.260
Pentamer5 (5'''')	30.14	2.84	1.19	0.602	11.88	0.14	0.295
Pentamer6 (5''''')	30.14	2.84	1.19	0.602	12.29	0.17	0.321
Hexamer1(6)	33.63	2.25	1.29	0.686	11.88	0.14	0.295
Hexamer2(6')	33.63	2.25	1.29	0.686	12.29	0.17	0.321
Hexamer3(6'')	33.63	2.25	1.29	0.686	12.64	0.18	0.344
Unretained compound (t_0)	5.19	1.17			7.31	0.2	
Last eluting compound (t_l)	46.63	1.84			22.82	0.18	
	Average	**2.75**	**1.21**		**Average**	**0.20**	

Table 4B: Retention times, peak widths, peak broadening factors and scaled retention factors for the on-line HILIC and RP-LC analysis of the cocoa extract.

Compound	HILIC				RP-LC (Long gradient)		
	Retention time (min)	Peak width (min)	Peak broadening factor (<β>)	Scaled retention factor	Retention time (min)	Peak width (min)	Scaled retention factor
Catechin (1)	62.27	20.42	1.02	0.07	0.75	0.09	0.278
Epicatechin (1')	62.27	20.42	1.02	0.066	0.85	0.10	0.410
Dimers (A-type)	109.36	15.54	1.03	0.176	0.67	0.05	0.179
Dimers	124.75	22.18	1.01	0.212	0.78	0.10	0.318
Dimers	124.75	22.18	1.01	0.212	1.09	0.08	0.710
Dimers pentose	149.02	12.46	1.04	0.269	0.80	0.05	0.343
Dimers hexose	170.51	9.33	1.08	0.320	1.17	0.06	0.811
Trimers	184.77	19.99	1.02	0.353	0.78	0.10	0.318
Trimers	184.77	19.99	1.02	0.353	0.98	0.10	0.571
Trimer pentose	209.38	6.68	1.14	0.411	0.84	0.05	0.394
Tetramers	232.30	12.84	1.04	0.465	0.78	0.10	0.318
Pentamers	270.72	18.19	1.02	0.555	0.78	0.10	0.318
Hexamers	303.08	14.64	1.03	0.631	0.78	0.10	0.318
Heptamers	331.47	15.54	1.03	0.698	0.78	0.10	0.318
Octamers	356.14	14.64	1.03	0.756	0.78	0.10	0.318
Unretained compound (t_0)	34.33	5.31			0.53	0.12	
Last eluting compound (t_l)	460.11	7.50			1.32	0.19	
	Average	**16.34**	**1.04**		**Average**	**0.09**	

Table 5B: Retention times, peak widths, peak broadening factors and scaled retention factors for the on-line HILIC and RP-LC analysis of the apple extract.

Compound	HILIC				RP-LC (Long gradient)		
	Retention time (min)	Peak width (min)	Peak broadening factor (<β>)	Scaled retention factor	Retention time (min)	Peak width (min)	Scaled retention factor
Catechin (1)	63.31	15.45	1.03	0.078	0.64	0.13	0.141
Epicatechin (1')	63.31	15.45	1.03	0.078	0.78	0.14	0.318
Dimers	122.47	23.77	1.01	0.244	0.7	0.14	0.217
Dimers	122.47	23.77	1.01	0.244	0.98	0.08	0.571
Trimers	197.55	20.14	1.02	0.456	0.78	0.14	0.318
Tetramers	225.08	23.29	1.01	0.534	0.78	0.14	0.318
Pentamers	263.29	19.27	1.02	0.641	0.78	0.14	0.318
Hexamers	294.80	16.55	1.02	0.730	0.78	0.14	0.318
Octamers	322.33	19.27	1.02	0.808	0.78	0.14	0.318
Unretained compound (t_0)	35.80	12.01			0.528	0.12	
Last eluting compound (t_l)	390.47	23.98			1.32	0.14	
	Average	**19.66**	**1.02**		**Average**	**0.13**	

Table 6B: Retention times, peak widths, peak broadening factors and scaled retention factors for the off-line HILIC and RP-LC analysis of the green tea extract (UV data at 320 and 370 nm).

Compound	HILIC				RP-LC (Long gradient)		
	Retention time (min)	Peak width (min)	Peak broadening factor (<β>)	Scaled retention factor	Retention time (min)	Peak width (min)	Scaled retention factor
p-coumaroylquinic acid	6.33	7.73	1.11	0.059	7.55	0.17	0.282
p-coumaroylquinic acid	6.33	7.73	1.11	0.059	9.36	0.15	0.361
quercetin-3-O-rhamnosylgalactoside	14.89	2.68	1.70	0.234	12.34	0.12	0.491
quercetin-3-O-rutinoside	14.89	2.68	1.70	0.234	12.52	0.15	0.499
quercetin-3-O-galactoside	9.51	1.62	2.49	0.124	12.83	0.16	0.513
quercetin-3-O-glucoside	9.51	1.62	2.49	0.124	13.11	0.14	0.525
kaempferol galactoside	9.51	1.62	2.49	0.124	14.15	0.17	0.570
kaempferol glucoside	9.51	1.62	2.49	0.124	14.78	0.19	0.597
myricetin galactoside	14.89	2.68	1.70	0.234	11.16	0.13	0.440
myricetin glucoside	14.89	2.68	1.70	0.234	11.35	0.17	0.448
apigenin glucosylarabinoside	18.67	1.65	2.45	0.311	11.01	0.12	0.433
apigenin glucosylarabinoside	18.67	1.65	2.45	0.311	11.12	0.13	0.438
quercetin dirhamnosylglucoside	22.97	2.63	1.73	0.399	12.25	0.15	0.487
quercetin dirhamnosylglucoside	22.97	2.63	1.73	0.399	12.53	0.18	0.499
quercetin galactosylrutinoside	26.18	2.48	1.80	0.465	11.57	0.12	0.458
quercetin galactosylrutinoside	26.18	2.48	1.80	0.465	11.91	0.15	0.472
kaempferol xylosylrutinoside	14.89	2.68	1.70	0.234	13.16	0.18	0.527
kaempferol xylosylrutinoside	14.89	2.68	1.70	0.234	13.76	0.15	0.553
Kaempferol rutinoside	11.90	2.07	2.05	0.173	13.42	0.12	0.538
Kaempferol rutinoside	11.90	2.07	2.05	0.173	14.07	0.17	0.567
Unretained compound (t_0)	3.46	1.24			1.07	0.11	
Last eluting compound (t_l)	52.32	6.15			24.02	0.17	
	Average	**2.24**	**2.01**		**Average**	**0.15**	

Table 7B: Retention times, peak widths, peak broadening factors and scaled retention factors for the off-line HILIC and RP-LC analysis of the green tea extract (UV data at 280 nm).

Compound*	HILIC				RP-LC (Long gradient)		
	Retention time (min)	Peak width (min)	Peak broadening factor (<β>)	Scaled retention factor	Retention time (min)	Peak width (min)	Scaled retention factor
Catechin (1a)	6.40	5.39	1.21	0.090	7.88	0.10	0.297
Epicatechin (1b)	6.40	5.39	1.21	0.090	9.66	0.14	0.374
Gallocatechin (1c)	8.02	5.39	1.21	0.147	5.10	0.13	0.176
Epigallocatechin (1d)	8.02	5.39	1.21	0.147	7.14	0.11	0.265
(epi)catechin gallate (1e)	10.17	5.39	1.21	0.223	12.87	0.06	0.514
(epi)catechin gallate (1f)	10.17	5.39	1.21	0.223	13.09	0.10	0.524
(epi)gallocatechin gallate1 (1g)	12.36	2.54	1.77	0.301	9.89	0.10	0.384
(epi)gallocatechin gallate2 (1g)	12.36	2.54	1.77	0.301	10.51	0.33	0.411
(epi)afzelechin gallate (1h)	8.70	5.39	1.21	0.171	15.28	0.15	0.619
methyl (epi)gallocatechin gallate (1j)	15.46	4.19	1.33	0.411	8.01	0.10	0.302
methylated (epi)gallocatechin gallate2	9.09	5.39	1.21	0.185	13.3	0.08	0.533
(epi)catechin dimer2 (2b)	12.79	2.54	1.77	0.316	8.71	0.11	0.333
(epi)catechin dimer3 (2c)	12.79	2.54	1.77	0.316	8.96	0.16	0.344
(epi)catechin dimer4 (2d)	12.79	2.54	1.77	0.316	12.48	0.10	0.497
(epi)gallocatechin dimer5	17.94	4.19	1.33	0.498	12.34	0.06	0.491
(epi)gallocatechin dimer6	17.94	4.19	1.33	0.498	12.52	0.10	0.499
(epi)catechin gallate dimer(2d)	16.80	4.19	1.33	0.458	10.94	0.08	0.430
(epi)gallocatechin gallate dimer1 (2f)	21.36	4.19	1.33	0.620	6.31	0.05	0.228
(epi)gallocatechin gallate dimer2 (2f)	21.36	4.19	1.33	0.620	7.37	0.10	0.275
(epi)catechin-(epi)gallocatechin5 (2k)	15.19	4.19	1.33	0.401	14.07	0.12	0.567
(epi)gallocatechin-(epi)gallocatechin gallate1 (2o)	18.98	4.19	1.33	0.535	9.10	0.13	0.350
(epi)gallocatechin-(epi)gallocatechin gallate2 (2p)	18.98	4.19	1.33	0.535	9.46	0.32	0.366
(epi)catechin trimer1 (3a)	20.34	4.19	1.33	0.583	9.41	0.32	0.363
(epi)catechin trimer2 (3b)	20.34	4.19	1.33	0.583	10.42	0.33	0.407
(epi)gallocatechin trimer (3c)	24.08	4.64	1.28	0.716	9.15	0.32	0.352
(epi)gallocatechin trimer (3d)	24.08	4.64	1.28	0.716	9.87	0.10	0.383

(epi)catechin-(epi)gallocatechin-(epi)gallocatechin (3d)	22.37	4.64	1.28	0.655	10.83	0.35	0.425
Unretained compound (t_0)	3.86	0.92			1.07	0.06	
Last eluting compound (t_l)	32.11	3.37			24.02	0.13	
	Average	**4.29**	**1.37**		**Average**	**0.16**	

*Exact sequence could not be established from the MS data alone.

The theoretical and practical peak capacities were calculated as follows:

1. Peak capacity (1-D) = $1 + \dfrac{t_g}{\dfrac{1}{n}\sum_{1}^{n} W_b}$

where t_g = total gradient time

n = number of peaks

W_b = base peak width

2. Theoretical peak capacity (N_T) = $N_1 \times N_2$

where N_1 = peak capacity in dimension 1

N_2 = peak capacity in dimension 2.

Finally, the practical peak capacities were calculated using the methods proposed by Liu *et al* [1] and Li *et al* [2]. Liu *et al* [1] practical peak capacity (N_p) is given by:

$N_p = N_T - ½ [N_2^2 \tan \gamma + N_1^2 \tan \alpha]$

where $\alpha = \alpha'(1-2\beta/\pi)$

$\alpha' = \tan^{-1} (N_2/N_1)$

$\gamma = \pi/2 - \alpha - \beta$

$\beta = \cos^{-1} (r)$, r is the square root of the correlation coefficient

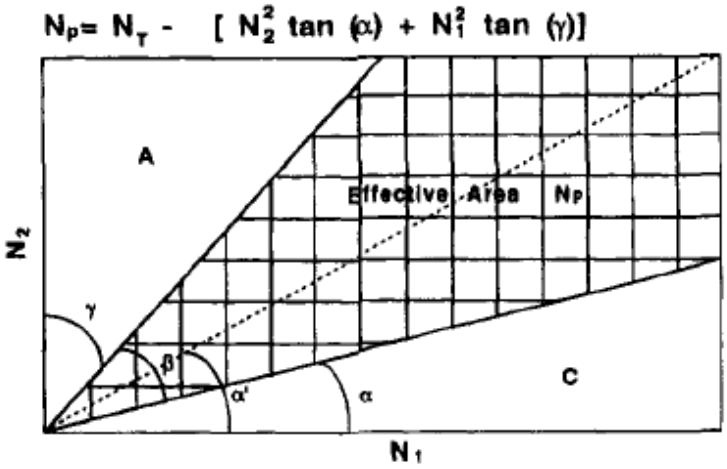

Figure 1B: Graphical presentation of the effective non-orthogonal 2D retention space for a peak spreading angle of β [1]. Derivation of values for α, α', γ and β are presented above.

While Li *et al* [1] peak capacity was calculated using:

$$n'_{p,2D} = \frac{n_1 n_2}{\sqrt{1 + 3.35\left(\frac{{}^2t_c n_1}{{}^1t_g}\right)^2}}$$

The peak broadening factor was calculated using:

$$< \beta >= \sqrt{1 + 0.214\left(\frac{t_s}{\sigma_1}\right)^2}$$

The isocratic peak capacity was calculated according to Neue [3]:

$$n_p = \frac{\sqrt{N}}{4R_s}\ln(k+1)$$

where k is the retention factor for the last eluting compound.

Table 8B: Summary of the results for the calculation of the practical peak capacities for the HILIC × RP-LC separations using the short and long gradients.

Parameter	Value						
	Cocoa (on-line)	**Cocoa (off-line, short gradient)**	**Cocoa (off-line, long gradient)**	**Apple (On-line)**	**Apple (off-line, long gradient)**	**Green tea (off-line, UV 280nm)**	**Green tea (off-line, UV 320 and 370 nm)**
[a]HILIC peak capacity, n_1	40	32	32	33	27	31	28
[a]RP peak capacity, n_2	20	54	137	20	112	121	125
Correlation coefficient, r^2	0.0231	0.0876	0.2092	0.0182	0.1651	0.0135	0.3694
r	0.1520	0.2960	0.4574	0.1349	0.4063	0.1162	0.6078
α	0.0450	0.1981	0.4057	0.0469	0.3554	0.0979	0.5616
α'	0.4636	1.0358	1.3413	0.5449	1.3342	1.3200	1.3504
β	0.4182	1.2703	1.0957	1.4355	1.1524	1.4543	0.9175
γ	0.1075	0.1023	0.0694	0.0884	0.0630	0.0186	0.0916
<β>	1.04	1.40	1.40	1.02	1.30	1.40	2.01
[c]Theoretical peak capacity, n_T	800	1728	4384	660	3024	3751	3500
[b]Practical peak capacity, n_p	742	1475	3512	617	2493	3568	2535
[d]Practical peak capacity, n_p	770	1237	3137	642	2334	2725	2186

[a] Calculated according to Neue [3].
[b] Calculated according to Liu *et al* [1].
[c] $n_T = n_1 \times n_2$.
[d] Calculated according to Li *et al* [2].

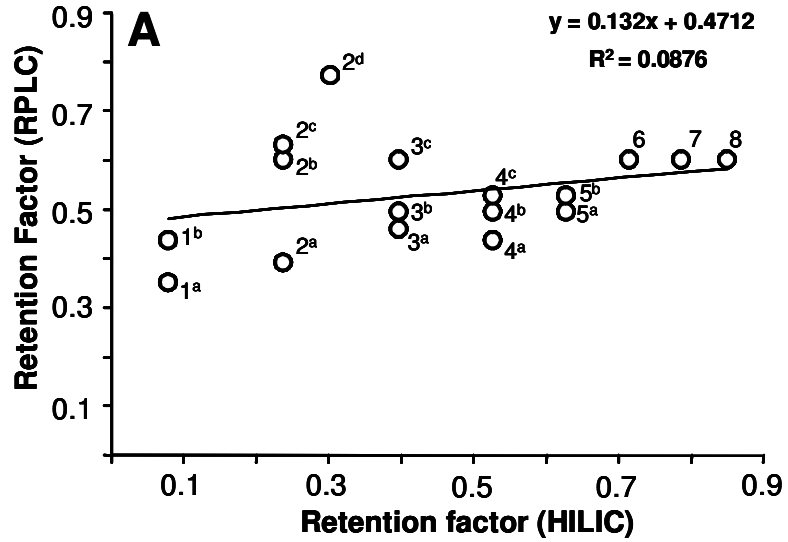
A
y = 0.132x + 0.4712
R² = 0.0876
Retention Factor (RPLC)
Retention factor (HILIC)
0.1
0.3
0.5
0.7
0.9

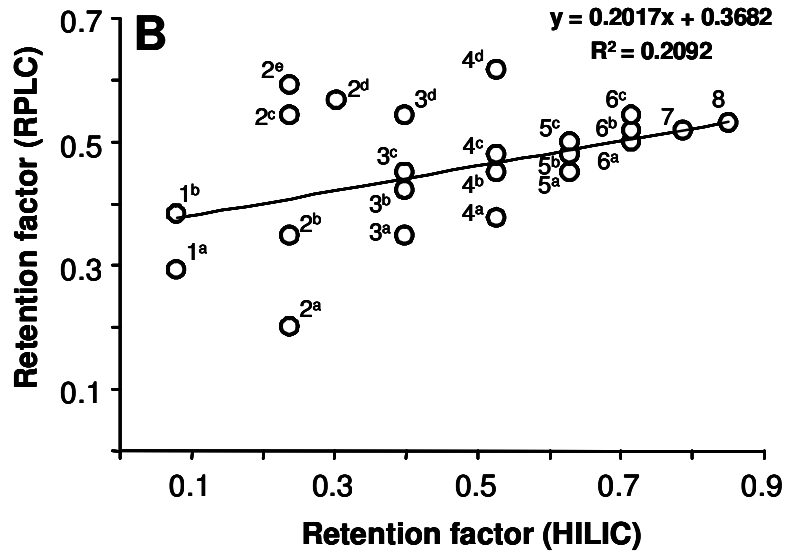
B
y = 0.2017x + 0.3682
R² = 0.2092
Retention factor (RPLC)
Retention factor (HILIC)
0.1
0.3
0.5
0.7
0.9

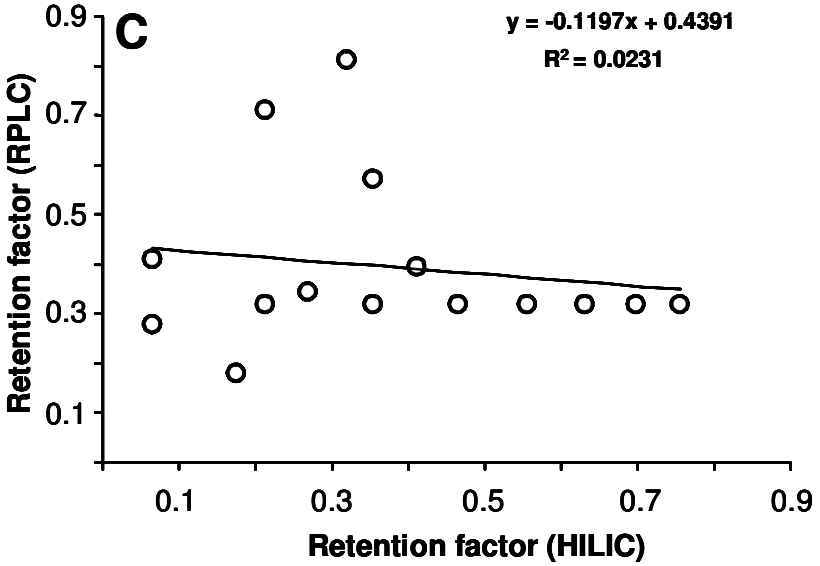
C
y = -0.1197x + 0.4391
R² = 0.0231
Retention factor (RPLC)
Retention factor (HILIC)
0.1
0.3
0.5
0.7
0.9

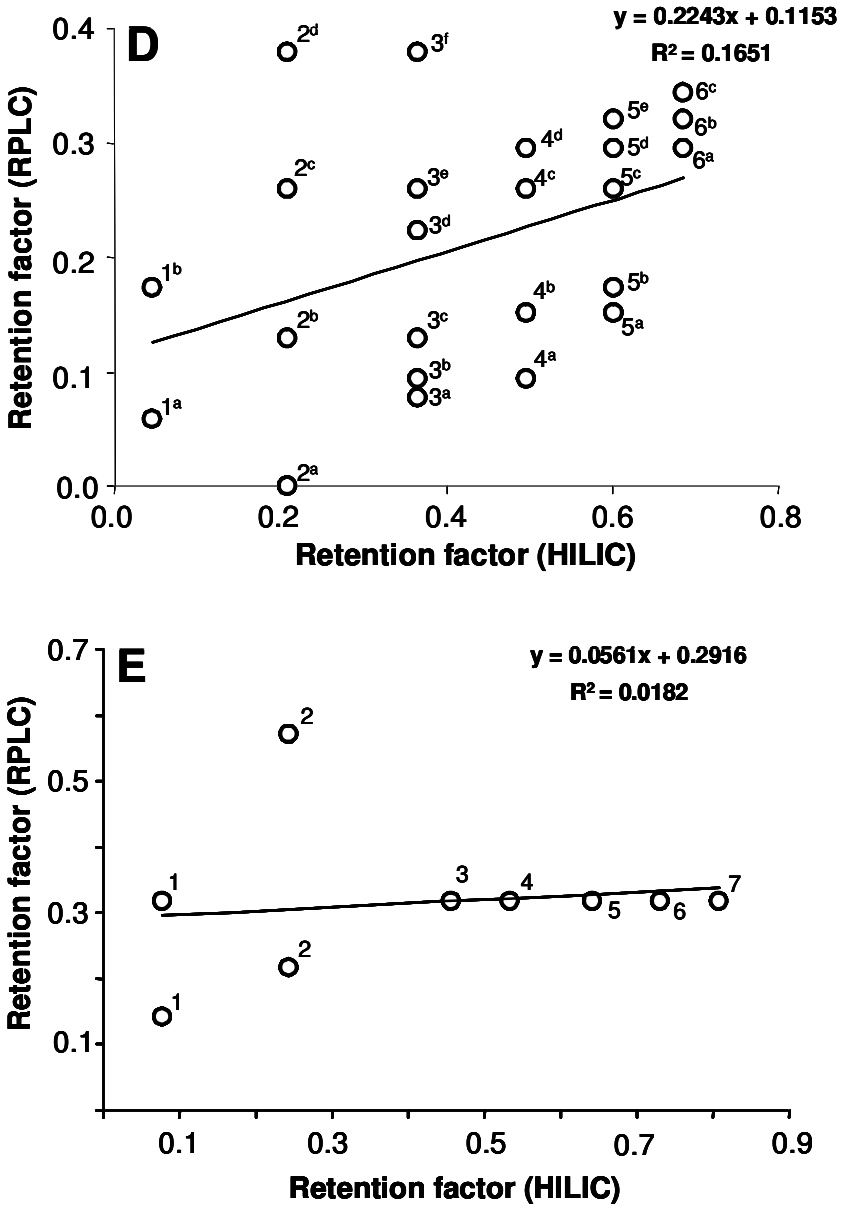

Figure 1B: Plots of the scaled retention factors for the procyanidins oligomers identified by HILIC × RP-LC in: (A) cocoa using a short gradient (off-line), (B) cocoa using a long gradient (off-line), (C) cocoa on-line, (D) apple using a long gradient and (E) apple on-line. Numbers indicate the degree of polymerisation (DP).

References

[1] Z. Liu, D.G. Patterson, M.L. Lee, Anal. Chem. 67 (1995) 3840.
[2] X. Li, D.R. Stoll, P.W. Carr, Anal. Chem. 81 (2009) 845.
[3] U.D. Neue, J. Chromatogr. A 1184 (2008) 107.

Appendix C

Additional Mass Spectra

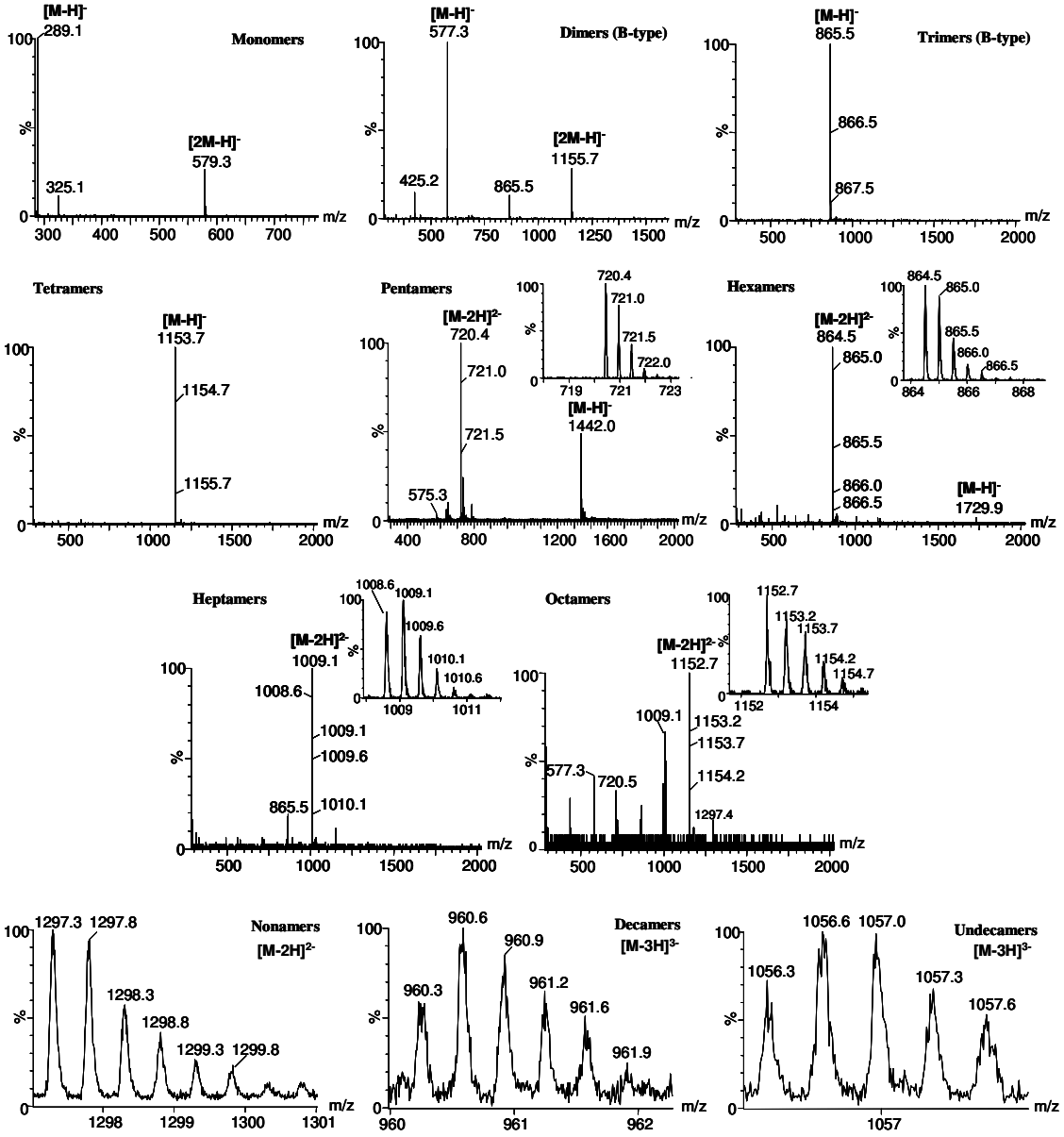

Figure 1C: Negative ESI mass spectra obtained from the HILIC–MS and RP-LC–MS analysis of oligomeric procyanidins in the cocoa extract.